UNIL | Université de Lausanne

Unicentre
CH-1015 Lausanne
http://serval.unil.ch

Year : 2015

WNT Signaling in Drosophila Neuromuscular Junctions

Anne-Marie Lüchtenborg

Anne-Marie Lüchtenborg, 2015, WNT Signaling in Drosophila Neuromuscular Junctions

Originally published at : Thesis, University of Lausanne

Posted at the University of Lausanne Open Archive http://serval.unil.ch
Document URN : urn:nbn:ch:serval-BIB_C2B038B424593

Droits d'auteur
L'Université de Lausanne attire expressément l'attention des utilisateurs sur le fait que tous les documents publiés dans l'Archive SERVAL sont protégés par le droit d'auteur, conformément à la loi fédérale sur le droit d'auteur et les droits voisins (LDA). A ce titre, il est indispensable d'obtenir le consentement préalable de l'auteur et/ou de l'éditeur avant toute utilisation d'une oeuvre ou d'une partie d'une oeuvre ne relevant pas d'une utilisation à des fins personnelles au sens de la LDA (art. 19, al. 1 lettre a). A défaut, tout contrevenant s'expose aux sanctions prévues par cette loi. Nous déclinons toute responsabilité en la matière.

Copyright
The University of Lausanne expressly draws the attention of users to the fact that all documents published in the SERVAL Archive are protected by copyright in accordance with federal law on copyright and similar rights (LDA). Accordingly it is indispensable to obtain prior consent from the author and/or publisher before any use of a work or part of a work for purposes other than personal use within the meaning of LDA (art. 19, para. 1 letter a). Failure to do so will expose offenders to the sanctions laid down by this law. We accept no liability in this respect.

UNIL | Université de Lausanne
Faculté de biologie et de médecine

Département de Pharmacologie et Toxicologie

WNT SIGNALING IN DROSOPHILA NEUROMUSCULAR JUNCTIONS

Thèse de doctorat en Neurosciences

présentée à la

Faculté de Biologie et de Médecine
de l'Université de Lausanne

par

Anne-Marie LÜCHTENBORG

Master of Science (Life Science) de l'Universität Konstanz, Allemagne

Jury

Prof. Jean-Pierre Hornung, Président
Prof. Vladimir Katanaev, Directeur
Prof. Esther Stöckli, Expert
Prof. Marie-Christine Broillet, Expert

Thèse n° 143

Lausanne 2015

Programme doctoral interuniversitaire en Neurosciences des Universités de Lausanne et Genève

LEMANIC NEURO SCIENCE DOCTORAL SCHOOL

UNIL | Université de Lausanne

UNIVERSITÉ DE GENÈVE

UNIL | Université de Lausanne

UNIVERSITÉ DE GENÈVE

Programme doctoral interuniversitaire en Neurosciences des Universités de Lausanne et Genève

Imprimatur

Vu le rapport présenté par le jury d'examen, composé de

Président	Monsieur Prof. Jean-Pierre **Hornung**
Directeur de thèse	Monsieur Prof. Vladimir **Katanaev**
Co-directeur de thèse	
Experts	Madame Prof. Esther **Stöckli**
	Madame Prof. Marie-Christine **Broillet**

le Conseil de Faculté autorise l'impression de la thèse de

Madame Anne-Marie Lüchtenborg

Master of Science Université de Konstanz

intitulée

WNT Signaling in Drosophila Neuromuscular Junctions

Lausanne, le 23 janvier 2015

pour Le Doyen
de la Faculté de Biologie et de Médecine

Prof. Jean-Pierre Hornung

TABLE OF CONTENTS

Acknowledgements **2**

Abstract **3**

Résumé **5**

Introduction **7**

Wnt signaling 7

The canonical Wnt pathway 8

The planar cell polarity pathway 11

The Wnt/Ca^{2+} pathway 11

Wingless signaling in *Drosophila* neuromuscular junctions 12

The neuromuscular junction 12

The presynaptic Wingless pathway 13

The postsynaptic Fz2 internalization pathway 18

Ankyrin 19

Mammalian Ankyrins 19

Drosophila Ankyrins 20

Ankyrin structure 21

Wnt signaling in Alzheimer's disease 23

Evidence for the relation of Alzheimer's Disease and Wnt signaling 25

Drosophila models of Alzheimer's Disease 26

Summary of the Results **28**

Article 1: Heterotrimeric Go protein links Wnt-Frizzled signaling with ankyrins to regulate the neuronal microtubule cytoskeleton 28

Gαo localization in NMJs 28

The role of Gαo in NMJs 29

Gαo in the Wg pathway 30

Interaction of Gαo with Ank2 30

Conservation of the interaction in mammals 31

Unpublished Results 32

Futsch genetically interacts with Wg-Fz2- Gαo 32

Article 2: Lack of evidence of the interaction of the Aβ peptide with the Wnt signaling cascade in Drosophila models of Alzheimer's disease 37

Discussion **39**

References **50**

Articles **60**

ACKNOWLEDGEMENTS

It is a pleasure to thank those who made this thesis possible.

First of all, I would like to express my gratitude to my thesis supervisor Prof. Vladimir Katanaev for his constant encouragement, effective guidance and valuable advice throughout the project as well as for his persistent personal support.

I am grateful to the members of my thesis committee, Prof. Esther Stöckli and Prof. Marie-Christine Broillet for kindly accepting to serve as the experts for my thesis and Prof. Jean-Pierre Hornung for kindly agreeing to preside the thesis jury.

I thank all members of the Katanaev lab for the supportive and fun working atmosphere. Especially I would like to thank Gonzalo Solis for many valuable suggestions, helpful advice and working "for me" in the Ankyrin project. Thank you also for proofreading the manuscript. Thanks to Alexey Koval for having an answer to every biochemistry question, Maja Babis for helping with the fly work and always having an open ear, Oleksii Bilousov for helping with crosses and Anne-Lise Maury-Fraering for technical assistance and moral support. I would also like to thank the former members of the group Natalya Katanayeva, Chen Lin, Vladimir Purvanov, Diane Egger-Adam, Damir Kopein and Silke Büstorf for helpful advices especially during the early parts of my project.

Special thanks go to Caroline Ronzaud for help with the French translations and her permanent interest in my work.

I also would like to thank the members of the DPT, the DGM and the CIF who helped me during my thesis.

My very special thanks go to my parents, Britta, Jörg, Daniel and to Margret and Wolfgang. Without your help and support, especially during the last year, this thesis would not have been possible.

To Roland and Fabienne, thank you for being by my side.

ABSTRACT

The Wnt -Wingless (Wg) in *Drosophila*- signaling is an evolutionary conserved, fundamental signal transduction pathway in animals, having a crucial role in early developmental processes. In the adult animal the Wnt cascade is mainly shut off; aberrant activation leads to cancer. One physiological exception in the adult animal is the activation of Wnt signaling in the nervous system. In the present work, we investigated Wg signaling in the *Drosophila* neuromuscular junctions (NMJs). The fly NMJs closely resemble the glutamatergic synapses in the mammalian central nervous system and serves as a model system to investigate the mechanism of synapse formation and stability. We demonstrate that the trimeric G-protein Go has a fundamental role in the presynaptic cell in the NMJ. It is implicated in the presynaptic Wg pathway, acting downstream of the ligand Wg and its receptor Frizzled2 (Fz2). Furthermore, we prove that the presynaptic Wg-Fz2-Gαo pathway is essential for correct NMJ formation. The neuronal protein Ankyrin2 (Ank2) localizes to the NMJ and has so far been considered to be a static player in NMJ formation, linking the plasma membrane to the cytoskeleton. We identify Ank2 as a direct target of Gαo. The physical and genetic interaction of Gαo with Ank2 represents a novel branch of the presynaptic Wg pathway, regulating the microtubule cytoskeleton in NMJ formation, jointly with the previously established Futsch-dependent branch, which controls microtubule stability downstream of the kinase Sgg (the homolog of GSK3β). We moreover demonstrate that the Gαo-Ankyrin interaction to regulate the cytoskeleton is conserved in mammalian neuronal cells. Our findings therefore provide a novel, universally valid regulation of the cytoskeleton in the nervous system.

Aberrant inactivation of the neuronal Wnt pathway is believed to be involved in the pathogenesis of the Aβ peptide in Alzheimer's disease (AD). We modeled AD in *Drosophila* by expressing Aβ42 in the nervous system and in the eye. Neuronal expression drastically shortens the life span of the flies. We prove that this effect depends on the expression specifically in glutamatergic neurons. However, Aβ42 does not induce any morphological changes in the NMJ; therefore this synapse is not suitable to study the mechanism of Aβ42 induced neurotoxicity. We furthermore demonstrate that genetic

activation of the Wnt pathway does not rescue the Aβ42 induced phenotypes – in opposition to the dominating view in the field. These results advice caution when interpreting data on the potential interaction of Wnt signaling and AD in other models.

RÉSUMÉ

La voie de signalisation Wnt (Wingless (Wg) chez la drosophile) est conservée dans l'évolution et fondamentale pour le développement des animaux. Cette signalisation est normalement inactive chez l'animal adulte; une activation anormale peut provoquer le cancer. Or, ceci n'est pas le cas dans le système nerveux des adultes. La présente thèse avait pour but d'analyser le rôle de la voie de signalisation Wingless dans la plaque motrice de *Drosophila melanogaster*. En effet, cette plaque ressemble fortement aux synapses glutaminergiques du système nerveux central des mammifères et procure ainsi un bon modèle pour l'étude des mécanismes impliqués dans la formation et la stabilisation des synapses. Nos résultats montrent que la protéine trimérique Go joue un rôle fondamental dans la fonction de la cellule présynaptique de la plaque motrice. Go est en effet impliqué dans la voie de signalisation Wg, opérant en aval du ligand Wg et de son récepteur Frizzled2. Nous avons pu démontrer que cette voie de signalisation Wg-Fz2-Gαo est essentielle pour le bon développement et le fonctionnement de la plaque motrice. Fait intéressant, nous avons montré que la protéine neuronale Ankyrin2 (Ank2), qui est connue pour jouer un rôle statique en liant la membrane plasmique au cytosquelette dans la plaque motrice, est une cible directe de Gαo. L'interaction physique et génétique entre Gαo et Ank2 constitue ainsi une bifurcation de la voie de signalisation présynaptique Wg. Cette voie régule le cytosquelette des microtubules en coopération avec la branche liée à la protéine Futsch. Cette protéine est l'homologue de la protéine liant les microtubules MAP1B des mammifères et contrôle la stabilité des microtubules opérant en aval de la kinase Sgg (l'homologue de GSK3β). De plus, la régulation du cytosquelette par l'interaction entre Gαo et Ankyrin est conservée chez les mammifères. Dans leur ensemble, nos résultats ont permis d'identifier un nouveau mode de régulation du cytosquelette dans le système nerveux, probablement valable de manière universelle.

La voie de signalisation Wnt est soupçonnée d'être impliquée dans la toxicité provoquée par le peptide Aβ dans le cadre de la maladie d'Alzheimer. Nous avons tenté de modéliser la maladie chez la drosophile en exprimant Aβ42 spécifiquement dans le cerveau. Cette expérience a montré que

l'expression neuronale d'Aβ42 réduit la durée de vie des mouches de manière significative par un mécanisme impliquant les cellules glutamatergiques. Par contre, aucune modification morphologique n'est provoquée par Aβ42 dans les plaques motrices glutamatergiques. Ces résultats montrent que ce modèle de Drosophile n'est pas adéquat pour l'étude de la maladie d'Alzheimer. De plus, l'activation génétique de la voie de signalisation Wg n'a pas réussi à restaurer les phénotypes de survie ou ceux des yeux causés par Aβ42. Ces résultats indiquent que l'implication de la voie de signalisation Wg dans la maladie d'Alzheimer doit être considérée avec prudence.

INTRODUCTION

WNT SIGNALING

The Wnt (Wingless, Wg, in *Drosophila*) signal transduction pathway is one of the fundamental signaling cascades in animal development. It is highly conserved throughout the animal kingdom (Logan and Nusse, 2004). During development, Wnt signal transduction defines crucial early processes like animal polarity, axis specification, segmentation and organogenesis (Wang et al., 2012). Later, Wnt signaling is implicated in CNS development ranging from the early steps including gastrulation and pattern formation to the later developmental processes like axon guidance and synaptogenesis to e.g. synaptic plasticity in adulthood (Figure 1) (Alves dos Santos and Smidt, 2011) . Missregulation of Wnt signaling leads to cancer and neurodegenerative diseases (Clevers and Nusse, 2012).

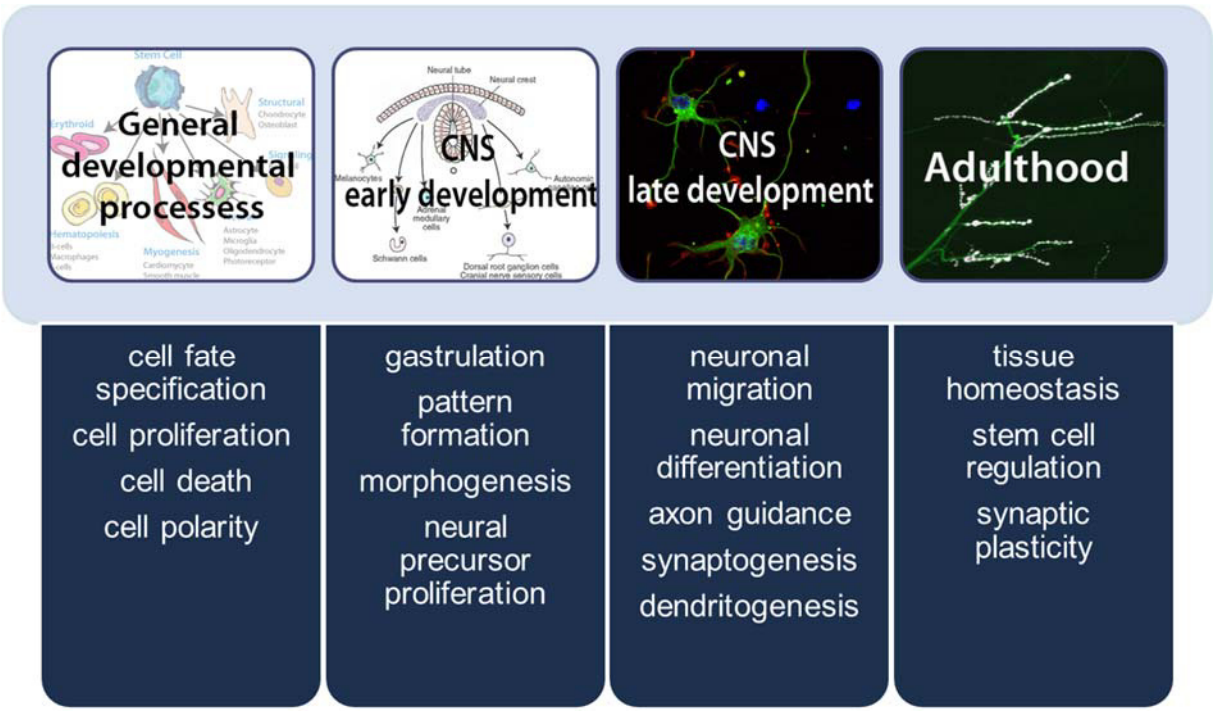

FIGURE 1 : Wnt signaling participates in CNS development from the regulation of early developmental processes until adulthood.

Wnts are a family of conserved morphogens consisting of 19 members in mammals and 7 in *Drosophila* (Miller, 2002), that are highly hydrophobic due to their posttranslational palmitoylation and N-glycosylation (Harterink and Korswagen, 2012; Willert et al., 2003). They are secreted from specialized cells and activate different signaling cascades in long- and short range target cells (Logan and Nusse, 2004). The posttranslational modification of Wnt impedes passive diffusion of the morphogen to long range target cells (Harterink and Korswagen, 2012). At present, the mechanism of Wnt secretion is incompletely understood and several mechanisms of active transport have been proposed (Logan and Nusse, 2004; Solis et al., 2013).

Wnt signaling is commonly divided into three branches: First, the transcription dependent, so called canonical Wnt-pathway, second, the non-canonical planar cell polarity pathway and third, the Wnt/Ca2+ pathway. Conventionally, these pathways have been considered independent from one another; it however becomes apparent that the activation of the pathways depends only in part on Wnt itself but mostly on the cellular context (Mikels and Nusse, 2006; Tao et al., 2005; Willert and Nusse, 2012). Therefore, the three cascades can also be considered as three "floors" of the same pathway which operate at different temporal modes (Koval and Katanaev, 2012).

THE CANONICAL WNT PATHWAY

The canonical, β-catenin dependent pathway was discovered in the early 1990s and is now the probably best studied among the three branches of Wnt signal transduction (Clevers and Nusse, 2012; Peifer et al., 1994). Its final outcome is the transcription of target genes; therefore the terminal effect of the signal occurs after hours to days.

In general, the ligand Wnt binds to a 7-transmembrane receptor of the Frizzled (Fz) family which is a member of the GPCR superfamily (Katanaev et al., 2005; Malbon, 2004). In the canonical pathway Wnts bind to Fz and the co-receptor low-density lipoprotein receptor-like protein 5/6 (Lrp5/6), a single-pass transmembrane receptor. The Wnt family of proteins consists of 19 members in mammals and 7 in *Drosophila,* while 19 human and 4 *Drosophila* Fz receptors are known (Wang et al., 2006).

Accordingly, the specificity of the signal is determined by the combination of ligand and receptor and the cellular environment. This binding activates the heterotrimeric G-protein downstream of the ligand-receptor complex (Katanaev and Tomlinson, 2006; Katanaev et al., 2005; Koval and Katanaev, 2011). Heterotrimeric G-proteins are evolutionary conserved. Of the Gα subunits four subfamilies exist in vertebrates: Gαi/o, Gαs, Gαq/11 and Gα12/13 (McCudden et al., 2005). Gαo was among the first α-subunit to be discovered and is the major Gα subunit in the brain (Sternweis and Robishaw, 1984; Wolfgang et al., 1990). In its inactive state, the trimeric G-protein exists as a trimer of the GDP-bound α-subunit and the β and γ subunits. Upon activation, GDP is exchanged to GTP leading to dissociation of the complex into the free α- and the βγ subunit. Both subunits can activate downstream signals (Gilman, 1987). Upon time GTP is hydrolyzed to GDP forming the free GDP-bound α-subunit. This can further reassociate with the βγ-dimer to reconstitute the trimeric complex (Figure 2).

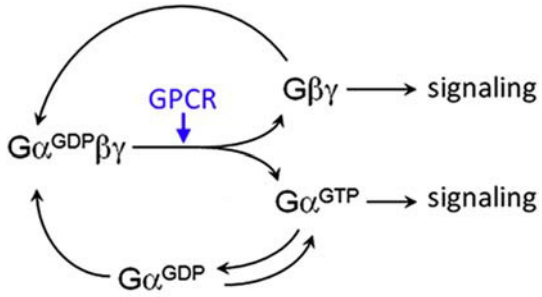

FIGURE 2: G-protein cycle. Upon activation of the trimeric G-protein ($G\alpha^{GDP}\beta\gamma$) by the G-protein coupled receptor (GPCR) the nucleotide GDP bound to the α-subunit is exchanged to GTP and the complex dissociates into the Gβγ-dimer and the $G\alpha^{GTP}$-subunit. Upon time, GTP bound to Gα hydrolyzes to GDP. Free $G\alpha^{GDP}$ is either recharged with GTP or associate again with the βγ-subunit to re-build the trimeric complex (modified from Lin et al., 2014).

The free Gα subunit binds the scaffolding protein Axin, while the βγ complex binds and recruits Dishevelled (Dvl, Dsh in Drosophila) (Egger-Adam and Katanaev, 2010). These interactions of Dvl and Axin with the G-protein subunits, together with binding of Dsh and Axin to the Fz and Lrp5/6 receptors, respectively (Egger-Adam and Katanaev, 2010; Mao et al., 2001; Wong et al., 2003), recruit the cytoplasmic proteins to the plasma membrane and destroy the Axin-based destruction complex. The destruction complex is a multiprotein complex which includes -amongst other proteins- Axin, adenomatous polyposis coli (APC) and the serin-threonin kinases casein kinase I (CKI) and glycogen

synthase kinase-3β (GSK3β, Shaggy (Sgg) in *Drosophila*). The function of the destruction complex is the sequential phosphorylation of β-catenin. Phosphorylated β-catenin is subsequently ubiquitinated by the E3-ubiquitin ligase β-TrCP and thereby tagged for proteasomal degradation (Aberle et al., 1997; Stamos and Weis, 2013). Upon binding of Wnt to Fz, the destruction complex is disassembled, leading to accumulation of β-catenin in the cytosol and its translocation into the nucleus. There, β-catenin binds to lymphoid enhancer-binding factor 1/T cell-specific transcription factor (TCF/LEF) and initiates the transcription of target genes (Logan and Nusse, 2004) (). An up-to date list of genes regulated by Wnt signaling is provided on the Wnt homepage (http://web.stanford.edu/group/nusselab/cgi-bin/wnt/).

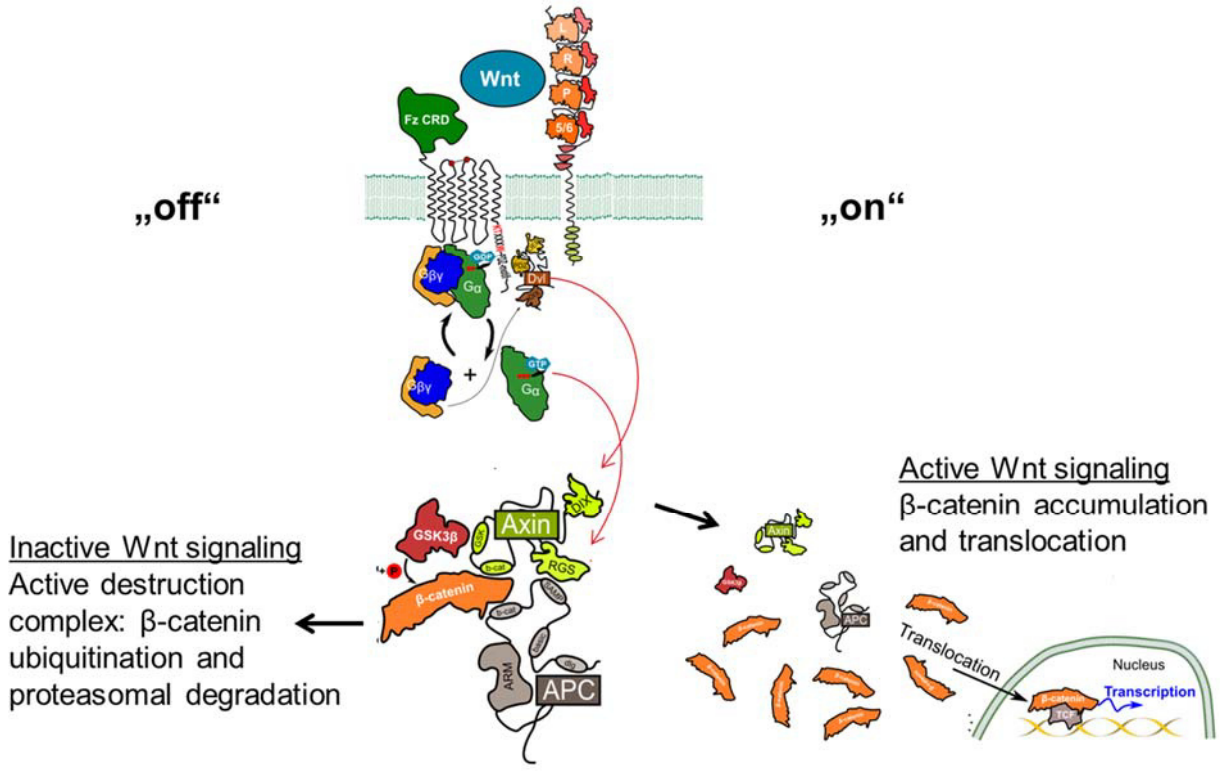

FIGURE 3: Scheme of canonical Wnt signaling: in the inactive ('off') state the Axin-based destruction complex is active, phosphorylating cytosolic β-catenin by the kinase GSK3β which targets it for ubiquitination and proteasomal degradation. Upon activation of the receptor Frizzled by the ligand Wnt ('on'), the trimeric G-protein is activated and dissociates into α- and βγ-subunits which cause together with the protein Dishevelled (Dvl) the inhibition of the destruction complex. Unphosphorylated β-catenin accumulates in the cytosol and ultimately translocates into the nucleus where it activates the transcription of target genes. Image courtesy: Alexey Koval.

THE PLANAR CELL POLARITY PATHWAY

Planar cell polarity (PCP) describes the phenomenon of specific orientation of cells in the plane of a tissue. It can be observed for example in the directional growth of body hair and the hair cells of the mammalian cochlea. A further example is the formation of oriented ommatidia in the flies' eyes. PCP is regulated by the second floor of Wnt signaling which is non-canonical, i.e. independent of β-catenin regulated transcription and by far less well understood than the canonical Wnt cascade (Gao, 2012). The final outcome of this pathway is the rearrangement of several proteins and the cytoskeleton and it takes minutes to hours to be accomplished. In the final asymmetrical protein localization, the receptor Fz and the cytosolic Dsh and Diego accumulate at the distal end of the cell; the proteins Van Gogh and Prickled at the proximal side (Shimada et al., 2001; Singh and Mlodzik, 2012; Strutt, 2001). Like in the canonical Wnt signal, the PCP pathway depends on the interaction of Fz with the trimeric G-protein Go (Katanaev and Tomlinson, 2006; Katanaev et al., 2005). Also involved in the relocalization and polarization of the cell signal are amongst others the small GTPases Rab5 and Rab11 and the actin regulator RhoA and Kermit (Lin and Katanaev, 2013; Purvanov et al., 2010; Strutt et al., 1997).

THE WNT/CA^{2+} PATHWAY

The Wnt/Ca^{2+} pathway displays the fastest signaling effect, taking only up to several minutes (Kühl et al., 2000a). It increases intracellular Ca^{2+} levels. This is achieved by activation of the phospholipase C in a G-protein dependent manner downstream of the Wnt-Fz ligand-receptor interaction, that ultimately results in increase in inositol-trisphosphate levels and intracellular Ca^{2+} release (Kühl et al., 2000b). The released Ca^{2+} levels activate the Ca^{2+}/calmodulin-dependent protein kinase II (CamKII) and protein kinase C which modulate the cellular response (Kühl et al., 2000a).

WINGLESS SIGNALING IN *DROSOPHILA* NEUROMUSCULAR JUNCTIONS

THE NEUROMUSCULAR JUNCTION

The neuromuscular junction (NMJ) of *Drosophila* larvae is a model for mammalian glutamatergic central nervous system synapses. Each syncytial body wall muscle of the *Drosophila* larva is innervated in a stereotypical manner by up to four neurons that form an arbor-like structure on the muscle. This arbor consists of many round cavities, the synaptic boutons. Each bouton contains around 20 active zones where the transmitter release takes place. On the postsynaptic side, boutons are surrounded by the subsynaptic reticulum (SSR). Here, the neurotransmitter receptors cluster opposite of the active zones. During growth of the larva, new boutons are added to the NMJ by budding, division or *de novo* formation accompanied by the formation of the postsynaptic SSR (Zito et al., 1999). Boutons are differentiated into type I, type II and type III boutons, dependent on their size, the neurotransmitter released and the thickness of the SSR. Type I boutons are glutamatergic and innervate every muscle of the *Drosophila* larva. These boutons are further subdivided into type Ib (big) and type Is (small) boutons (Jan and Jan, 1976). Additional regulation is provided by modulatory synapses of type II and III boutons that release different neurotransmitters (Menon et al., 2013).

Several components of mammalian glutamatergic synapses have been found in the *Drosophila* NMJ (Menon et al., 2013). The ionotropic glutamate receptor GluR in the postsynaptic density is for example homolog to the mammalian AMPA-type GluR and the protein discs large (Dlg) that accumulates in the SSR is the *Drosophila* ortholog of the mammalian postsynaptic scaffolding protein PSD-95 (Lahey et al., 1994).

The advantages of the NMJ as model for mammalian glutamatergic synapses are -besides the advantages of *Drosophila* genetics- the large size, the easy accessibility both for morphological and for (electro-) physiological investigations and the possibility for live imaging (Zito et al., 1999).

THE PRESYNAPTIC WINGLESS PATHWAY

Wg signaling is active both in the pre- and in the postsynaptic cell. Figure 4 displays an overview of the current understanding of Wg signaling in the NMJ.

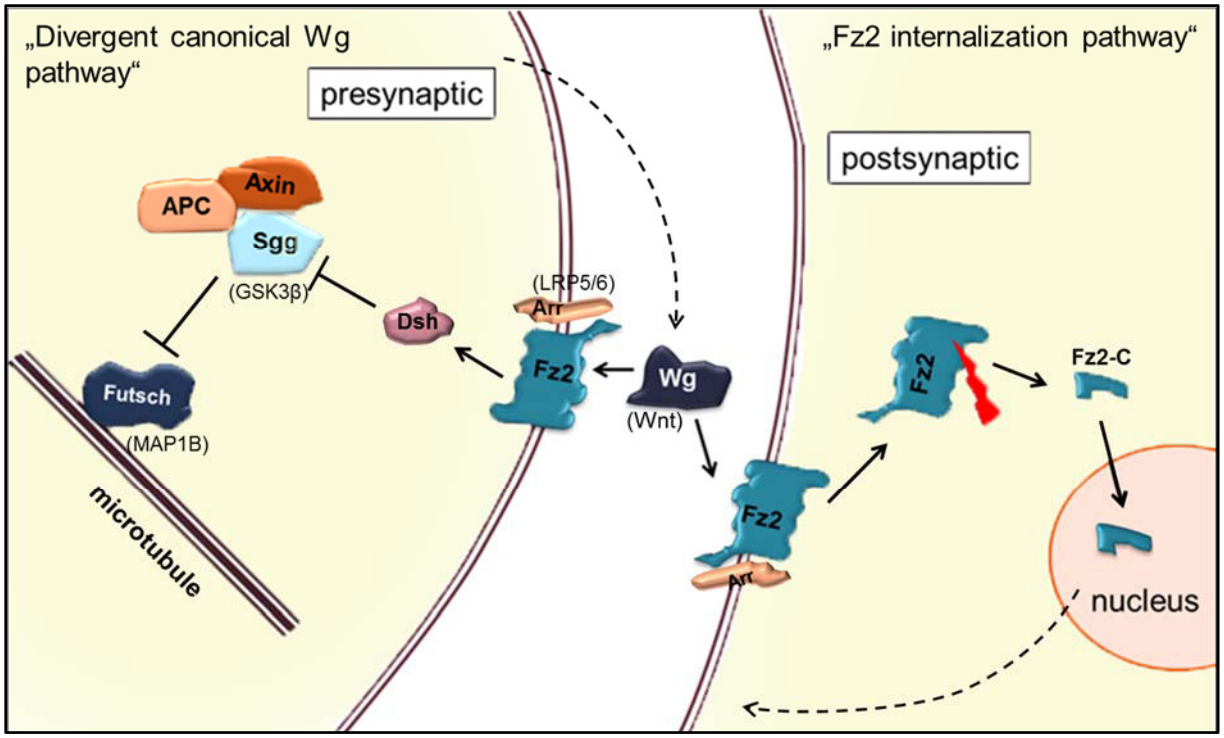

FIGURE 4: Schematic representation of the pre-and postsynaptic Wg signaling in the *Drosophila* NMJ. Wg is released from the neuron and binds pre-and postsynaptically to the receptor Frizzled2. In the presynaptic cell an β-catenin and transcription independent signaling cascade is active, leading to structural rearrangement of the microtubule cytoskeleton through the phosphorylation of the microtubule binding protein Futsch by the kinase Sgg. On the postsynaptic side, Wg signal leads to internalization of the receptor, cleavage of its C-terminal peptide (Fz2-C) and the nuclear translocation of Fz2-C. Mammalian homologues to the *Drosophila* protein are indicated in brackets.

In the presynaptic cell of the NMJ several proteins of the canonical Wg pathway are present: Wg and Arrow (Arr, the *Drosophila* homolog of Lrp5/6) are both distributed in a punctate manner in the presynaptic cell in the axon and enriched in the synaptic boutons; Fz2 is present in the motoneurons and NMJ; Dsh is also located in the axon and shows a more diffuse and evenly distributed pattern in the boutons, and Sgg is evenly distributed along the axon and shows a clear, dense presynaptic

localization in the boutons (Miech et al., 2008; Packard et al., 2002). The presynaptic cell is however devoid of β-catenin (Armadillo, Arm, in *Drosophila*) - some remaining Arm immunofluorescent signal in the nerve could be attributed to the ensheathing glial cell (Miech et al., 2008; Packard et al., 2002), suggesting a β-catenin independent Wg pathway in the synapse. Indeed, expression of the constitutively active form of β-catenin or of the transcription factor TCF/pangolin did not rescue the phenotypes associated with expression of dominant-negative form of Dsh. Furthermore a dominant-negative TCF did not suppress the phenotypes induced by a dominant-negative Sgg construct (Miech et al., 2008). Taken together this demonstrates that the presynaptic Wg pathway is transcription independent.

WINGLESS

In the larval NMJ Wg is expressed in neurons and glial cells but not in the muscles (Kerr et al., 2014; Packard et al., 2002). Wg is secreted presumably from type Ib boutons and distributes around the synaptic boutons (Packard et al., 2002). Secretion is enhanced after physiological or experimental stimulation of the synapse (Ataman et al., 2008; Tan et al., 2013). Since this stimulation induces presynaptic synaptopod and ghost bouton formation that might further develop into mature boutons, potentially the Wg signaling regulates the NMJ morphology in an activity dependent manner (Ataman et al., 2008; Tan et al., 2013). Glial cells also secrete Wg but blocking this secretion did not influence the presynaptic cell. Instead, Wg from glial cells might have an impact on postsynaptic NMJ formation (Kerr et al., 2014).

The requirement of Wg for NMJ formation has been tested with temperature-sensitive Wg mutants (Wg^{ts}), which were shifted to restrictive temperature only in late larval stages to overcome the embryonic lethality of wg mutations. Wg^{ts} mutants show severe morphological defects both in pre-and postsynapse: The neuron forms large, irregular cavities with an altered staining of the microtubule-binding protein Futsch. In wild-type synapses, Futsch appears bundled and forms loops in the terminal boutons. Wg^{ts} larvae show instead a more diffuse localization of Futsch (Miech et al., 2008; Roos et

al., 2000). Furthermore, the presynaptic terminals are filled with vesicles, while mitochondria and active zones are missing (Packard et al., 2002). In addition to these presynaptic defects, the postsynaptic SSR is partially lacking and the glutamate receptor GluRII seems to be more diffusely localized in wg mutants than in the wild type condition. Cumulatively these defects are reflected in a decreased bouton number (Miech et al., 2008; Packard et al., 2002).

In contrast to the mutant phenotypes, overexpression of Wg in the presynaptic cell resulted in an increase in bouton numbers. Moreover, presynaptic overexperssion of Wg rescued the mutant bouton number, indicating an important role of presynaptic Wg in bouton formation (Packard et al., 2002).

FRIZZLED2

The receptor Fz2 is expressed both in the neuron and the muscle (Packard et al., 2002). Fz2 mutation induces NMJ defects that resemble the ones induced by the wg mutation: the NMJ morphology is abnormal and the bouton number is heavily reduced. Postsynaptically, the SSR is thinner and partially lost which indicates an inaccurate pre-and postsynaptic apposition (Mathew et al., 2005; Mosca and Schwarz, 2010). Moreover an increase in ghost boutons can be observed in fz2 mutants compared to control (Mosca and Schwarz, 2010).

So far, these defects have been mainly attributed to a function of Fz2 in the postsynaptic cell where the receptor is cleaved and internalized (Mathew et al., 2005) (see below). It has been demonstrated that postsynaptic expression of Fz2 could rescue these fz2 mutant phenotypes, indicating an important postsynaptic role of Fz2 (Mathew et al., 2005; Mosca and Schwarz, 2010). However, a presynaptic rescue experiment has not been performed until now.

SHAGGY

The serine-threonine kinase Sgg is expressed in a variety of tissues and exerts a vast amount of functions throughout development and adulthood. In the larval nervous system, Sgg is strongly expressed and localizes to the axons and the NMJ. It is enriched at the presynaptic NMJ arbor and distributes rather uniformly in the presynaptic boutons (Bobinnec et al., 2006; Franco et al., 2004; Packard et al., 2002).

Sgg functions as a negative regulator of bouton formation in the presynaptic cell. Sgg loss-of-function mutants or larvae expressing a dominant-negative "kinase-null" form of Sgg form more boutons and satellite boutons. In contrast, overexpression of Sgg decreased the bouton number (Franco et al., 2004). Furthermore, expression of a Sgg mini-gene in the presynaptic cell rescued loss-of-function phenotypes, but postsynaptic expression of the dominant-negative Sgg did not have any effect on the NMJ (Franco et al., 2004). Cumulatively these results prove the presynaptic role of Sgg in NMJ formation.

Several lines of evidence suggest that this role is the regulation of the microtubule cytoskeleton via phosphorylation of the microtubule binding protein Futsch. First, SggDN larvae display significantly more Futsch-positive microtubule loops than the control (Franco et al., 2004). Furthermore, futsch mutants suppressed formation of ectopic boutons induced by Wg overexpression or dominant-negative Sgg (Franco et al., 2004; Gögel et al., 2006; Miech et al., 2008). Last, it has been demonstrated in vitro and in vivo that Futsch is phosphorylated by Sgg (Gögel et al., 2006).

FUTSCH

Futsch is a large protein of more than 570 kDa which is the *Drosophila* homolog of the mammalian microtubule binding protein MAP1B (Hummel et al., 2000). The C- and N-termini are highly conserved between mammals and flies and the central domain of Futsch shares sequence similarity with the neurofilament proteins (Hummel et al., 2000).

Futsch is, like MAP1B, tightly associated with microtubules in vivo and in vitro (Gögel et al., 2006; Hummel et al., 2000; Lepicard et al., 2014; Roos et al., 2000; Ruiz-Canada et al., 2004). In the *Drosophila* NMJ, Futsch and tubulin form loops in the terminal boutons that are parallel to the muscle surface. These loops seem to be correlated with structural rearrangement of the synapse, for example during growth of the NMJ (Roos et al., 2000). The structures are disrupted and tubulin is present in a rather diffuse pattern in futsch mutants (Roos et al., 2000). However, Futsch is not only crucial for the localization of tubulin: a recent work found a reduced number of active zones in Futsch mutants that seems to be independent of the stabilization of tubulin by Futsch, but most likely depends on the interconnection of the active zone and the microtubules by Futsch (Lepicard et al., 2014).

Futsch also influences the overall appearance of the NMJ. Loss-of-function futsch mutants have a reduced number of boutons and an altered NMJ phenotype compared to the wild-type. This effect is partially rescued when the microtubule binding, N-terminal and the C-terminal domain of Futsch are reintroduced in the presynaptic cell (Gögel et al., 2006; Roos et al., 2000). Futsch can be phosphorylated by Sgg and moreover, the Wg overexpression phenotype is suppressed in a futsch$^{+/-}$ background. Therefore it has been proposed that the Wg pathway might act through this microtubule-binding protein (Gögel et al., 2006; Hummel et al., 2000; Roos et al., 2000). In this scenario, phosphorylation of Futsch by Sgg regulates Futsch activity. However, the partial rescue of the futsch mutant phenotype by the microtubule-binding parts of Futsch could not be improved when the Sgg phosphorylation site is included in the introduced gene (Gögel et al., 2006), suggesting a mechanism of Wg signaling that is independent of Sgg phosphorylation. In addition, no change in the immunofluorescence signal with an antibody against phosphorylated Futsch could be observed in a Sgg hypomorph and a dominant-negative Sgg construct (Gögel et al., 2006). Thus, it remains unclear whether phosphorylation by Sgg is crucial for the role of Futsch in NMJ formation.

THE POSTSYNAPTIC FZ2 INTERNALIZATION PATHWAY

In addition to the described presynaptic Wg pathway, another Fz2 dependent signaling cascade is active in NMJ: the postsynaptic Fz2 nuclear internalization (FNI) pathway (Figure 4). Fz2 is expressed both in neurons and in the muscle where it is enriched in the postsynaptic density surrounding the presynaptic terminals (Mathew et al., 2005). Postsynaptic overexpression of Fz2 was able to rescue the bouton number and ghost bouton defect of fz2 mutants, indicating an important role of postsynaptic Fz2 for proper NMJ formation (Mosca and Schwarz, 2010). Furthermore, the other proteins described before for the presynaptic Wg pathway (Wg, Arr, Dsh and Sgg) are also evenly distributed in the muscle – which holds also true for cytoplasmic β-catenin. However, the nuclei in the muscle are devoid of β-catenin (Miech et al., 2008; Packard et al., 2002) suggesting again at another "divergent" Wg pathway in the postsynaptic cell.

As mentioned before, Wg is expressed in neurons and glial cells and secreted from the presynaptic terminal and subsequently endocytosed by the muscle (Kerr et al., 2014; Packard et al., 2002). At the SSR it is possibly sequestered by the heparansulfate proteoglycan Perlecan/Trol which enables the activation of the postsynaptic Fz2 pathway (Kamimura et al., 2013). Upon activation, Fz2 is internalized, cleaved and shuttled to the nucleus dGRIP-dependent manner (Ataman et al., 2006; Mathew et al., 2005). The C-terminal Fz2 peptide (Fz2-C) translocates into the nucleus in a process involving the proteins importin-β11 and importin-α2, while the N-terminal part of the protein stays in the in proximity of the nucleus (Mathew et al., 2005; Mosca and Schwarz, 2010). The C-terminal peptide associates with the perinuclear reticulum and the protein laminC (Speese et al., 2012). The Fz2-C/laminC complex binds RNA but not DNA (Speese et al., 2012). Therefore, unlike previously hypothesized, Fz2-C seems to regulate RNA trafficking and local translation, but no transcription. This goes along with the notion, that the nuclear import of the Fz2-C peptide is not crucial for presynaptic bouton formation and microtubule organization, suggesting that the nuclear import of Fz2 controls only a postsynaptic subset of Fz2 function in the NMJ, potentially the local organization of the SSR (Higashi-Kovtun et al., 2010; Mathew et al., 2005; Mosca and Schwarz, 2010).

ANKYRIN

MAMMALIAN ANKYRINS

Ankyrins were first discovered as a linker between the actin-spectrin cytoskeleton and the plasma membrane in human erythrocytes and were given their name after their "anchor" function (Bennett and Stenbuck, 1979). The first Ankyrin discovered was called AnkyrinR (AnkR, for "restricted") and was later on found to be not only expressed in erythrocytes but in a vast variety of tissues including the brain, where its localization is limited to cell bodies and dendrites of a subset of neurons (Bennett, 1979; Bennett and Davis, 1981; Tse et al., 1991). In the follwing years, numerous studies demonstrated the existence of several AnkR isoforms and various protein-protein interactions (Bennett and Davis, 1981; Bennett and Healy, 2009; Davis and Bennett, 1994). In 1991, a second ankyrin gene was discovered that encodes the brain AnkB (B for "brain" or "broad" expression) (Otto et al., 1991; Tse et al., 1991). This protein exists in two splice variants of 220 kDa and 440 KDa which are differentially expressed during development. In developing, unmyelinated neurons the 440 kDa form predominates and is replaced by the 220 kDa AnkB when myelination is completed (Chan et al., 1993; Kunimoto, 1995; Kunimoto et al., 1991). In the brain a third anykrin gene encodes for the giant AnkG (G for "giant" or "general"). AnkG is neural specific in its 480 kDa and 270 kDa isoforms. Several smaller alternative splice variants exist and are expressed in a wide range of tissues (Kordeli et al., 1995; Peters et al., 1995). AnkG is more closely related to AnkB than to AnkR. While their unstructured C-termini display only 20 % homology, high identity is found in small stretches spread across the tail regions (Kordeli et al., 1995). In neurons, AnkG localizes to the axon initial segment and the nodes of Ranvier and is possibly involved in targeting specific proteins to these important subcellular locations (Jenkins and Bennett, 2001; Kordeli et al., 1995).

DROSOPHILA ANKYRINS

In *Drosophila*, two Ankyrin genes exist: ank1 and ank2 (Bouley et al., 2000; Dubreuil and Yu, 1994). Ank1 shares 53% similarity with human brain AnkB, but is in contrast to AnkB is widely expressed throughout the *Drosophila* life cycle.

In contrast, the expression pattern of the second *Drosophila* ank gene discovered, ank2, resembles the pattern of mammalian AnkB: it was found to be exclusively neuronal and the expression was found to be time-restricted to late embryonic and larval development when the nervous system is developing (Bouley et al., 2000). However, the authors of this first study on Ank2 reported only a single short isoform of 1159 aa in length, which is now referred to as Ank2S. Detailed analysis of the subcellular localization revealed that Ank2S is restricted to the neuronal cell body (Hortsch et al., 2002). Later, a group of larger isoforms of at least 4 transcripts between 2386 aa and 2465 aa was discovered. These proteins are now collectively referred to as Ank2M according to their medium size. Transcripts of this group localize along the axon but are excluded from the cell body (Hortsch et al., 2002). Mutations disrupting the Ank2M isoforms are lethal suggesting that the function of the protein is essential for survival (Hortsch et al., 2002).

Two giant isoforms of Ank2 emerged in two genetic screens, using transposon insertion or EMS induced mutations, which were carried out to find novel genes that are important for synaptic stability and to identify players in the process of synaptic remodeling (Koch et al., 2008; Pielage et al., 2008). These large isoforms are fusions of the previously known ank2 gene with the downstream genes SP2523 and CG32377 with unknown function (Koch et al., 2008; Pielage et al., 2008). According to their size, these constructs were called Ank2L for Ank2-Sp2523 and Ank2XL for Ank2-CG32377 (Koch et al., 2008). Disruption of these large isoforms leads to severe morphological defects of the NMJ: instead of boutons, large swellings that lack interbouton regions are created which go in hand with a reduction of bouton number. In addition the neuron retracts from the NMJ, the microtubule cytoskeleton seems to be disturbed and vacuolization can be detected in ank2L mutant synaptic

terminals (Koch et al., 2008; Pielage et al., 2008). Synaptic vesicles are also accumulating in the axon, hinting at a role of Ank2 in transport (Koch et al., 2008).

Ank2L and AnkXL are expressed in the peripheral and central nervous system. Both proteins are present in the axons and in the NMJ, albeit Ank2L to a somewhat lower level than Ank2XL (Koch et al., 2008; Pielage et al., 2008). In the axon Ank2XL and Ank2L surround the Futsch staining and high illumination microscopy revealed that Ank2L forms a lattice with a 200 nm interval in axons and interbouton regions (Pielage et al., 2008). In the boutons, Ank2L presents a more homogenous distribution while Ank2XL shows a granular pattern. Both isoforms do not overlap with active zone markers and therefore seem to be restricted to periactive zones (Koch et al., 2008).

ANKYRIN STRUCTURE

Ank proteins share a common structure with a globular N-terminal head, a ZU5 domain, a death domain and a variable C-terminal tail (Figure 5). The head domain consists of twenty-four 33aa long ankyrin repeats that are organized in four equal domains which mediate the interaction with transmembrane proteins like ion channels, e.g. the voltage dependent Na-channel; cell adhesion molecules like proteins of the L1CAM family; and cytosolic proteins like tubulin and MAP1 (Bennett and Davis, 1981; Bennett and Healy, 2009; Davis and Bennett, 1994). The ankyrin repeats are helically arranged and form a solenoid that might act as a reversible spring in cells that are mechanically challenged (Lee et al., 2006; Michaely et al., 2002). The ZU5 domain interacts with spectrin and anchors thereby the membrane bound proteins to the underlying actin cytoskeleton (Ipsaro et al., 2009). The death domain mediates interaction with other death-domain containing proteins. The C-terminal tail is in general unstructured. An exception is the C-terminus of *Drosophila* Ank2XL harboring 92 KEY repeats which are sequences of 76 aa in length that share the identifier amino acids K-E-Y. The KEY region of Ank2XL is weakly homologous to futsch, titin, unc-89 and the neurofilament heavy chain (Koch et al., 2008).

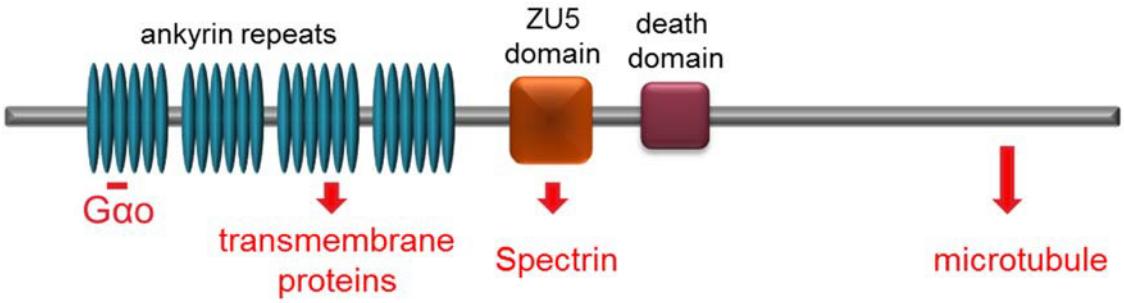

FIGURE 5: Schematic representation of Ankyrin displaying 24 anykrin repeats, organized in 4 domains, a ZU5 domain, a death domain and the unstructured C-terminus. The interaction partners of the different domains are indicated.

The C-terminal tails of the large isoforms seem to have a crucial function for proper NMJ development since all mutations that were discovered in the two NMJ screens were localized in this part of the protein (Koch et al., 2008; Pielage et al., 2008). Indeed, the C-terminus of Ank2L efficiently binds microtubule in vitro and is sufficient to ensure the trafficking of the protein to the NMJ (Pielage et al., 2008). The expression of this C-terminal construct does however not rescue the phenotypes observed in the mutants which suggests an additional role of the N-terminal part of Ank2 for proper NMJ development.

Recently, several studies have linked the AnkG gene to psychiatric disorders like schizophrenia and bipolar disorder (Gella et al., 2011; Logue et al., 2013; Wirgenes et al., 2014; Yuan et al., 2012). Yet the exact function of Ankyrins in the body is still the matter of research. The current view of their physiological role is somewhat static: they are thought to mediate the localization of ion channels and cell adhesion molecules to specific compartments of the cell –being it excitable membranes in the nervous system or the calcium homeostasis compartment in striated muscle. The giant Ank2 isoforms in *Drosophila* are presently seen as a linker between the microtubule cytoskeleton and membrane proteins. There are however reports that uncover a regulatory function of AnkG on Nav1.6 channel gating (Shirahata et al., 2006).

WNT SIGNALING IN ALZHEIMER'S DISEASE

The Wnt signaling pathway does not only play a physiological role in the adult nervous system, but mounting evidence show that it is also implicated in several neurological disorders like schizophrenia, autism, mood disorders, epilepsy, and Alzheimer's disease (AD) (Inestrosa et al., 2012).

AD is a terminal, progressive neurodegenerative disease that accounts for 50-75% of all dementia cases and affects >35 million people worldwide with an increasing tendency (Prince et al., 2013). AD patients show cognitive symptoms like amnesia (memory loss), aphasia (loss of the ability to comprehend and produce language), apraxia (the inability to perform learned movements) and agnosia (the inability to process sensory information), often accompanied with psychiatric symptoms like depression and hallucinations.

The first neuropathological changes in the brain can be detected even before the onset of the first clinical symptoms (Blennow et al., 2006). The neuropathological hallmarks of the disease are the intracellular fibrillary tangles consisting of aggregated, hyperphosphorylated Tau protein and the extracellular plagues which are mainly composed of aggregated amyloid peptide Aβ (Figure 6). According to the amyloid hypothesis, the Aβ peptide is the underlying cause for neuronal death (Hardy and Higgins, 1992). Aβ is produced by proteolytic cleavage of the amyloid precursor protein (APP) (Haass and Selkoe, 2007). APP is a transmembrane protein that is processed in either the amyloidogenic or the non-amyloidogenic pathway. In the non-amyloidogenic pathway, APP is cleaved on the luminal juxtamembrane position by the α-secretase ADAM10 into the soluble extracellular sAPPα and the C83 fragment. This cleavage occurs inside the Aβ sequence. In the amyloidogenic pathway APP is first processed by the β-secretase BACE1 into sAPPβ and the membrane bound C-terminal fragment C99. C99 is further cleaved inside its transmembrane domain by the γ-secretase complex to release the free Aβ peptide of 37 to 43 aa length and the APP intracellular domain (Kummer and Heneka, 2014) (Figure 6). Different combinations of α, β and γ-secretases and alternative cleavage sites lead to generation of many different peptides – of which the mechanism of

production and (patho-)physiological functions are still unclear (Kummer and Heneka, 2014; Saito et al., 2011). The two major forms of the amyloid peptide are the 40 aa and the 42 aa forms. Aβ42 is more hydrophobic than Aβ40, oligomerizes faster and has more severe neurotoxic effects in mice and cell culture (Snyder et al., 1994). It is the main component of the characteristic plaques in AD patients' brains. In the early-onset familial forms of AD, mutations in APP and the secretases have been correlated with an increase of the Aβ42/Aβ40 ratio or a faster Aβ42 production, suggesting a major pathogenic role of Aβ42 (Haass and Selkoe, 2007). It is however not yet clear in which form Aβ exerts its toxicity: in its soluble monomeric or oligomeric state or aggregated, fibrillar or in form of plaques.

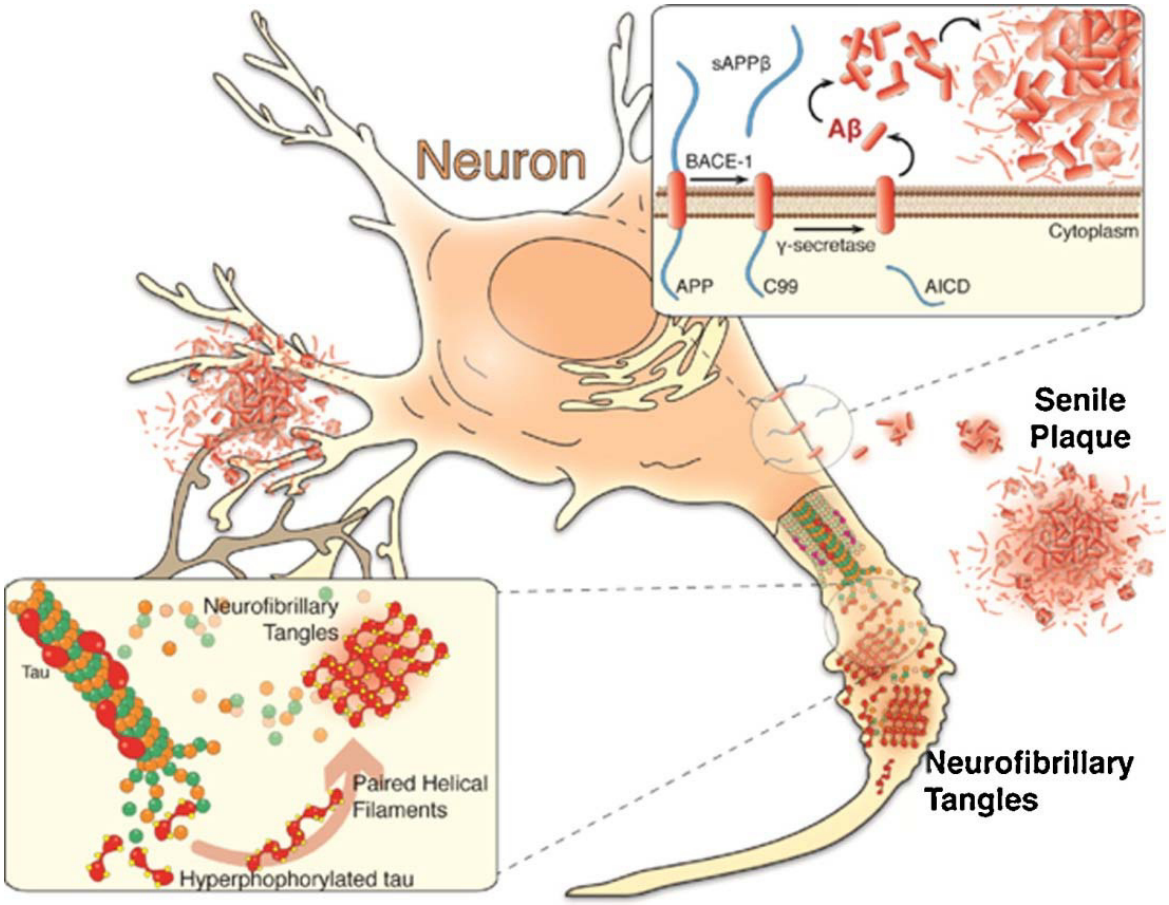

FIGURE 6: The hallmarks of AD. Intracellular neurofibrilary tangles consisting of hyperphosphorylated Tau and extracellular plaques comprising aggregated Aβ peptide. Aβ is produced in a two-step cleavage process of the transmembrane protein APP (Ríos et al., 2014)

EVIDENCE FOR THE RELATION OF ALZHEIMER'S DISEASE AND WNT SIGNALING

In the last years, AD has been related to abnormal Wnt signaling in the brain. In post-mortem patients' brains the GSK3β level was found to be increased compared to age-matched non-demented controls and the kinase seems to be more active (DaRocha-Souto et al., 2012; Hooper et al., 2008; Pei et al., 1997). Lithium chloride inhibits, amongst other targets, GSK3β (O'Brien and Klein, 2009). It has a neuroprotective effect and has therefore been tested as a drug against AD in small scale clinical trials; however with inconsistent results (Forlenza et al., 2012). In animal models and primary cell cultures it has been demonstrated mainly by lithium chloride administration that Aβ load and Aβ induced toxicity depend on GSK3β activity (De Ferrari et al., 2003; Noble et al., 2005; Phiel et al., 2003; Toledo and Inestrosa, 2010). Furthermore, lithium chloride administration ameliorated behavioral impairments and reduced tau aggregates and axonal degeneration (Noble et al., 2005; Toledo and Inestrosa, 2010).

GSK3β is the key kinase in the Wnt pathway, but it regulates a vast amount of other proteins as well. The potential implication of GSK3β in the pathomechanism of AD does not allow by itself to conclude a role of Wnt signaling in AD. But interestingly, some studies show that Wnt3a administration is neuroprotective in AD models and that this effect depends on Fz1 (Alvarez et al., 2004; Chacón et al., 2008; De Ferrari et al., 2003).

Further, the levels of total and free β-catenin are reduced in patients with a familiar form of AD where the secretase presenilin 1 is mutated (Liu et al., 2014; Zhang et al., 1998). A similar destabilization of β-catenin was observed in primary cultures that were treated with Aβ oligomers. This effect could be rescued by administration of the Wnt3a conditioned medium (Alvarez et al., 2004; Liu et al., 2014). In PC-12 cells, this rescue was transcription dependent (Chacón et al., 2008).

Additionally, a reduction of Lrp6 levels in human AD brains has been reported which correlated with the cognitive impairment of the patients (De Ferrari et al., 2007; Liu et al., 2014). Conditional knock-out of Lrp6 in the mouse brain resulted in a slightly higher level of Aβ and plaque load in an Lrp6 KO-AD mouse model. In this model, Lrp6 expression suppressed Aβ production (Liu et al., 2014). In

neuronal cell cultures β-catenin levels were reduced upon downregulation of Lrp6 (Liu et al., 2014). These results suggest a vicious circle in which the loss of Lrp6 increases the amount of amyloid peptide which in turn inhibits the Wnt pathway and further reduces Lrp6.

Last, the amount of Dickkopf (Dkk), the natural Wnt antagonist, was found to be elevated in AD brains (Caricasole et al., 2004). Its expression is induced by Aβ in hippocampal slices and primary cultures of rat cortical neurons (Caricasole et al., 2004; Purro et al., 2014). When Dkk is inhibited, the Aβ induced synaptic loss is blocked in brain slices and behavior is improved (Purro et al., 2014; Seib et al., 2013).

In addition to the aforementioned changes in the human brain and the knowledge gathered from animal models and cell culture experiments, some biochemical interactions hint at a relation of the Wnt pathway and AD: in vitro experiments have demonstrated that the Aβ peptide binds to Fz5 (Magdesian et al., 2008) and Lrp6 interacts with APP (Liu et al., 2014).

All the above described results suggest a suppression of the canonical Wnt signaling in AD. In addition, some results indicate an overactivation of the non-canonical Wnt5a pathway which might regulate neuroinflammation (Li et al., 2011).

DROSOPHILA MODELS OF ALZHEIMER'S DISEASE

Drosophila melanogaster expresses an APP-like protein (APPL) (Rosen et al., 1989). This protein differs however in the sequence from the human APP in the Aβ-cleavage region. In addition, *Drosophila* lack endogenous, functional β-secretase. Consequently, flies by themselves do not develop an AD-like disease.

Several genetic *Drosophila* AD models have been created. Generally speaking, one can mimic the disease by expressing the human proteins that are responsible for Aβ production or by directly expressing Aβ in neurons. To the end of the first method, usually human APP and the β-secretase BACE1 are expressed in the fly brain (Mhatre et al., 2014a). The human APP is first processed by

BACE1 and in a second step by the endogenous γ-secretase. Obviously, this model allows studying the effects of the different mutations in the enzymes and possible modulators of APP and BACE1 activity. The second approach is the direct neuronal expression of the human Aβ peptide, in various lengths and with or without mutations, fused to a secretion peptide like the pre-proenkephalin sequence or the signal sequence of the *Drosophila* necrotic gene to ensure the extracellular deposition of the mammalian peptide (Crowther et al., 2005; Finelli et al., 2004; Sofola et al., 2010). This model allows the direct investigation of the effect of Aβ peptide. Since the start of the expression can be regulated in *Drosophila*, it can be used to study late onset Aβ production (Sofola et al., 2010; Mhatre et al., 2014b).

Both *Drosophila* AD models induce phenotypes that resemble the human disease: a shortened life span, memory deficits, reduced locomotion, Aβ depositions and the formation of plaques in the fly brain, and neuronal loss (Finelli et al., 2004; Iijima et al., 2004; Prüßing et al., 2013). Also, vacuolization can be observed which is reminiscent of the atrophy observed in AD patients' brains (Sarantseva et al., 2009). Therefore *Drosophila* models of AD can be used to investigate in a relative simple manner the genetic background of the disease as well as screen for modifiers and drugs against AD.

SUMMARY OF THE RESULTS

ARTICLE 1: HETEROTRIMERIC GO PROTEIN LINKS WNT-FRIZZLED SIGNALING WITH ANKYRINS TO REGULATE THE NEURONAL MICROTUBULE CYTOSKELETON

MY CONTRIBUTION TO THE ARTICLE:

- *I performed and analyzed all experiments of the paper, except the experiments of the cell culture part and the biochemical characterization of the mutant Gαo[G203T]. I have also analyzed the data of the mammalian cell culture. I wrote the first version of the manuscript.*

Although the role of the Wg signal transduction in the *Drosophila* NMJ has been investigated for more than a decade, understanding of the cascade is still very incomplete. In this work, we identified the trimeric protein Gαo as a transducer of the presynaptic Wg signaling and prove the signaling cascade Wg-Fz2-Gαo by genetic interaction studies. We pinpoint the neuronal protein Ankyrin as a downstream transducer of Wg signaling, providing a second regulator of the presynaptic cytoskeleton. Moreover, we provide evidence that this pathway is conserved in mammals.

GαO LOCALIZATION IN NMJS

We first tested whether Gαo is expressed in the *Drosophila* NMJ. We found a clear immunofluorescent signal that colocalizes with presynaptic markers like Bruchpilot (Brp) and the membrane HRP-staining in the synaptic boutons and the interconnecting neurites, demonstrating the presynaptic localization of the protein. In contrast, we found only limited overlap with the postsynaptic marker CD8-GFP-Sh or discs large (Dlg) suggesting that the major localization of Gαo is presynaptic. We also analyzed the localization of the Gβ subunit and found that its distribution differs

somewhat from Gαo. In the postsynaptic cell Gβ spreads around the presynaptic boutons. This indicates that in the postsynaptic cell Gβγ functions with a different Gα subunit.

THE ROLE OF GαO IN NMJS

We next investigated the role of Gαo in the NMJ. We first measured the electrophysiological properties of NMJs with altered Gαo levels and analyzed the locomotion of the larvae. Motoneuronal-specific overexpression of the constitutively active Gαo, Gαo[Q205L], or RNAi-induced downregulation of Gαo using the driver line OK371-Gal4 changed the amplitude and area under the curve of evoked excitatory junctional potential (EJP), the area under the curve and the frequency of miniature EJPs. Also, the quantal content was decreased upon alteration of Gαo levels. Taken together these results suggest a presynaptic role of Gαo in NMJ function. Presynaptic alteration of Gαo levels also changed the locomotion of the larvae.

In order to further understand the role of Gαo in NMJs we analyzed the NMJ morphology in detail. RNAi induced downregulation of Gαo in the presynaptic cell with the motoneuronal driver lines OK371-Gal4 and D42-Gal4 resulted in the formation of aberrant NMJs. Contrary to the wild type boutons, elongated stretches were formed – an effect that was rescued upon reintroduction of Gαo but not of an unrelated protein. Gαo transheterozygous mutants that unexpectedly survived until late third instar larval stage showed similar phenotypes. Also pertussis toxin that uncouples the α-subunit of Go from the receptor and therefore serves as a specific inhibitor of Gαo, similarly altered NMJ morphology. Quantification of the number of boutons in these conditions showed a significant decrease in all cases. The observed phenotype resembles closely the previously published phenotype of wg mutants (Packard et al., 2002) and the phenotypes we observed upon downregulation of wg or fz2 with the drivers lines OK371-Gal4, D42-Gal4 and elav-Gal4, as well as in fz2 mutants. Expression of Fz2 in the presynaptic cell in the fz2 mutant background is able to rescue the fz2 mutant phenotype just like the postsynaptic rescue (Mathew et al., 2005) providing more evidence for the importance of the presynaptic Wg pathway.

We next analyzed the overexpression phenotypes of Gαo in different nucleotide states. In addition to the constitutively active mutant which we used for the electrophysiology experiment, we also analyzed the wild type form and Gαo[G203T]. Wild type Gαo predominantly binds GDP but shuttles between GDP and GTP upon activation; the Gαo[G203T] mutant has a reduced affinity for GTP but does not behave as a dominant negative. Overexpression of those different forms of Gαo increased the number of boutons which seem to be smaller that wild type. This phenotype was also observed when Wg or Fz2 were overexpressed or Sgg downregulated, but not when Fz1 was overexpressed.

GαO IN THE WG PATHWAY

The similar phenotypes of Gαo, Wg and Fz2 suggest an implication of the protein in the Wg/Fz2 pathway. We therefore performed genetic rescue experiments to unequivocally prove the participation of Gαo in the divergent Wg pathway in the NMJ. Overexpression of Gαo[Q205L] and Gαo[G203T] in RNAi-wg, RNAi-fz2 and fz2 mutant background rescued the reduced bouton number and the morphology of the NMJ in all cases, effectively suggesting that Gαo acts as a downstream transducer of Wg-Fz2 signaling.

INTERACTION OF GαO WITH ANK2

In a yeast-two-hybrid screen, performed to identify binding partners of Gαo with Gαo as bait and a *Drosophila* head cDNA library as prey, we identified the neuronal protein Ank2 as a high confidence Gαo partner. The interaction was localized between aa 47 and 123 of Ank2. Since this protein is implicated in the NMJ structure, we investigated whether it is a downstream effector of Gαo in the NMJ. We first confirmed the binding in a biochemical pulldown experiment and found that a MBP-tagged construction of the first 2 anykrin domains efficiently bound monomeric Gαo regardless of its nucleotide state, however not the heterotrimeric (αβγ) Go protein. Therefore, Ank2 behaves as a true effector of Gαo in the cell.

We further confirmed this in *Drosophila* by genetic interactions. Downregulation or mutation of ank2 also decreased the bouton number and resulted in an aberrant NMJ morphology similar to that

observed in loss of Gαo, Wg or Fz2. Overexpression of Gαo or downregulation of Sgg failed to restore the NMJ phenotypes of ank2 mutants as it was expected from a downstream effector. One might argue that Ank2 could also just localize Gαo to the plasma membrane. The localization of Gαo was however unaffected in ank2 mutants. In addition, overexpression of Wg or Fz2 could not rescue the phenotypes introduced by RNAi-ank2 and Fz2 localization was not changed in RNAi-ank2. It has previously been demonstrated that loss of ank2 induces synaptic retraction (Pielage et al., 2008). We recapitulated those findings and could demonstrate that expression of Gαo[G205L] could not restore that effect. We next analyzed the localization of Ank2 in RNAi-Gαo and Gαo mutants and found Ank2 retraction in a subset of boutons. In contrast we found a large number of ghost boutons – presynaptic protrusions that lack the postsynaptic marker - in NMJ overexpressing Gαo in an ank2 mutant background. Taken together those results suggest that Ank2 indeed functions downstream of the Wg/Fz2/Gαo signaling cascade in the NMJ.

CONSERVATION OF THE INTERACTION IN MAMMALS

We completed our findings of the Gαo-Ank2 interaction in the nervous system by analyzing these proteins in a mammalian system, the mouse N2A cell culture. Expression of Gαo in N2A cells induced neurite outgrowth in around 60 % of the cells. In this neurite outgrowth system, we downregulated the two anykrins (AnkB and AnkG) which are expressed in this cell type either individually or simultaneously and assessed the ability of the cells to grow neurites. Both the number of cells that produced neurites as well as the number of neurites per differentiating cell were significantly reduced in the single knock-down and even further reduced upon double knock-down. The most remarkable effect was however the cell morphology. While Gαo expression usually induces the cells to form neurites in a radial manner, downregulation of AnkB or AnkG induced a fibroblast-like, bilateral neurite outgrowth. Upon downregulation of both AnkB and AnkG the cell changed from the microtubule based neurite outgrowth to an actin based mechanism of lammelipodia formation. This effect was specific for Gαo induced neurite outgrowth as MARK2 induced neurite outgrowth was not affected by Ank reductions.

Since Ankyrins bind to microtubule, we tested whether inhibition of microtubule polymerization by nocodazole had an effect on neurite outgrowth – and indeed, we observed similar phenotypes to downregulation of Ankyrin in a dose dependent manner. Overexpression of Ankyrins in N2A cells expressing Gαo increased the length of the neurites but did not affect their number, indicating again that Gαo and Ankyrins interact in neurite formation. Interestingly, AnkB accumulated in neurite tips in the Gαo-induced neurite outgrowth system. Taken together these results demonstrate the conservation of the novel Gαo-Ankyrin interaction in the nervous system across animal taxa.

UNPUBLISHED RESULTS

FUTSCH GENETICALLY INTERACTS WITH WG-FZ2- GαO

Futsch, the *Drosophila* homolog of the mammalian MAP1B, can influence the microtubule stability and dynamics depending on its phosphorylation state (Roos et al., 2000). Loss-of-function *futsch* mutants have a reduced number of boutons and an altered NMJ phenotype compared to the wild-type (Gögel et al., 2006; Roos et al., 2000). Since Futsch can be phosphorylated by Sgg, it has been proposed that the Wg pathway might act through this microtubule-binding protein (Gögel et al., 2006; Hummel et al., 2000; Roos et al., 2000). Furthermore, *futsch* mutants suppressed formation of ectopic boutons induced by Wg overexpression or dominant-negative Sgg (Franco et al., 2004; Miech et al., 2008). Futsch has been found to aberrantly accumulate in *ank2L* mutants (Pielage et al., 2008).

To further address the role of Futsch, we analyzed the morphology of NMJ overexpressing Futsch in the presynaptic cell. In 50% of the analyzed NMJ we detected an aberrant phenotype represented by large structures composed of ‘entangled’ boutons. These boutons were attached to one another instead of being aligned and separated by neurites (Figure 7A). Quantification showed that Futsch overexpression significantly increased the bouton number compared to the wild-type larvae (Figure 7B).

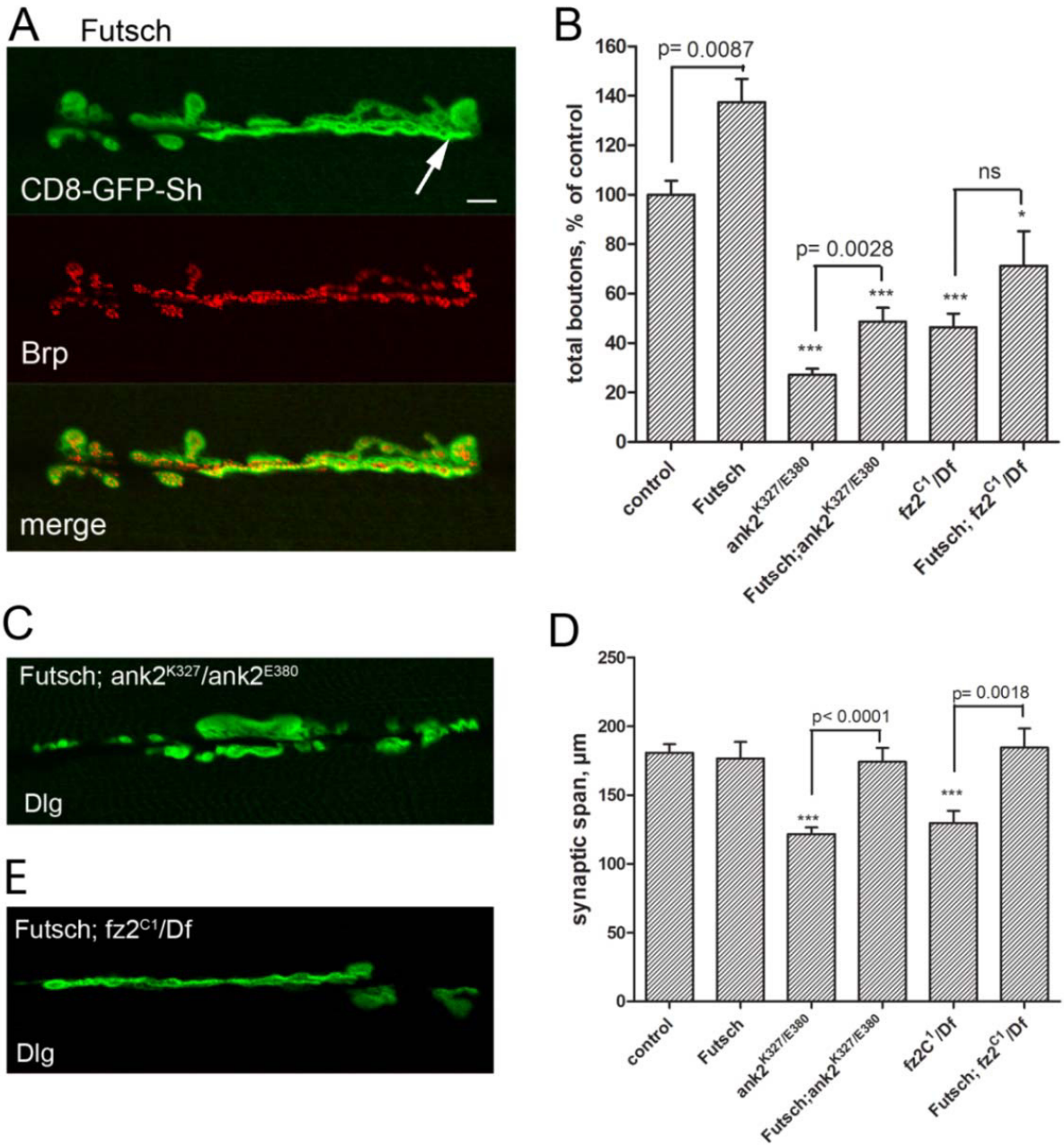

FIGURE 7: Futsch genetically interacts with Ank2. (A) Overexpression of Futsch in the presynaptic cell results in increased formation of boutons which in part lack the separation by neurites (arrow). The circular boutons formed by the postsynaptic density (CD8-GFP-Sh, green) often attach to one another. The presynaptic cell marked by immunostaining with antibodies against Brp (red) forms normal synapses opposite the subsynaptic reticulum. Futsch interacts with Ank2. (B) Quantification of the bouton number in different genotypes, depicted as mean±SEM, ***: $p<0.001$ compared to control. (C) However, Futsch overexpression fails to rescue ank2 genetic mutant NMJ morphology. (D) The synaptic span of different genotypes is increased by Futsch. (E) Futsch fails to rescue fz2 genetic mutant.

We used this dominant phenotype to perform epistasis experiments between Futsch and Ank2. In the ank2 null background, overexpression of Futsch failed to induce the dominant Futsch phenotype (entangled boutons). However, Futsch overexpression slightly rescued the bouton number defects of the ank2 mutant, but the resultant bouton number was still significantly reduced by more than 50% compared to the control (Figure 7B,C). However, the synaptic span is significantly shorter in ank2 mutants and this decrease is rescued by Futsch overexpression (Figure 7D). The reduced bouton density in ank2 mutants is thus not rescued by Futsch overexpression (not shown). These findings indicate a parallelism of two branches of the signaling pathway in the synapse which cooperatively regulate NMJ formation.

However, the conclusion about the epistatic relationship between Futsch and Ank2 is complicated by our subsequent observation: overexpression of Futsch in the null fz2 background also failed to produce the dominant Futsch phenotypes or rescue fz2 defects (Figure 7B, E). Formally, this observation suggests that Fz2 is epistatic to Futsch in bouton formation, and contradicts the previous findings where the inability of overexpressed Wg or dominant negative Sgg to rescue futsch loss-of-function NMJ phenotypes was taken as a proof of Futsch being a downstream component of the Wg pathway (Franco et al., 2004; Miech et al., 2008). However, it can be hypothesized that in the absence of the active Wg-Fz2 signaling, Sgg remains active to phosphorylate and inhibit Futsch even despite overproduction of the latter. In contrast to the bouton number, the NMJ length which is significantly reduced in fz2 mutants, is rescued upon Futsch overexpression (Figure 7D). Futsch therefore seems to be functional and downstream of Fz2 in NMJ formation.

Although the exact epistasis relationships among Futsch, Ank2, and components of the Wg pathway are refractory to unequivocal determination, we further provide evidence for strong genetic interactions among these proteins. Indeed, overexpression of Futsch in the backgrounds of RNAi-driven downregulation of wg, fz2, Gαo and ank2 was able to fully rescue the RNAi phenotypes and produce the dominant Futsch-overexpression entangled boutons (Figure 8A-E). For example, in the majority of the NMJs co-expressing Futsch and RNAi-Gαo the RNAi phenotype was rescued to the

wild-type morphology (Figure 8A), and 30% of the NMJs displayed the Futsch overexpression-like phenotype with the entangled boutons (see Figure 7A); the bouton number in the rescue experiment was significantly increased as compared to the RNAi-Gαo NMJ (Figure 8E). Futsch similarly rescues the RNAi-wg and RNAi-fz2 phenotypes both morphologically and quantitatively (Figure 8B, C, E). Finally, coexpression of RNAi-ank2L and Futsch resulted in complete rescue of the *RNAi-ank2L* phenotype in 44% of the NMJ; additionally, one third of the NMJs showed the Futsch overexpression-like morphology (Figure 8D). Quantification also proved the rescue in bouton numbers (Figure 8E).

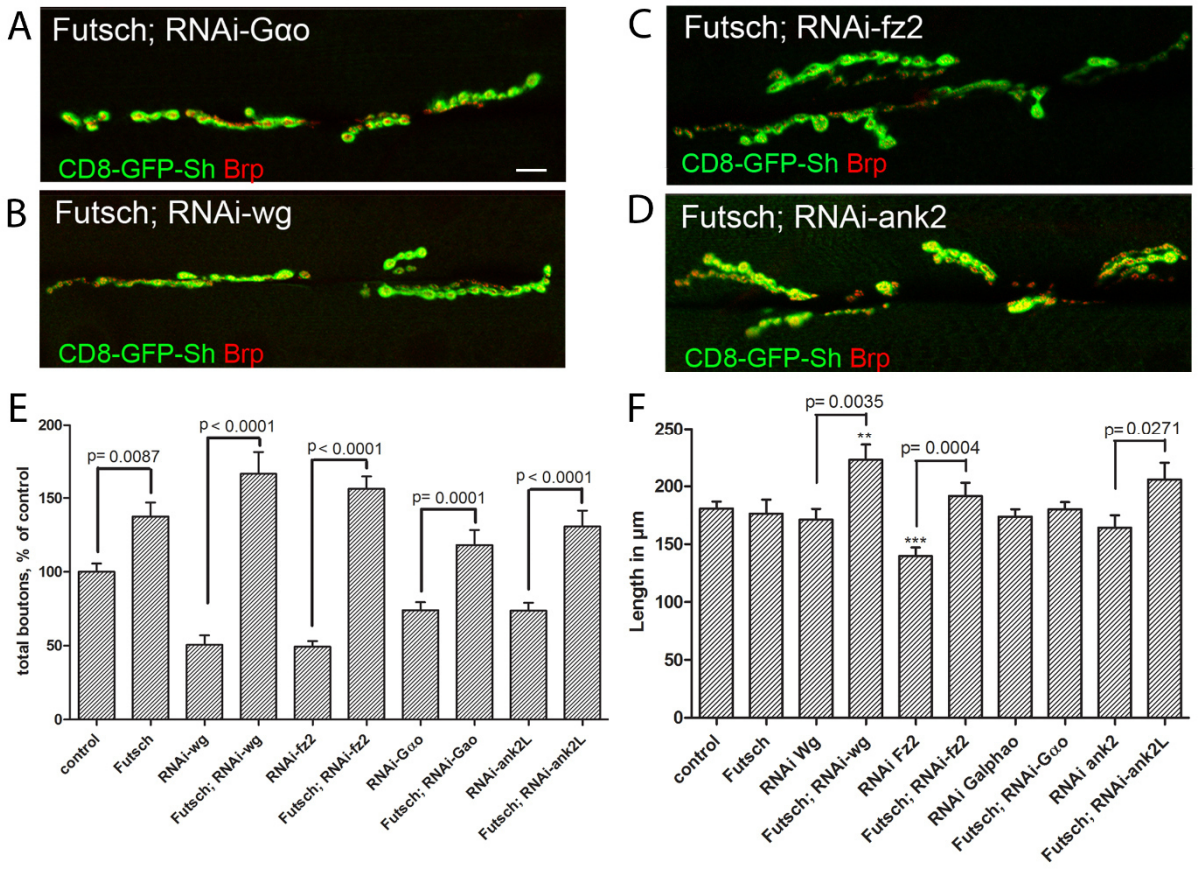

FIGURE 8: Futsch genetically interacts with the Wg-Go pathway. (A-D) Futsch overexpression rescues the phenotypes of *RNAi-Gαo* (A), *RNAi-wg* (B), *RNAi-fz2* (C) and *RNAi-ank2L* (D). (E) Quantification of the bouton number in different genotypes, in mean ±SEM. (F) Quantification of the NMJ length in mean ±SEM, **: p<0.01; ***: p<0.001 compared to control.

Interestingly, Futsch overexpression increased the NMJ length in an RNAi-wg, RNAi-fz2 or RNAi-ankL background compared to the respective RNAi lines (Figure 8F) further proving that Futsch is downstream of Wg-Fz2-Ank2L. However, the NMJ length in Futsch;RNAi-Gαo larvae stayed constant. Possibly the Futsch induced outgrowth depends on direct interaction of Futsch and Gαo, which remains to be investigated.

In conclusion, Futsch emerges as an important player in the Wg-Fz2-Gαo-Sgg signaling pathway in the NMJ. It also genetically interacts with Ank2 in NMJ formation and coordinates with Ank2 the microtubule rearrangements required for NMJ growth and remodeling.

ARTICLE 2: LACK OF EVIDENCE OF THE INTERACTION OF THE AB PEPTIDE WITH THE WNT SIGNALING CASCADE IN DROSOPHILA MODELS OF ALZHEIMER'S DISEASE

MY CONTRIBUTION TO THE ARTICLE:

- *I have designed, performed and analyzed the experiments and wrote the manuscript.*

The link between the Wnt pathway and AD has been studied in rodent experiments and cell culture assays using mostly indirect, pharmacological approaches. In this work, we used the genetic model *Drosophila* to investigate in detail this interaction.

In order to study the effect of the human Aβ peptide on the *Drosophila* nervous system we used the previously established read-out for AD in *Drosophila*, the life span. In concordance with previous reports, we demonstrated that expression of human Aβ42 in the *Drosophila* nervous system using the pan-neuronal driver line elav-Gal4 drastically shortens the median life span of the flies from 30 to 10 days. Similarly, the life span was reduced by 62% when Aβ42 was expressed exclusively in the motoneurons using the driver line D42-Gal4. To increase the amount of Aβ42 expressed in the cells, we introduced a second driver line, OK371-Gal4, which also drives expression in the motoneurons, in addition to D42-Gal4. Higher expression levels further decreased the survival, demonstrating that the effect is dose-dependent. These results suggest that the effect of human Aβ42 on the flies' survival is mainly through the glutamatergic neurons.

We further aimed at investigating in detail the toxicity of Aβ42 using the larval NMJ as model which in general allows to investigate the function of proteins in a glutamatergic synapse on a single cell-to-cell contact level. Previous studies have reported slight changes in NMJ morphology and bouton number upon introduction of the Aβ42 peptide or APP and BACE, which lead to Aβ production

(Folwell et al., 2010; Mhatre et al., 2014a). In contrast, we discovered that neuronal expression of a secreted Aβ42 does not change the NMJ morphology, regardless of which driver line was used. Therefore, this otherwise very useful larval synapse seems to be inappropriate to study the Aβ toxicity in *Drosophila*.

Due to the impossibility to study the Aβ toxicity in detail in the NMJ, we went back to the adult organisms' life span as a read-out to investigate the potential interaction of Aβ42 with the Wg-Fz2 pathway. We co-expressed the peptide with the receptor Fz2 or with RNAi-Sgg, to overactivate the cascade with both the pan-neuronal elav-Gal4 and the motoneuron driver D42-Gal4. We also tried to co-express the constitutively active form Gαo[Q205L] with Aβ42, but this combination was lethal. D42-driven expression slightly rescued the survival. This was however due to a titration effect since expression of the unrelated construct UAS-myr-mRFP similarly improved survival. Elav-Gal4 driven expression did not affect the median life span, although the maximal life span increased upon overexpression of Fz2.

The finding that overactivation of the Wg cascade does not rescue the observed phenotype is corroborated by our finding in the *Drosophila* eye. The *Drosophila* eye is composed of about 800 ommatidia which are normally distributed in an ordered manner and form a neat array. Small changes in ommatidia structure, e.g. evoked by changes in levels important for eye formation, manifest themselves in an easily visible alteration in the lattice. Defective ommatidial arrangement is collectively called eye roughness. Expression of human Aβ42 with the driver GMR-Gal4 leads to a rough eye phenotype in the compound eye (Sanokawa-Akakura et al., 2010). Co-expression of RNAi-sgg or Gαo[Q205L] does not rescue this phenotype. These results confirm in a second setting that genetic activation of the Wg pathway does not rescue the Aβ toxicity.

Cumulatively, those results indicate that even though pharmacological inhibition of GSK3β in rodents ameliorated Aβ induced phenotypes, genetic activation of the Wg pathway (in the *Drosophila* system) has no beneficial effect.

DISCUSSION

The present thesis work presents a novel, alternative branch of the presynaptic divergent Wg signal transduction pathway and demonstrates that the Wg pathway seems not to capable of blocking Aβ42 induced neurotoxicity in a *Drosophila* model of AD.

In the first study, we investigated the presynaptic Wg pathway in the *Drosophila* NMJ as a model for glutamatergic synapses. We uncover the role of the trimeric G-protein Go in the NMJ and unequivocally prove its participation in the presynaptic Wg signal transduction pathway downstream of Wg and Fz2. We furthermore demonstrate that Gαo physically and genetically interacts with the neuronal protein Ank2 and that this interaction is conserved from flies to mammals. In addition, the microtubule binding protein Futsch genetically interacts with the Wg pathway. Taken together our results establish the Gαo-Ank2 interaction as a second branch of the Wg pathway in parallel to the Futsch dependent branch to reorganize the cytoskeleton in synapses.

Gαo is highly expressed in the mammalian and *Drosophila* brain, accounting to up to 1.5% of the total membrane protein fraction (Sternweis and Robishaw, 1984; Wolfgang et al., 1990). In the NMJ, Gαo is expressed in the motoneuron which we demonstrate by immunohistochemistry and confocal microscopy. A large body of evidence demonstrates that presynaptic Gαo is fundamental for proper NMJ formation and function. Altering expression levels or activity of Gαo in the presynaptic cell results in strong neurophysiological and morphological defects: Gαo mutation, presynaptic downregulation or expression of pertussis toxin, that specifically uncouples Go from its receptor, induce bouton loss and changes in NMJ morphology. Presynaptic overexpression has the opposite effect. In addition, presynaptic expression of Gαo in the Gαo mutant or RNAi-Gαo background rescues the NMJ defects, unequivocally identifying presynaptic Go as indispensable for NMJ formation. Also the physiological properties, like the amplitude of evoked potentials, the frequency of spontaneous potentials and the quantal content – a measure for synaptic efficacy - depend on adjusted

Gαo levels in the fly NMJ, as found for electrophysiological properties of mammalian synapses (Goh and Pennefather, 1989; Tang and Lovinger, 2000)

In contrast to the α-subunit, the βγ-complex is not only expressed presynaptically but localizes also postsynaptically around the synaptic boutons. This postsynaptic expression in the absence of a Gαo signal suggests that βγ couples to another α subunit in the postsynaptic cell like in other systems (Egger-Adam and Katanaev, 2008; von Maltzahn et al., 2012; Nichols et al., 2013).

The phenotypes that Gαo mutation and presynaptic Gαo downregulation induce in the NMJ are reminiscent of the ones elicited by mutation or downregulation Wg or Fz2. The same holds true for overexpression of Gαo which causes an increase of bouton formation that resembles Wg or Fz2 overexpression or downregulation of Sgg. These results indicate a common signal transduction pathway of these proteins. The existence of a presynaptic Wg pathway was already established several years ago (Miech et al., 2008; Packard et al., 2002). The participation of the proteins Wg, Fz2, Arr, Dsh and Sgg has been inferred from similar mutant phenotpyes (Miech et al., 2008). Our comprehensive study provides mechanistic insights in the signaling transduction cascade demonstrating unequivocally that the novel player Gαo signals, like Sgg, downstream from Wg and Fz2. Although Gαo has been established as an immediate transducer of the Wg signal in other contexts, its role in the divergent presynaptic Wg pathway has never been investigated. Here, we demonstrate that interestingly Gαo exhibits a positive function in NMJ formation in both nucleotide states: Gαo[G203T] or Gαo[Q205L] induce the formation of many very compact boutons. Additionally, these two forms rescue Wg or Fz2 knockdown or mutation defects. The mutant Gαo[G203T] exists largely in its GDP bound state due to its reduced affinity for GTP. The mutant is however still able to bind GTP, as is the mutant Gαi[G203T] which only partially inhibited the functions of Gαi (Inoue et al., 1995; Winitz et al., 1994). The mutant therefore acts as dominant-negative in an effector specific way. In the case of the NMJ, Gαo[G203T] thus partially exists in its free GDP bound state able to exert downstream functions. Sufficient free GDP bound Gα-subunit has been predicted to exist in the cell (Katanaev and Chornomorets, 2007). In other contexts both

GαoGDP and GαoGTP also elicit downstream signals, demonstrating the active role of GαoGDP in the signal transduction (Egger-Adam and Katanaev, 2010; Kopein and Katanaev, 2009; Lin et al., 2014; Purvanov et al., 2010).

Several proteins of the canonical Wg pathway (Wg, Arr, Dsh, Sgg) are not only expressed in the presynaptic cell but are also evenly distributed in the muscle. However, the muscle nuclei (but not the cytoplasm) are devoid of β-catenin (Miech et al., 2008). Interestingly, postsynaptic Fz2 is cleaved and transported into the nucleus in the Fz2 nuclear import pathway (Mathew et al., 2005). The mechanism of this postsynaptic pathway has been investigated in more details during the last years; but the final outcome of the signal remains still unclear (Ataman et al., 2006; Mathew et al., 2005; Mosca and Schwarz, 2010; Speese et al., 2012). Fz2 mutation phenotypes in the NMJ can be rescued by postsynaptic Fz2 expression (Mathew et al., 2005 and our results). This finding leads to the hypothesis, that postsynaptic Wg signaling might be a major contributor to NMJ development (Budnik and Salinas, 2011). However, we unambiguously prove that the presynaptic Wg pathway is crucial for accurate NMJ formation: Presynaptic downregulation of Fz2 (as well as Wg and Gαo) induces bouton loss and morphological NMJ changes similar to those of fz2 mutants. Contrary, presynaptic overactivation of the Wg pathway enhances bouton formation. Moreover, presynaptic Fz2 overexpression is just as well capable of rescuing fz2 mutant phenotypes as is the postsynaptic Fz2 expression. Neuronal Fz2 therefore proves to be indispensable for correct NMJ formation. The pre- and postsynaptic pathway may have however redundant mechanism to control bouton formation. Endogenous levels of postsynaptic Fz2 are not sufficient to rescue the phenotypes of presynaptic RNAi-fz2; overexpression of the receptor on the other hand rescues the mutant phenotypes. Potentially, the overactivated pathway might induce the activation of a secondary mechanism such as the inhibition of lamininA that leads to restoration of bouton morphology (Tsai et al., 2012). Of note, mutations of the Fz2 coreceptor arrow induce a similar phenotype as wg or fz2 mutants. This phenotype is also rescued both by pre- and postsynaptic reintroduction of the protein (Miech et al., 2008). Taken together this indicates that the pre- and postsynaptic Wg/Fz2 pathway function together in NMJ development.

We identify the neuronal protein Ank2 as a target of Gαo in the presynaptic Wg pathway. Gαo physically binds to Ank2 in the first Ankyrin domain. We demonstrate that the monomeric Gαo subunit but not the trimeric G-protein binds to Ank2; and that this interaction occurs irrespective of the nucleotide state of Gαo. Therefore Ank2 acts as a real target of Gαo in the NMJ, and this is independent of the nucleotide state of Gαo.

Ank2 forms a lattice-like structure in synaptic boutons and participates in NMJ formation and stability (Koch et al., 2008; Pielage et al., 2008). Mutation of the protein cause severe morphological bouton defects, Futsch accumulation, presynaptic retractions and reduction of the bouton number and the synaptic span (Koch et al., 2008; Pielage et al., 2008). Presynaptic downregulation of Ank2 reduces the bouton number and changes the NMJ morphology similar to RNAi-Gαo, RNAi-fz2 and RNAi-wg. Our epistatic experiments furthermore place Ank2 downstream of Wg, Fz2 and Gαo, demonstrating that Ank2 acts as a transducer of the Wg signaling in the bouton formation and synaptic retractions. So far Ank2 was considered to be a static player in the NMJ formation and bouton stability (Koch et al., 2008; Pielage et al., 2008). Here, we provide evidence for a direct regulatory mechanism of this protein via the Wg signal transduction pathway by physical interaction with Gαo. This interaction might be crucial for the function of Ank2. Previously it has been demonstrated that the C-terminal domain of Ank2L binds to microtubule (Pielage et al., 2008). However, the microtubule binding domain of Ank2 was not sufficient to rescue the presynaptic defects (Pielage et al., 2008). This indicates that additional domains and interactions of the protein are required for NMJ formation – for example the first Ankyrin domain that binds Gαo; while phosphorylation of Ank2 by CK2A might be required for NMJ stability (Bulat et al., 2014).

Ghost boutons are small protrusions of the neuron that lack the postsynaptic SSR. Upon time, they might evolve into mature boutons. While overexpression of Gαo[Q205L] in ank2 mutants did not rescue the bouton density or synaptic retractions indicating that ank2 is downstream of Gαo in bouton formation and stability, it strongly induced the formation of ghost boutons. The excessive ghost bouton formation might indicate that Gαo initiates bouton outgrowth while Ank2 supports the bouton

maturation and stability. This idea is supported by the NMJ span data. Ank2 mutant larvae have a reduced NMJ length compared to control. The NMJ length reduction is rescued by RNAi-sgg and Gowt overexpression – contrary to the bouton formation. This indicates that the NMJ length is regulated by a Gαo and Sgg dependent pathway, independent of Ank2.

It is tempting to speculate that the Wg pathway regulates the NMJ outgrowth via the Futsch dependent branch of the Wg pathway. Indeed, we have observed that the reduced length of the ank2 mutant NMJ is rescued by overexpression of Futsch. Previously, it has been proposed that phosphorylation of Futsch by Sgg downstream of Wg might cause the final microtubule rearrangement in the synapse (Ciani et al., 2004; Franco et al., 2004; Gögel et al., 2006; Hummel et al., 2000; Miech et al., 2008; Roos et al., 2000). In addition, Futsch localization is abnormal in ank2 mutants (Pielage et al., 2008). Overexpression of Futsch increases the bouton number and leads to formation of entangled boutons. Futsch overexpression in ank2 mutants does however not rescue the morphological defects of the boutons and only marginally rescues the bouton number. These results indicate that the NMJ formation might be regulated by two branches of the Wg pathway: the Sgg-Futsch dependent branch and the Gαo-Ank2 branch.

Interestingly, our experiments furthermore place Ank2 downstream from Sgg - a kinase component of the Axin-based complex of proteins playing the negative role in Wg signaling. This indicates a link between the two branches. Furthermore, high expression levels of the C-terminal domain of Ank2L in the presynapse induced satellite bouton formation (Pielage et al., 2008), pointing out that the two branches are not exclusive but interactive. At present we propose that the microtubule-binding protein Futsch may be a linker between Sgg and Ank2.

The mechanism of the interplay of Sgg, Ank2 and Futsch needs some further refinement. It remains to be investigated whether Sgg directly phosphorylates Ank2 and whether Ank2 physically interacts with Futsch and/or Sgg. Since Ank2 is a giant protein, until now flies overexpressing the whole protein are not available. Those flies would however allow performing additional epistasis experiment to illuminate the relation between the mentioned proteins and the cytoskeleton.

Taken together, the Fz2-Go-Sgg-Futsch branch might regulate NMJ outgrowth and induce bouton formation and is linked via Futsch and possibly Sgg to the novel second branch, the Wg-Fz-Go-Ank2 cascade, which is required for maturation of the boutons and synaptic stability. Jointly, these two branches regulate the microtubule cytoskeleton required for NMJ formation and remodeling (Figure 9).

We furthermore demonstrate that the Gαo-Ankyrin interaction is conserved in mammals. In mammalian neuroblastoma cells, Gαo induced neurite outgrowth depends on the mammalian AnkB and AnkG. Moreover, as in *Drosophila*, the microtubule cytoskeleton seems to be regulated by these interactions. Our results therefore provide insights in a general mechanism for synapse formation and regulation which is potentially implicated in development, memory formation and neurodegenerative diseases.

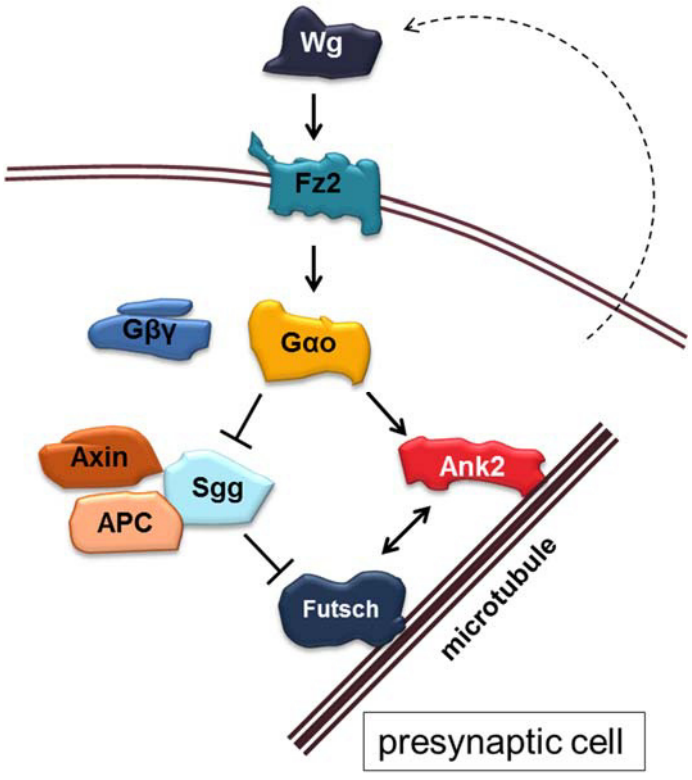

FIGURE 9: Model of microtubule cytoskeleton regulation during NMJ formation. The heterotrimeric Go protein is a direct transducer of the Wg/Fz2 signal. Upon activation of Go and dissociation into α and βγ-subunit the Sgg-containing destruction complex which inhibits phosphorylation of Futsch. In parallel, Gαo binds to Ank2, also a microtubule binding protein. This combined action coordinately regulates the microtubule cytoskeleton, as required for synaptic remodeling.

The second study aimed at investigating the interplay between the neuronal Wg signaling cascade and AD in *Drosophila*. During the last decade, a body of evidence suggests the implication of the Wnt pathway in AD. Mainly the group of N. Inestrosa has demonstrated in animal models, primary cell culture and cell lines that Aβ induced toxicity can be attenuated by administration of lithium chloride or Wnt3a (Alvarez et al., 2004; Chacón et al., 2008). The effect of Wnt3a is conveyed by Fz1 and could be inhibited by sFRP (Chacón et al., 2008) Those results provide evidence for an inactivation or attenuation of the Wnt signaling cascade in the disease and laid the ground for the hypothesis that the Wnt signaling cascade may serve as a drug target against AD (Inestrosa et al., 2012). However, most of the experiments investigating the relation of Wnt signaling and Aβ toxicity rely on pharmacological inhibition of the Wnt signaling cascade. This only provides indirect evidence for the interaction. We therefore studied the AD-Wnt interaction in a genetic model – the fruit fly.

We benefitted from the previously established *Drosophila* AD model that contains a secretion sequence–tagged Aβ42 peptide (Sanokawa-Akakura et al., 2010) and expressed this pan-neuronally or specifically in glutamatergic neurons. As expected, expression of Aβ42 significantly shortened the life span of the flies. This is reminiscent of the decreased life expectancy of AD patients (Zanetti et al., 2009). Furthermore, we show that the decreased survival in flies is caused by Aβ expression in glutamatergic synapses. In AD patients' brains, the first changes are seen in the entorhinal cortex, followed by the hippocampus; in both structures glutamate is the major neurotransmitter. Decrease of presynaptic glutamatergic boutons density correlates with progression of the dementia (Bell et al., 2007). In humans, the glutamatergic system is directly linked to AD in various ways; amongst others, it is suggested that Aβ induces cell death via glutamate-mediated excitotoxicity, dysregulation of NMDAR activity and oxidative stress (Francis, 2003; Miguel-Hidalgo et al., 2002; reviewed in Revett et al., 2013) . The importance of the glutamatergic system for Aβ induced neurotoxicity can therefore be confirmed in the *Drosophila* AD model.

We sought to explore the molecular details of the Aβ toxicity in the glutamatergic synapses and its interaction with Wg in the NMJ. To this end, we expressed Aβ42 pan-neuronally or in the

motoneurons and studied the morphology of the NMJ. In general, NMJs are an easy-to-use model and widely accepted to study the role and function of proteins and pathways in glutamatergic synapses. In the case of AD, investigating NMJ defects could shed light on the molecular mechanism of Aβ42 toxicity that ultimately results in premature cell death. Surprisingly, in our experiments Aβ did not induce any morphological change regardless of which driver line was used. This is reflected by a stable bouton number compared to control. The *Drosophila* larval NMJ therefore does not seem to be an appropriate model synapse to study AD.

There are several hypothetical explanations for this outcome. First, potentially only high levels of Aβ42, for example in highly concentrated soluble or in the aggregated form, induce morphological changes and ultimately cell death. The short larval life span might however impede the accumulation of enough Aβ peptide to affect the synapse. Alternatively, chronic exposure of the synapse to the Aβ peptide might induce some changes which would lead to neuronal death – these changes might however be slow and subtle in the beginning, and consequently no effect can be observed in the larval NMJ. Similarly, in mouse hippocampal primary cultures Aβ effects the postsynaptic density, i.e. it decreases PSD95 (the homolog of Dlg) and GluR1 levels in a time-dependent manner only after 12 to 19 days in vitro (Almeida et al., 2005). Adult AD flies show an age-dependent reduction in locomotion (Iijima et al., 2004). The movement capability of adult flies worsens progressively with the amount of secreted Aβ (Iijima et al., 2004). Possibly, structural differences become apparent in the adult NMJ during aging of the fly. Although the adult NMJ is not very well established as model synapse, it might be interesting to investigate the impact of Aβ in this structure.

It has been reported previously that expression of human APP and BACE or Aβ42 slightly alters the synaptic bouton morphology and decreases the total bouton number by approximately 20 % (Folwell et al., 2010; Mhatre et al., 2014a). In our study, we used a different Aβ peptide that is coupled to the pro-preenkephalin secretion sequence (Iijima et al., 2004). Since the construct we used did not alter the NMJ morphology, it might be hypothesized that the constructs with different secretion sequences are processed differently. It has been suggested that cleavage of APP can occur in the ER and that Aβ

damages the cells by inducing ER stress (Fonseca et al., 2013; Wild-Bode et al., 1997). One explanation of the phenotypes might therefore be that the NMJ alterations shown in the other studies arise from an intracellular effect. Alternatively, the aggregation state of the peptides might differ. Different forms of Aβ are not equally prone to aggregation; e.g. Aβ42 with the arctic mutation forms more oligomers and deposits than wild type Aβ42 (Iijima et al., 2008). Moreover, these different aggregations induce different phenotypes (Iijima et al., 2008). Potentially the way of Aβ production could influences the aggregation state. Since we used three different driver lines, and no line showed a NMJ phenotype, we can rule out an effect of expression efficiency of the peptide as well as the time of the induction of the expression which differs between driver lines.

Activation of the Wnt pathway is believed to rescue Aβ induced neurotoxicity. We aimed at studying this Wnt-Aβ interaction in the genetic model *Drosophila*. Due to the impossibility to study the interaction on the synapse level in the NMJ, we used the flies' life span and the eye as two independent read-outs. While expression of Aβ induced as expected premature death and the rough-eye phenotype, expression of Fz2, RNAi-Sgg or GαoGTP which overactivate the Wg pathway did not have any effect on the life span or the eye roughness; suggesting that contrary to previous studies, activation of the Wg cascade does not rescue the neurotoxic effects of Aβ42.

A previous work in a different AD model in *Drosophila*, using the arctic mutation of the Aβ42 peptide (Aβ42arc), reported an interaction of Sgg and Aβ toxicity (Sofola et al., 2010). Aβ42arc was found in a family with early onset AD (Nilsberth et al., 2001). In *Drosophila*, expression of Aβ42arc leads to locomotor defects and reduced survival similar to the wild-type Aβ42 (Sofola et al., 2010). Aβ42arc is very prone to oligomerization and aggregation and was found in a fibrillar form when the first signs of locomotion defects became apparent in the Aβ42arc flies (Iijima et al., 2008; Sofola et al., 2010). Phosphorylation of Sgg at Ser9 suppresses its kinase activity. The level of Ser9 phosphorylation of Sgg was slightly reduced by expression of arcAβ42; feeding the flies with lithium chloride in contrast significantly increased the phosphorylation (Sofola et al., 2010). Moreover, the kinase inactive Sgg mutant SggS9E or treatment with lithium partially rescued the shortened life span and locomotor

deficits of Aβ42arc flies, potentially due to a decreased Aβ42 concentration which results from the reduced overall protein synthesis in lithium treated flies (Sofola et al., 2010; Sofola-Adesakin et al., 2014). In contrast, wild-type Aβ42 did not alter Sgg phosphorylation in tau expressing flies and addition of lithium chloride had no effect (Folwell et al., 2010). The differences might be explained by the arctic mutation in contrast to the wild-type peptide. In mice Aβ42arc accumulates intracellularly (Lord et al., 2006; Sahlin et al., 2007), suggesting that at least in parts, it exerts its toxicity via a divergent pathogenic mechanism, potentially directly influencing the phosphorylation of Sgg.

In the studies described, the life span of the flies was ameliorated by lithium (Folwell et al., 2010). Lithium is however a very unspecific inhibitor of Sgg, targeting also many other proteins (O'Brien and Klein, 2009). Our results show that RNAi-sgg or UAS-Fz2 did not rescue the life span. Taken together, these data suggest that the effect of lithium on the wild-type Aβ toxicity is independent of the Fz2-Sgg pathway in *Drosophila*.

In the mammalian and cell culture systems, the activation of the Wnt pathway has also been mainly achieved pharmacologically with lithium chloride. Few experiments with cultured cell demonstrate a direct implication of Wnt in Aβ induced neurotoxicity. In the mainly dopaminergic PC12 cell culture, it was demonstrated that Wnt3a overexpression decreases Aβ induced cell death by 20% (Chacón et al., 2008). Additionally, exposure of hippocampal neurons to Wnt3a conditioned medium seemed to protect the cells from Aβ induced apoptosis in a Fz1 and transcription dependent mechanism (Alvarez et al., 2004; Chacón et al., 2008). Aβ was found to reduce β-catenin levels in these systems, and Wnt3a protected the cytoplasmic β-catenin level from the reduction (Alvarez et al., 2004; Liu et al., 2014). Lithium showed a stronger β-catenin stabilizing effect than Wnt3a (Alvarez et al., 2004). The direct proof of the interrelation of Wnt signaling and Aβ is until now not very solid. Moreover, the lack of connection in our fly model questions the cell culture systems results. Altogether, the contradictory results suggest that caution should be taken when interpreting data on Aβ -Wnt interaction in AD.

In conclusion, the present thesis identifies the trimeric G-protein Go as a crucial player of the synaptic divergent Wg pathway in NMJ formation. Gαo interacts with the neuronal protein Ank2 to regulate the microtubule cytoskeleton downstream of Wg and the receptor Fz2 in a novel branch of the signaling cascade. Moreover, the Gαo-Ank2 interaction is conserved in mammals, indicating that the Wg-Fz2-Gαo-Ank2 pathway is universal for synapse formation and stability. Furthermore, the results presented herein show that in a *Drosophila* model of AD the Wg pathway does not rescue Aβ induced neurotoxicity. This advises caution when interpreting data from other animal models on the interaction of Aβ and the Wnt-pathway, as potential drug target against AD.

REFERENCES

Aberle, H., Bauer, A., Stappert, J., Kispert, A., and Kemler, R. (1997). β-catenin is a target for the ubiquitin–proteasome pathway. EMBO J. *16*, 3797–3804.

Almeida, C.G., Tampellini, D., Takahashi, R.H., Greengard, P., Lin, M.T., Snyder, E.M., and Gouras, G.K. (2005). Beta-amyloid accumulation in APP mutant neurons reduces PSD-95 and GluR1 in synapses. Neurobiol. Dis. *20*, 187–198.

Alvarez, A.R., Godoy, J.A., Mullendorff, K., Olivares, G.H., Bronfman, M., and Inestrosa, N.C. (2004). Wnt-3a overcomes beta-amyloid toxicity in rat hippocampal neurons. Exp. Cell Res. *297*, 186–196.

Alves dos Santos, M.T.M., and Smidt, M.P. (2011). En1 and Wnt signaling in midbrain dopaminergic neuronal development. Neural Develop. *6*, 23.

Ataman, B., Ashley, J., Gorczyca, D., Gorczyca, M., Mathew, D., Wichmann, C., Sigrist, S.J., and Budnik, V. (2006). Nuclear trafficking of Drosophila Frizzled-2 during synapse development requires the PDZ protein dGRIP. Proc. Natl. Acad. Sci. U. S. A. *103*, 7841–7846.

Ataman, B., Ashley, J., Gorczyca, M., Ramachandran, P., Fouquet, W., Sigrist, S.J., and Budnik, V. (2008). Rapid Activity-Dependent Modifications in Synaptic Structure and Function Require Bidirectional Wnt Signaling. Neuron *57*, 705–718.

Bell, K.F.S., Bennett, D.A., and Cuello, A.C. (2007). Paradoxical upregulation of glutamatergic presynaptic boutons during mild cognitive impairment. J. Neurosci. Off. J. Soc. Neurosci. *27*, 10810–10817.

Bennett, V. (1979). Immunoreactive forms of human erythrocyte ankyrin are present in diverse cells and tissues. Nature *281*, 597–599.

Bennett, V., and Davis, J. (1981). Erythrocyte ankyrin: immunoreactive analogues are associated with mitotic structures in cultured cells and with microtubules in brain. Proc. Natl. Acad. Sci. U. S. A. *78*, 7550–7554.

Bennett, V., and Healy, J. (2009). Membrane Domains Based on Ankyrin and Spectrin Associated with Cell-Cell Interactions. Cold Spring Harb. Perspect. Biol. *1*.

Bennett, V., and Stenbuck, P.J. (1979). Identification and partial purification of ankyrin, the high affinity membrane attachment site for human erythrocyte spectrin. J. Biol. Chem. *254*, 2533–2541.

Blennow, K., de Leon, M.J., and Zetterberg, H. (2006). Alzheimer's disease. The Lancet *368*, 387–403.

Bobinnec, Y., Morin, X., and Debec, A. (2006). Shaggy/GSK-3β kinase localizes to the centrosome and to specialized cytoskeletal structures in Drosophila. Cell Motil. Cytoskeleton *63*, 313–320.

Bouley, M., Tian, M.-Z., Paisley, K., Shen, Y.-C., Malhotra, J.D., and Hortsch, M. (2000). The L1-Type Cell Adhesion Molecule Neuroglian Influences the Stability of Neural Ankyrin in the Drosophila Embryo But Not Its Axonal Localization. J. Neurosci. *20*, 4515–4523.

Budnik, V., and Salinas, P.C. (2011). Wnt signaling during synaptic development and plasticity. Curr. Opin. Neurobiol. *21*, 151–159.

Bulat, V., Rast, M., and Pielage, J. (2014). Presynaptic CK2 promotes synapse organization and stability by targeting Ankyrin2. J. Cell Biol. *204*, 77–94.

Caricasole, A., Copani, A., Caraci, F., Aronica, E., Rozemuller, A.J., Caruso, A., Storto, M., Gaviraghi, G., Terstappen, G.C., and Nicoletti, F. (2004). Induction of Dickkopf-1, a negative modulator of the Wnt pathway, is associated with neuronal degeneration in Alzheimer's brain. J. Neurosci. Off. J. Soc. Neurosci. *24*, 6021–6027.

Chacón, M.A., Varela-Nallar, L., and Inestrosa, N.C. (2008). Frizzled-1 is involved in the neuroprotective effect of Wnt3a against Abeta oligomers. J. Cell. Physiol. *217*, 215–227.

Chan, W., Kordeli, E., and Bennett, V. (1993). 440-kD ankyrinB: structure of the major developmentally regulated domain and selective localization in unmyelinated axons. J. Cell Biol. *123*, 1463–1473.

Ciani, L., Krylova, O., Smalley, M.J., Dale, T.C., and Salinas, P.C. (2004). A divergent canonical WNT-signaling pathway regulates microtubule dynamics Dishevelled signals locally to stabilize microtubules. J. Cell Biol. *164*, 243–253.

Clevers, H., and Nusse, R. (2012). Wnt/β-Catenin Signaling and Disease. Cell *149*, 1192–1205.

Crowther, D.C., Kinghorn, K.J., Miranda, E., Page, R., Curry, J.A., Duthie, F. a. I., Gubb, D.C., and Lomas, D.A. (2005). Intraneuronal Abeta, non-amyloid aggregates and neurodegeneration in a Drosophila model of Alzheimer's disease. Neuroscience *132*, 123–135.

DaRocha-Souto, B., Coma, M., Pérez-Nievas, B.G., Scotton, T.C., Siao, M., Sánchez-Ferrer, P., Hashimoto, T., Fan, Z., Hudry, E., Barroeta, I., et al. (2012). Activation of glycogen synthase kinase-3 beta mediates β-amyloid induced neuritic damage in Alzheimer's disease. Neurobiol. Dis. *45*, 425–437.

Davis, J.Q., and Bennett, V. (1994). Ankyrin binding activity shared by the neurofascin/L1/NrCAM family of nervous system cell adhesion molecules. J. Biol. Chem. *269*, 27163–27166.

Dubreuil, R.R., and Yu, J. (1994). Ankyrin and beta-spectrin accumulate independently of alpha-spectrin in Drosophila. Proc. Natl. Acad. Sci. *91*, 10285–10289.

Egger-Adam, D., and Katanaev, V.L. (2008). Trimeric G protein-dependent signaling by Frizzled receptors in animal development. Front. Biosci. J. Virtual Libr. *13*, 4740–4755.

Egger-Adam, D., and Katanaev, V.L. (2010). The trimeric G protein Go inflicts a double impact on axin in the Wnt/frizzled signaling pathway. Dev. Dyn. Off. Publ. Am. Assoc. Anat. *239*, 168–183.

De Ferrari, G.V., Chacón, M.A., Barría, M.I., Garrido, J.L., Godoy, J.A., Olivares, G., Reyes, A.E., Alvarez, A., Bronfman, M., and Inestrosa, N.C. (2003). Activation of Wnt signaling rescues neurodegeneration and behavioral impairments induced by beta-amyloid fibrils. Mol. Psychiatry *8*, 195–208.

De Ferrari, G.V., Papassotiropoulos, A., Biechele, T., Wavrant De-Vrieze, F., Avila, M.E., Major, M.B., Myers, A., Sáez, K., Henríquez, J.P., Zhao, A., et al. (2007). Common genetic variation within the low-density lipoprotein receptor-related protein 6 and late-onset Alzheimer's disease. Proc. Natl. Acad. Sci. U. S. A. *104*, 9434–9439.

Finelli, A., Kelkar, A., Song, H.-J., Yang, H., and Konsolaki, M. (2004). A model for studying Alzheimer's Abeta42-induced toxicity in Drosophila melanogaster. Mol. Cell. Neurosci. *26*, 365–375.

Folwell, J., Cowan, C.M., Ubhi, K.K., Shiabh, H., Newman, T.A., Shepherd, D., and Mudher, A. (2010). Abeta exacerbates the neuronal dysfunction caused by human tau expression in a Drosophila model of Alzheimer's disease. Exp. Neurol. *223*, 401–409.

Fonseca, A.C.R.G., Ferreiro, E., Oliveira, C.R., Cardoso, S.M., and Pereira, C.F. (2013). Activation of the endoplasmic reticulum stress response by the amyloid-beta 1-40 peptide in brain endothelial cells. Biochim. Biophys. Acta *1832*, 2191–2203.

Forlenza, P.D.O.V., Paula, V.J. de, Machado-Vieira, R., Diniz, B.S., and Gattaz, W.F. (2012). Does Lithium Prevent Alzheimer's Disease? Drugs Aging *29*, 335–342.

Francis, P.T. (2003). Glutamatergic systems in Alzheimer's disease. Int. J. Geriatr. Psychiatry *18*, S15–S21.

Franco, B., Bogdanik, L., Bobinnec, Y., Debec, A., Bockaert, J., Parmentier, M.-L., and Grau, Y. (2004). Shaggy, the homolog of glycogen synthase kinase 3, controls neuromuscular junction growth in Drosophila. J. Neurosci. Off. J. Soc. Neurosci. *24*, 6573–6577.

Gao, B. (2012). Chapter Eleven - Wnt Regulation of Planar Cell Polarity (PCP). In Current Topics in Developmental Biology, Yingzi Yang, ed. (Academic Press), pp. 263–295.

Gella, A., Segura, M., Durany, N., Pfuhlmann, B., Stöber, G., and Gawlik, M. (2011). Is Ankyrin a genetic risk factor for psychiatric phenotypes? BMC Psychiatry *11*, 103.

Gilman, A.G. (1987). G proteins: transducers of receptor-generated signals. Annu. Rev. Biochem. *56*, 615–649.

Gögel, S., Wakefield, S., Tear, G., Klämbt, C., and Gordon-Weeks, P.R. (2006). The Drosophila microtubule associated protein Futsch is phosphorylated by Shaggy/Zeste-white 3 at an homologous GSK3beta phosphorylation site in MAP1B. Mol. Cell. Neurosci. *33*, 188–199.

Goh, J.W., and Pennefather, P.S. (1989). A pertussis toxin-sensitive G protein in hippocampal long-term potentiation. Science *244*, 980–983.

Haass, C., and Selkoe, D.J. (2007). Soluble protein oligomers in neurodegeneration: lessons from the Alzheimer's amyloid β-peptide. Nat. Rev. Mol. Cell Biol. *8*, 101–112.

Hardy, J.A., and Higgins, G.A. (1992). Alzheimer's disease: the amyloid cascade hypothesis. Science *256*, 184–185.

Harterink, M., and Korswagen, H.C. (2012). Dissecting the Wnt secretion pathway: key questions on the modification and intracellular trafficking of Wnt proteins. Acta Physiol. Oxf. Engl. *204*, 8–16.

Higashi-Kovtun, M.E., Mosca, T.J., Dickman, D.K., Meinertzhagen, I.A., and Schwarz, T.L. (2010). Importin-β11 Regulates Synaptic Phosphorylated Mothers Against Decapentaplegic, and Thereby Influences Synaptic Development and Function at the Drosophila Neuromuscular Junction. J. Neurosci. *30*, 5253–5268.

Hooper, C., Killick, R., and Lovestone, S. (2008). The GSK3 hypothesis of Alzheimer's disease. J. Neurochem. *104*, 1433–1439.

Hortsch, M., Paisley, K.L., Tian, M.-Z., Qian, M., Bouley, M., and Chandler, R. (2002). The axonal localization of large Drosophila ankyrin2 protein isoforms is essential for neuronal functionality. Mol. Cell. Neurosci. *20*, 43–55.

Hummel, T., Krukkert, K., Roos, J., Davis, G., and Klämbt, C. (2000). Drosophila Futsch/22C10 Is a MAP1B-like Protein Required for Dendritic and Axonal Development. Neuron *26*, 357–370.

Iijima, K., Liu, H.-P., Chiang, A.-S., Hearn, S.A., Konsolaki, M., and Zhong, Y. (2004). Dissecting the pathological effects of human A?40 and A?42 in Drosophila: A potential model for Alzheimer's disease. Proc. Natl. Acad. Sci. U. S. A. *101*, 6623–6628.

Iijima, K., Chiang, H.-C., Hearn, S.A., Hakker, I., Gatt, A., Shenton, C., Granger, L., Leung, A., Iijima-Ando, K., and Zhong, Y. (2008). A?42 Mutants with Different Aggregation Profiles Induce Distinct Pathologies in Drosophila. PLoS ONE *3*.

Inestrosa, N.C., Montecinos-Oliva, C., and Fuenzalida, M. (2012). Wnt signaling: role in Alzheimer disease and schizophrenia. J. Neuroimmune Pharmacol. Off. J. Soc. NeuroImmune Pharmacol. *7*, 788–807.

Inoue, S., Hoshino, S., Kukimoto, I., Ui, M., and Katada, T. (1995). Purification and characterization of the G203T mutant alpha i-2 subunit of GTP-binding protein expressed in baculovirus-infected Sf9 cells. J. Biochem. (Tokyo) *118*, 650–657.

Ipsaro, J.J., Huang, L., and Mondragón, A. (2009). Structures of the spectrin-ankyrin interaction binding domains. Blood *113*, 5385–5393.

Jan, L.Y., and Jan, Y.N. (1976). L-glutamate as an excitatory transmitter at the Drosophila larval neuromuscular junction. J. Physiol. *262*, 215–236.

Jenkins, S.M., and Bennett, V. (2001). Ankyrin-G coordinates assembly of the spectrin-based membrane skeleton, voltage-gated sodium channels, and L1 CAMs at Purkinje neuron initial segments. J. Cell Biol. *155*, 739–746.

Kamimura, K., Ueno, K., Nakagawa, J., Hamada, R., Saitoe, M., and Maeda, N. (2013). Perlecan regulates bidirectional Wnt signaling at the Drosophila neuromuscular junction. J. Cell Biol. *200*, 219–233.

Katanaev, V.L., and Chornomorets, M. (2007). Kinetic diversity in G-protein-coupled receptor signalling. Biochem. J. *401*, 485–495.

Katanaev, V.L., and Tomlinson, A. (2006). Dual roles for the trimeric G protein Go in asymmetric cell division in Drosophila. Proc. Natl. Acad. Sci. U. S. A. *103*, 6524–6529.

Katanaev, V.L., Ponzielli, R., Sémériva, M., and Tomlinson, A. (2005). Trimeric G protein-dependent frizzled signaling in Drosophila. Cell *120*, 111–122.

Kerr, K.S., Fuentes-Medel, Y., Brewer, C., Barria, R., Ashley, J., Abruzzi, K.C., Sheehan, A., Tasdemir-Yilmaz, O.E., Freeman, M.R., and Budnik, V. (2014). Glial Wingless/Wnt Regulates Glutamate Receptor Clustering and Synaptic Physiology at the Drosophila Neuromuscular Junction. J. Neurosci. *34*, 2910–2920.

Koch, I., Schwarz, H., Beuchle, D., Goellner, B., Langegger, M., and Aberle, H. (2008). Drosophila ankyrin 2 is required for synaptic stability. Neuron *58*, 210–222.

Kopein, D., and Katanaev, V.L. (2009). Drosophila GoLoco-protein Pins is a target of Galpha(o)-mediated G protein-coupled receptor signaling. Mol. Biol. Cell *20*, 3865–3877.

Kordeli, E., Lambert, S., and Bennett, V. (1995). AnkyrinG. A new ankyrin gene with neural-specific isoforms localized at the axonal initial segment and node of Ranvier. J. Biol. Chem. *270*, 2352–2359.

Koval, A., and Katanaev, V.L. (2011). Wnt3a stimulation elicits G-protein-coupled receptor properties of mammalian Frizzled proteins. Biochem. J. *433*, 435–440.

Koval, A., and Katanaev, V.L. (2012). Platforms for high-throughput screening of Wnt/Frizzled antagonists. Drug Discov. Today *17*, 1316–1322.

Kühl, M., Sheldahl, L.C., Malbon, C.C., and Moon, R.T. (2000a). Ca2+/Calmodulin-dependent Protein Kinase II Is Stimulated by Wnt and Frizzled Homologs and Promotes Ventral Cell Fates in Xenopus. J. Biol. Chem. *275*, 12701–12711.

Kühl, M., Sheldahl, L.C., Park, M., Miller, J.R., and Moon, R.T. (2000b). The Wnt/Ca2+ pathway: a new vertebrate Wnt signaling pathway takes shape. Trends Genet. *16*, 279–283.

Kummer, M.P., and Heneka, M.T. (2014). Truncated and modified amyloid-beta species. Alzheimers Res. Ther. *6*, 28.

Kunimoto, M. (1995). A neuron-specific isoform of brain ankyrin, 440-kD ankyrinB, is targeted to the axons of rat cerebellar neurons. J. Cell Biol. *131*, 1821–1829.

Kunimoto, M., Otto, E., and Bennett, V. (1991). A new 440-kD isoform is the major ankyrin in neonatal rat brain. J. Cell Biol. *115*, 1319–1331.

Lahey, T., Gorczyca, M., Jia, X.X., and Budnik, V. (1994). The Drosophila tumor suppressor gene dlg is required for normal synaptic bouton structure. Neuron *13*, 823–835.

Lee, G., Abdi, K., Jiang, Y., Michaely, P., Bennett, V., and Marszalek, P.E. (2006). Nanospring behaviour of ankyrin repeats. Nature *440*, 246–249.

Lepicard, S., Franco, B., Bock, F. de, and Parmentier, M.-L. (2014). A Presynaptic Role of Microtubule-Associated Protein 1/Futsch in Drosophila: Regulation of Active Zone Number and Neurotransmitter Release. J. Neurosci. *34*, 6759–6771.

Li, B., Zhong, L., Yang, X., Andersson, T., Huang, M., and Tang, S.-J. (2011). WNT5A signaling contributes to Aβ-induced neuroinflammation and neurotoxicity. PloS One *6*, e22920.

Lin, C., and Katanaev, V.L. (2013). Kermit Interacts with Gαo, Vang, and Motor Proteins in Drosophila Planar Cell Polarity. PLoS ONE *8*, e76885.

Lin, C., Koval, A., Tishchenko, S., Gabdulkhakov, A., Tin, U., Solis, G.P., and Katanaev, V.L. (2014). Double suppression of the Gα protein activity by RGS proteins. Mol. Cell *53*, 663–671.

Liu, C.-C., Tsai, C.-W., Deak, F., Rogers, J., Penuliar, M., Sung, Y.M., Maher, J.N., Fu, Y., Li, X., Xu, H., et al. (2014). Deficiency in LRP6-Mediated Wnt Signaling Contributes to Synaptic Abnormalities and Amyloid Pathology in Alzheimer's Disease. Neuron *84*, 63–77.

Logan, C.Y., and Nusse, R. (2004). The Wnt signaling pathway in development and disease. Annu. Rev. Cell Dev. Biol. *20*, 781–810.

Logue, M.W., Solovieff, N., Leussis, M.P., Wolf, E.J., Melista, E., Baldwin, C., Koenen, K.C., Petryshen, T.L., and Miller, M.W. (2013). The ankyrin-3 gene is associated with posttraumatic stress disorder and externalizing comorbidity. Psychoneuroendocrinology *38*, 2249–2257.

Lord, A., Kalimo, H., Eckman, C., Zhang, X.-Q., Lannfelt, L., and Nilsson, L.N.G. (2006). The Arctic Alzheimer mutation facilitates early intraneuronal Abeta aggregation and senile plaque formation in transgenic mice. Neurobiol. Aging *27*, 67–77.

Magdesian, M.H., Carvalho, M.M.V.F., Mendes, F.A., Saraiva, L.M., Juliano, M.A., Juliano, L., Garcia-Abreu, J., and Ferreira, S.T. (2008). Amyloid-beta binds to the extracellular cysteine-rich domain of Frizzled and inhibits Wnt/beta-catenin signaling. J. Biol. Chem. *283*, 9359–9368.

Malbon, C.C. (2004). Frizzleds: new members of the superfamily of G-protein-coupled receptors. Front. Biosci. J. Virtual Libr. *9*, 1048–1058.

Von Maltzahn, J., Bentzinger, C.F., and Rudnicki, M.A. (2012). Wnt7a-Fzd7 signalling directly activates the Akt/mTOR anabolic growth pathway in skeletal muscle. Nat. Cell Biol. *14*, 186–191.

Mao, J., Wang, J., Liu, B., Pan, W., Farr III, G.H., Flynn, C., Yuan, H., Takada, S., Kimelman, D., Li, L., et al. (2001). Low-Density Lipoprotein Receptor-Related Protein-5 Binds to Axin and Regulates the Canonical Wnt Signaling Pathway. Mol. Cell *7*, 801–809.

Mathew, D., Ataman, B., Chen, J., Zhang, Y., Cumberledge, S., and Budnik, V. (2005). Wingless signaling at synapses is through cleavage and nuclear import of receptor DFrizzled2. Science *310*, 1344–1347.

McCudden, C.R., Hains, M.D., Kimple, R.J., Siderovski, D.P., and Willard, F.S. (2005). G-protein signaling: back to the future. Cell. Mol. Life Sci. *62*, 551–577.

Menon, K.P., Carrillo, R.A., and Zinn, K. (2013). Development and plasticity of the Drosophila larval neuromuscular junction. Wiley Interdiscip. Rev. Dev. Biol. *2*, 647–670.

Mhatre, S.D., Satyasi, V., Killen, M., Paddock, B.E., Moir, R.D., Saunders, A.J., and Marenda, D.R. (2014a). Synaptic abnormalities in a Drosophila model of Alzheimer's disease. Dis. Model. Mech. *7*, 373–385.

Mhatre, S.D., Michelson, S.J., Gomes, J., Tabb, L.P., Saunders, A.J., and Marenda, D.R. (2014b). Development and characterization of an aged onset model of Alzheimer's disease in Drosophila melanogaster. Exp. Neurol. *261C*, 772–781.

Michaely, P., Tomchick, D.R., Machius, M., and Anderson, R.G.W. (2002). Crystal structure of a 12 ANK repeat stack from human ankyrinR. EMBO J. *21*, 6387–6396.

Miech, C., Pauer, H.-U., He, X., and Schwarz, T.L. (2008). Presynaptic local signaling by a canonical wingless pathway regulates development of the Drosophila neuromuscular junction. J. Neurosci. Off. J. Soc. Neurosci. *28*, 10875–10884.

Miguel-Hidalgo, J.J., Alvarez, X.A., Cacabelos, R., and Quack, G. (2002). Neuroprotection by memantine against neurodegeneration induced by beta-amyloid(1-40). Brain Res. *958*, 210–221.

Mikels, A.J., and Nusse, R. (2006). Purified Wnt5a protein activates or inhibits beta-catenin-TCF signaling depending on receptor context. PLoS Biol. *4*, e115.

Miller, J.R. (2002). The Wnts. Genome Biol. *3*, REVIEWS3001.

Mosca, T.J., and Schwarz, T.L. (2010). The nuclear import of Frizzled2-C by Importins-beta11 and alpha2 promotes postsynaptic development. Nat. Neurosci. *13*, 935–943.

Nichols, A.S., Floyd, D.H., Bruinsma, S.P., Narzinski, K., and Baranski, T.J. (2013). Frizzled receptors signal through G proteins. Cell. Signal. *25*, 1468–1475.

Nilsberth, C., Westlind-Danielsson, A., Eckman, C.B., Condron, M.M., Axelman, K., Forsell, C., Stenh, C., Luthman, J., Teplow, D.B., Younkin, S.G., et al. (2001). The "Arctic" APP mutation

(E693G) causes Alzheimer's disease by enhanced Abeta protofibril formation. Nat. Neurosci. *4*, 887–893.

Noble, W., Planel, E., Zehr, C., Olm, V., Meyerson, J., Suleman, F., Gaynor, K., Wang, L., LaFrancois, J., Feinstein, B., et al. (2005). Inhibition of glycogen synthase kinase-3 by lithium correlates with reduced tauopathy and degeneration in vivo. Proc. Natl. Acad. Sci. U. S. A. *102*, 6990–6995.

O'Brien, W.T., and Klein, P.S. (2009). Validating GSK3 as an in vivo target of lithium action. Biochem. Soc. Trans. *37*, 1133–1138.

Otto, E., Kunimoto, M., McLaughlin, T., and Bennett, V. (1991). Isolation and characterization of cDNAs encoding human brain ankyrins reveal a family of alternatively spliced genes. J. Cell Biol. *114*, 241–253.

Packard, M., Koo, E.S., Gorczyca, M., Sharpe, J., Cumberledge, S., and Budnik, V. (2002). The Drosophila Wnt, wingless, provides an essential signal for pre- and postsynaptic differentiation. Cell *111*, 319–330.

Pei, J.J., Tanaka, T., Tung, Y.C., Braak, E., Iqbal, K., and Grundke-Iqbal, I. (1997). Distribution, levels, and activity of glycogen synthase kinase-3 in the Alzheimer disease brain. J. Neuropathol. Exp. Neurol. *56*, 70–78.

Peifer, M., Pai, L.M., and Casey, M. (1994). Phosphorylation of the Drosophila adherens junction protein Armadillo: roles for wingless signal and zeste-white 3 kinase. Dev. Biol. *166*, 543–556.

Peters, L.L., John, K.M., Lu, F.M., Eicher, E.M., Higgins, A., Yialamas, M., Turtzo, L.C., Otsuka, A.J., and Lux, S.E. (1995). Ank3 (epithelial ankyrin), a widely distributed new member of the ankyrin gene family and the major ankyrin in kidney, is expressed in alternatively spliced forms, including forms that lack the repeat domain. J. Cell Biol. *130*, 313–330.

Phiel, C.J., Wilson, C.A., Lee, V.M.-Y., and Klein, P.S. (2003). GSK-3alpha regulates production of Alzheimer's disease amyloid-beta peptides. Nature *423*, 435–439.

Pielage, J., Cheng, L., Fetter, R.D., Carlton, P.M., Sedat, J.W., and Davis, G.W. (2008). A presynaptic giant ankyrin stabilizes the NMJ through regulation of presynaptic microtubules and transsynaptic cell adhesion. Neuron *58*, 195–209.

Prince, M., Bryce, R., Albanese, E., Wimo, A., Ribeiro, W., and Ferri, C.P. (2013). The global prevalence of dementia: A systematic review and metaanalysis. Alzheimers Dement. J. Alzheimers Assoc. *9*, 63–75.e2.

Prüßing, K., Voigt, A., and Schulz, J.B. (2013). Drosophila melanogaster as a model organism for Alzheimer's disease. Mol. Neurodegener. *8*, 35.

Purro, S.A., Galli, S., and Salinas, P.C. (2014). Dysfunction of Wnt signaling and synaptic disassembly in neurodegenerative diseases. J. Mol. Cell Biol. *6*, 75–80.

Purvanov, V., Koval, A., and Katanaev, V.L. (2010). A direct and functional interaction between Go and Rab5 during G protein-coupled receptor signaling. Sci. Signal. *3*, ra65.

Revett, T.J., Baker, G.B., Jhamandas, J., and Kar, S. (2013). Glutamate system, amyloid b peptides and tau protein: functional interrelationships and relevance to Alzheimer disease pathology. J. Psychiatry Neurosci. JPN *38*, 6–23.

Ríos, J.A., Cisternas, P., Arrese, M., Barja, S., and Inestrosa, N.C. (2014). Is Alzheimer's disease related to metabolic syndrome? A Wnt signaling conundrum. Prog. Neurobiol. *121*, 125–146.

Roos, J., Hummel, T., Ng, N., Klämbt, C., and Davis, G.W. (2000). Drosophila Futsch regulates synaptic microtubule organization and is necessary for synaptic growth. Neuron *26*, 371–382.

Rosen, D.R., Martin-Morris, L., Luo, L.Q., and White, K. (1989). A Drosophila gene encoding a protein resembling the human beta-amyloid protein precursor. Proc. Natl. Acad. Sci. U. S. A. *86*, 2478–2482.

Ruiz-Canada, C., Ashley, J., Moeckel-Cole, S., Drier, E., Yin, J., and Budnik, V. (2004). New Synaptic Bouton Formation Is Disrupted by Misregulation of Microtubule Stability in aPKC Mutants. Neuron *42*, 567–580.

Sahlin, C., Lord, A., Magnusson, K., Englund, H., Almeida, C.G., Greengard, P., Nyberg, F., Gouras, G.K., Lannfelt, L., and Nilsson, L.N.G. (2007). The Arctic Alzheimer mutation favors intracellular amyloid-beta production by making amyloid precursor protein less available to alpha-secretase. J. Neurochem. *101*, 854–862.

Saito, T., Suemoto, T., Brouwers, N., Sleegers, K., Funamoto, S., Mihira, N., Matsuba, Y., Yamada, K., Nilsson, P., Takano, J., et al. (2011). Potent amyloidogenicity and pathogenicity of Aβ43. Nat. Neurosci. *14*, 1023–1032.

Sanokawa-Akakura, R., Cao, W., Allan, K., Patel, K., Ganesh, A., Heiman, G., Burke, R., Kemp, F.W., Bogden, J.D., Camakaris, J., et al. (2010). Control of Alzheimer's Amyloid Beta Toxicity by the High Molecular Weight Immunophilin FKBP52 and Copper Homeostasis in Drosophila. PLoS ONE *5*.

Sarantseva, S., Timoshenko, S., Bolshakova, O., Karaseva, E., Rodin, D., Schwarzman, A.L., and Vitek, M.P. (2009). Apolipoprotein E-Mimetics Inhibit Neurodegeneration and Restore Cognitive Functions in a Transgenic Drosophila Model of Alzheimer's Disease. PLoS ONE *4*, e8191.

Seib, D.R.M., Corsini, N.S., Ellwanger, K., Plaas, C., Mateos, A., Pitzer, C., Niehrs, C., Celikel, T., and Martin-Villalba, A. (2013). Loss of Dickkopf-1 Restores Neurogenesis in Old Age and Counteracts Cognitive Decline. Cell Stem Cell *12*, 204–214.

Shimada, Y., Usui, T., Yanagawa, S., Takeichi, M., and Uemura, T. (2001). Asymmetric colocalization of Flamingo, a seven-pass transmembrane cadherin, and Dishevelled in planar cell polarization. Curr. Biol. CB *11*, 859–863.

Shirahata, E., Iwasaki, H., Takagi, M., Lin, C., Bennett, V., Okamura, Y., and Hayasaka, K. (2006). Ankyrin-G Regulates Inactivation Gating of the Neuronal Sodium Channel, Nav1.6. J. Neurophysiol. *96*, 1347–1357.

Singh, J., and Mlodzik, M. (2012). Planar Cell Polarity Signaling: Coordination of cellular orientation across tissues. Wiley Interdiscip. Rev. Dev. Biol. *1*, 479–499.

Snyder, S.W., Ladror, U.S., Wade, W.S., Wang, G.T., Barrett, L.W., Matayoshi, E.D., Huffaker, H.J., Krafft, G.A., and Holzman, T.F. (1994). Amyloid-beta aggregation: selective inhibition of aggregation in mixtures of amyloid with different chain lengths. Biophys. J. *67*, 1216–1228.

Sofola, O., Kerr, F., Rogers, I., Killick, R., Augustin, H., Gandy, C., Allen, M.J., Hardy, J., Lovestone, S., and Partridge, L. (2010). Inhibition of GSK-3 Ameliorates Aβ Pathology in an Adult-Onset Drosophila Model of Alzheimer's Disease. PLoS Genet *6*, e1001087.

Sofola-Adesakin, O., Castillo-Quan, J.I., Rallis, C., Tain, L.S., Bjedov, I., Rogers, I., Li, L., Martinez, P., Khericha, M., Cabecinha, M., et al. (2014). Lithium suppresses Aβ pathology by inhibiting translation in an adult Drosophila model of Alzheimer's disease. Front. Aging Neurosci. *6*, 190.

Solis, G.P., Luchtenborg, A.-M., and Katanaev, V.L. (2013). Wnt Secretion and Gradient Formation. Int. J. Mol. Sci. *14*, 5130–5145.

Speese, S.D., Ashley, J., Jokhi, V., Nunnari, J., Barria, R., Li, Y., Ataman, B., Koon, A., Chang, Y.-T., Li, Q., et al. (2012). Nuclear envelope budding enables large ribonucleoprotein particle export during synaptic Wnt signaling. Cell *149*, 832–846.

Stamos, J.L., and Weis, W.I. (2013). The β-catenin destruction complex. Cold Spring Harb. Perspect. Biol. *5*, a007898.

Sternweis, P.C., and Robishaw, J.D. (1984). Isolation of two proteins with high affinity for guanine nucleotides from membranes of bovine brain. J. Biol. Chem. *259*, 13806–13813.

Strutt, D.I. (2001). Asymmetric Localization of Frizzled and the Establishment of Cell Polarity in the Drosophila Wing. Mol. Cell *7*, 367–375.

Strutt, D.I., Weber, U., and Mlodzik, M. (1997). The role of RhoA in tissue polarity and Frizzled signalling. Nature *387*, 292–295.

Tan, Y., Yu, D., Busto, G.U., Wilson, C., and Davis, R.L. (2013). Wnt signaling is required for long-term memory formation. Cell Rep. *4*, 1082–1089.

Tang, K.-C., and Lovinger, D.M. (2000). Role of Pertussis Toxin–Sensitive G-Proteins in Synaptic Transmission and Plasticity at Corticostriatal Synapses. J. Neurophysiol. *83*, 60–69.

Tao, Q., Yokota, C., Puck, H., Kofron, M., Birsoy, B., Yan, D., Asashima, M., Wylie, C.C., Lin, X., and Heasman, J. (2005). Maternal wnt11 activates the canonical wnt signaling pathway required for axis formation in Xenopus embryos. Cell *120*, 857–871.

Toledo, E.M., and Inestrosa, N.C. (2010). Activation of Wnt signaling by lithium and rosiglitazone reduced spatial memory impairment and neurodegeneration in brains of an APPswe/PSEN1DeltaE9 mouse model of Alzheimer's disease. Mol. Psychiatry *15*, 272–285, 228.

Tsai, P.-I., Wang, M., Kao, H.-H., Cheng, Y.-J., Lin, Y.-J., Chen, R.-H., and Chien, C.-T. (2012). Activity-dependent retrograde laminin A signaling regulates synapse growth at Drosophila neuromuscular junctions. Proc. Natl. Acad. Sci. *109*, 17699–17704.

Tse, W.T., Menninger, J.C., Yang-Feng, T.L., Francke, U., Sahr, K.E., Lux, S.E., Ward, D.C., and Forget, B.G. (1991). Isolation and chromosomal localization of a novel nonerythroid ankyrin gene. Genomics *10*, 858–866.

Wang, H., Liu, T., and Malbon, C.C. (2006). Structure-function analysis of Frizzleds. Cell. Signal. *18*, 934–941.

Wang, J., Sinha, T., and Wynshaw-Boris, A. (2012). Wnt Signaling in Mammalian Development: Lessons from Mouse Genetics. Cold Spring Harb. Perspect. Biol. *4*.

Wild-Bode, C., Yamazaki, T., Capell, A., Leimer, U., Steiner, H., Ihara, Y., and Haass, C. (1997). Intracellular generation and accumulation of amyloid beta-peptide terminating at amino acid 42. J. Biol. Chem. *272*, 16085–16088.

Willert, K., and Nusse, R. (2012). Wnt Proteins. Cold Spring Harb. Perspect. Biol. *4*.

Willert, K., Brown, J.D., Danenberg, E., Duncan, A.W., Weissman, I.L., Reya, T., Yates, J.R., and Nusse, R. (2003). Wnt proteins are lipid-modified and can act as stem cell growth factors. Nature *423*, 448–452.

Winitz, S., Gupta, S.K., Qian, N.X., Heasley, L.E., Nemenoff, R.A., and Johnson, G.L. (1994). Expression of a mutant Gi2 alpha subunit inhibits ATP and thrombin stimulation of cytoplasmic phospholipase A2-mediated arachidonic acid release independent of Ca2+ and mitogen-activated protein kinase regulation. J. Biol. Chem. *269*, 1889–1895.

Wirgenes, K.V., Tesli, M., Inderhaug, E., Athanasiu, L., Agartz, I., Melle, I., Hughes, T., Andreassen, O.A., and Djurovic, S. (2014). ANK3 gene expression in bipolar disorder and schizophrenia. Br. J. Psychiatry J. Ment. Sci. *205*, 244–245.

Wolfgang, W.J., Quan, F., Goldsmith, P., Unson, C., Spiegel, A., and Forte, M. (1990). Immunolocalization of G protein alpha-subunits in the Drosophila CNS. J. Neurosci. Off. J. Soc. Neurosci. *10*, 1014–1024.

Wong, H.-C., Bourdelas, A., Krauss, A., Lee, H.-J., Shao, Y., Wu, D., Mlodzik, M., Shi, D.-L., and Zheng, J. (2003). Direct Binding of the PDZ Domain of Dishevelled to a Conserved Internal Sequence in the C-Terminal Region of Frizzled. Mol. Cell *12*, 1251–1260.

Yuan, A., Yi, Z., Wang, Q., Sun, J., Li, Z., Du, Y., Zhang, C., Yu, T., Fan, J., Li, H., et al. (2012). ANK3 as a risk gene for schizophrenia: new data in Han Chinese and meta analysis. Am. J. Med. Genet. Part B Neuropsychiatr. Genet. Off. Publ. Int. Soc. Psychiatr. Genet. *159B*, 997–1005.

Zanetti, O., Solerte, S.B., and Cantoni, F. (2009). Life expectancy in Alzheimer's disease (AD). Arch. Gerontol. Geriatr. *49*, 237–243.

Zhang, Z., Hartmann, H., Do, V.M., Abramowski, D., Sturchler-Pierrat, C., Staufenbiel, M., Sommer, B., van de Wetering, M., Clevers, H., Saftig, P., et al. (1998). Destabilization of beta-catenin by mutations in presenilin-1 potentiates neuronal apoptosis. Nature *395*, 698–702.

Zito, K., Parnas, D., Fetter, R.D., Isacoff, E.Y., and Goodman, C.S. (1999). Watching a synapse grow: noninvasive confocal imaging of synaptic growth in Drosophila. Neuron *22*, 719–729.

ARTICLES

1. Lüchtenborg, A.-M., Solis G.P, Egger-Adam D., Koval A., Lin C., Blanchard M.G., Kellenberger S. & Katanaev V.L.

   Heterotrimeric Go protein links Wnt-Frizzled signaling with ankyrins to regulate the neuronal microtubule cytoskeleton.

   Development. 2014 Sep;141(17):3399-409

2. Lüchtenborg, A.-M. & Katanaev, V.L.

   Lack of evidence of the interaction of the Aβ peptide with the Wnt signaling cascade in Drosophila models of Alzheimer's disease.

   Mol Brain. 2014 Nov 12;7(1):81

FURTHER MANUSCRIPT NOT INCLUDED IN THE THESIS:

3. Solis G.P., Lüchtenborg, A.-M.& Katanaev, V.L.

   Wnt secretion and gradient formation.

   Int J Mol Sci. 2013 Mar 1;14(3):5130-45

© 2014. Published by The Company of Biologists Ltd | Development (2014) 141, 3399-3409 doi:10.1242/dev.106773

RESEARCH ARTICLE

Heterotrimeric Go protein links Wnt-Frizzled signaling with ankyrins to regulate the neuronal microtubule cytoskeleton

Anne-Marie Lüchtenborg[1,2], Gonzalo P. Solis[1], Diane Egger-Adam[2], Alexey Koval[1], Chen Lin[1,2], Maxime G. Blanchard[1], Stephan Kellenberger[1] and Vladimir L. Katanaev[1,2,*]

ABSTRACT

Drosophila neuromuscular junctions (NMJs) represent a powerful model system with which to study glutamatergic synapse formation and remodeling. Several proteins have been implicated in these processes, including components of canonical Wingless (*Drosophila* Wnt1) signaling and the giant isoforms of the membrane-cytoskeleton linker Ankyrin 2, but possible interconnections and cooperation between these proteins were unknown. Here, we demonstrate that the heterotrimeric G protein Go functions as a transducer of Wingless-Frizzled 2 signaling in the synapse. We identify Ankyrin 2 as a target of Go signaling required for NMJ formation. Moreover, the Go-ankyrin interaction is conserved in the mammalian neurite outgrowth pathway. Without ankyrins, a major switch in the Go-induced neuronal cytoskeleton program is observed, from microtubule-dependent neurite outgrowth to actin-dependent lamellopodial induction. These findings describe a novel mechanism regulating the microtubule cytoskeleton in the nervous system. Our work in *Drosophila* and mammalian cells suggests that this mechanism might be generally applicable in nervous system development and function.

KEY WORDS: *Drosophila*, Neuromuscular junction, Wnt, Frizzled, G protein, Ankyrin, Microtubules

INTRODUCTION

Go is the most abundant heterotrimeric G protein in the central nervous system of both vertebrates and invertebrates (Sternweis and Robishaw, 1984; Wolfgang et al., 1990). It is the immediate transducer of a number of G protein-coupled receptors (GPCRs), including receptors of the Frizzled (Fz) family (Egger-Adam and Katanaev, 2008). In *Drosophila*, Go is involved in transduction of the Wingless (Wg; *Drosophila* Wnt1) signal (Katanaev et al., 2005). Go can physically interact with Fz proteins, and binding of Wnt ligands to Fz induces an exchange of the guanine nucleotide on the Gα subunit of Go (Gαo) (Koval and Katanaev, 2011). The initial heterotrimeric complex then dissociates into free Gα-GTP and the Gβγ dimer; both are involved in downstream signaling. The intrinsic GTPase activity of Gα leads to hydrolysis of GTP to GDP; the resultant Gα-GDP can continue to signal or associates back with Gβγ to bind GPCRs (Gilman, 1987; Katanaev, 2010).

[1]Department of Pharmacology and Toxicology, Faculty of Biology and Medicine, University of Lausanne, Rue du Bugnon 27, Lausanne 1005, Switzerland. [2]Department of Biology, University of Konstanz, Universitätsstrasse 10, Box 643, Konstanz 78457, Germany.

*Author for correspondence (vladimir.katanaev@unil.ch)

This is an Open Access article distributed under the terms of the Creative Commons Attribution License (http://creativecommons.org/licenses/by/3.0), which permits unrestricted use, distribution and reproduction in any medium provided that the original work is properly attributed.

Received 4 December 2013; Accepted 9 July 2014

The evolutionarily conserved Wg pathway is important for numerous developmental programs and cellular processes (Logan and Nusse, 2004). In the nervous system of *Drosophila*, Wg signaling is involved in the formation of neuromuscular junctions (NMJs) (Packard et al., 2002; Miech et al., 2008). Being a glutamatergic synapse, the *Drosophila* NMJ provides a useful experimental model with which to study mammalian central nervous system synapses, their formation and remodeling (Collins and DiAntonio, 2007). The *Drosophila* NMJ is a beads-on-a-string-like structure that is formed at the axon terminus and is composed of distinct circular structures – the synaptic boutons – which contain active zones for neurotransmitter release. During growth, the NMJ is subject to remodeling to build additional synapses on the growing muscle, which is achieved by the formation of new boutons as well as by budding off from the existing boutons (Zito et al., 1999). These processes require cytoskeletal rearrangements (Roos et al., 2000) and depend on the proper response to the Wg ligand, which is produced presynaptically (Packard et al., 2002; Korkut et al., 2009).

In canonical Wnt signaling, binding of the ligand to Fz and a co-receptor, LRP5/6 (Arrow in *Drosophila*), leads to reorganization of the cytoplasmic β-catenin-destruction machinery, which contains, among other proteins, glycogen synthase kinase 3β [GSK3β; Shaggy (Sgg) in *Drosophila*]. Receptors (Fz and LRP5/6) are activated by Wnt signal to disassemble the destruction complex, leading to the stabilization of β-catenin, its translocation into the nucleus and the induction of transcription of Wnt target genes (Logan and Nusse, 2004).

However, this canonical pathway is not active in the *Drosophila* NMJ. Instead, on the postsynaptic side of the NMJ the Wg signal is transduced via endocytosis and cleavage of Frizzled 2 (Fz2) and nuclear import of its C-terminal fragment, which is required for the proper transcription-dependent establishment of postsynaptic densities (Mathew et al., 2005; Mosca and Schwarz, 2010). On the presynaptic side, the Wg pathway does not involve β-catenin nor transcription but does require inhibition of Sgg activity (Miech et al., 2008); Sgg in the presynapse is proposed to regulate the stability of the microtubule cytoskeleton through phosphorylation of the microtubule-binding protein Futsch (*Drosophila* MAP1B) (Franco et al., 2004; Gogel et al., 2006; Miech et al., 2008). The microtubule cytoskeleton in the presynaptic NMJ cell is also under the control of Ankyrin 2 (Hortsch et al., 2002; Koch et al., 2008; Pielage et al., 2008).

Ankyrins (Ank) are highly abundant modular proteins that mediate protein-protein interactions, mainly serving as adaptors for linking the cytoskeleton to the plasma membrane (Bennett and Baines, 2001). Mammalian genomes encode three Ank genes [*AnkR* (*Ank1*), *AnkB* (*Ank2*) and *AnkG* (*Ank3*)], whereas *Drosophila* has two [*Ank1* (also known as *Ank* – FlyBase) and *Ank2*] (Dubreuil and Yu, 1994; Bouley et al., 2000). *Ank2* is expressed exclusively in neurons and exists in several splicing variants (Koch et al., 2008;

Development (2014) 141, 3399-3409 doi:10.1242/dev.106773

Pielage et al., 2008). The larger isoforms (Ank2M, Ank2L and Ank2XL) are localized to axons and play important roles in NMJ formation and function (Hortsch et al., 2002; Koch et al., 2008; Pielage et al., 2008). The C-terminal part of Ank2L can bind to microtubules (Pielage et al., 2008). Despite the well-established role of Ank2 in NMJ formation, its function has been considered somewhat passive and its mode of regulation has not been clarified. Here, we show that Gαo binds to Ank2 and that these proteins and the Wg pathway components Wg, Fz2, and Sgg jointly coordinate the formation of the NMJ. We also show that the functional Gαo-Ank interaction is conserved from insects to mammals.

RESULTS

Go is abundant in the NMJ and is required for normal NMJ physiology

Since Go is abundant in neurons and is involved in Fz signaling, we investigated its presence and function in the NMJ. To visualize the synaptic boutons, we used the postsynaptic marker CD8-GFP-Sh (Zito et al., 1999) or Discs large (Dlg; Dlg1 – FlyBase) (Guan et al., 1996) (Fig. 1A; supplementary material Fig. S1A). For the presynaptic side we used the marker Bruchpilot (Brp) (Wagh et al., 2006) (Fig. 1B) or performed anti-HRP staining (Jan and Jan, 1982) (supplementary material Fig. S1A,B). Using two different anti-Gαo antibodies (see Materials and Methods), we found strong anti-Gαo staining in boutons as well as in axons (Fig. 1C; supplementary material Fig. S1A-D). Comparison of Gαo staining with the markers revealed that Gαo is expressed in the presynaptic cell, overlapping with Brp (Fig. 1D-F; supplementary material Fig. S1C,D) and anti-HRP (supplementary material Fig. S1A,B). This is particularly evident at high magnification, which shows the anti-Gαo staining encircled by postsynaptic Dlg and CD8-GFP-Sh (supplementary material Fig. S1B,D). Interestingly, this pattern is different from that of anti-Gβ13F staining, which recognizes the major Gβ subunit in *Drosophila* (Katanayeva et al., 2010): this pan-G protein Gβ subunit shows both pre- and postsynaptic staining, the latter being even broader than the CD8-GFP-Sh pattern (supplementary material Fig. S1H) or that of anti-Dlg (not shown). A role of Gβ13F both in the nervous system (Schaefer et al.,

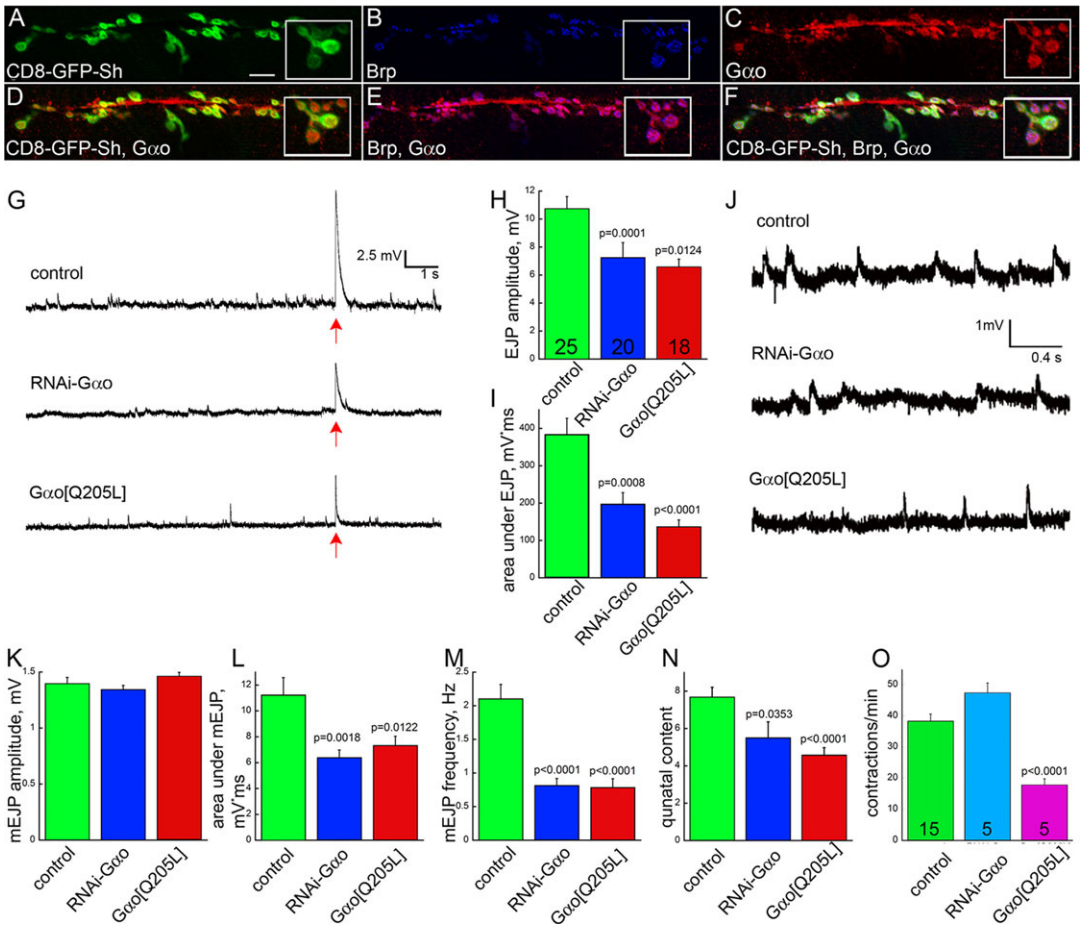

Fig. 1. Gαo is expressed in the presynaptic cell of the NMJ and is required for normal NMJ physiology. (A-F) Gαo (red in C-F) is expressed in the presynaptic side of the NMJ and is barely detected postsynaptically, as judged by colocalization with Brp (blue in B,E,F) but only partial overlap with CD8-GFP-Sh (green in A,D,F). Insets are enlargements of the terminal boutons. Scale bar: 10 μm. (G) Representative traces of spontaneous NMJ activity and one illumination-evoked action potential [arrow indicates the time of illumination; arrow thickness is in scale with the length of illumination (20 ms)] recorded from control (*OK371-Gal4;UAS-ChR2*), RNAi-Gαo (*OK371-Gal4;UAS-ChR2/UAS-RNAi-Gαo*) and Gαo[Q205L] (*OK371-Gal4;UAS-ChR2/UAS-Gαo[Q205L]*) larvae. (H,I) Quantification of amplitude (H) and area under the peak (I) of excitatory junctional potentials (EJPs) from individual muscles from the three genotypes; the number of muscles analyzed is shown in H. (J) Higher magnification of a region in G to show representative traces of spontaneous NMJ activity. (K-M) Quantification of amplitude (K), area (L) and frequency (M) of spontaneous miniature EJPs (mEJPs) of the three genotypes, recorded in the same muscles as in H. (N) Quantal content of the three genotypes calculated as EJP/mEJP. (O) Locomotion activity measured as the number of contractions per minute of third instar larvae of the three genotypes; the number of animals tested is shown in the bars. *P*-values are shown where the observed differences between the mutant and control conditions are statistically significant ($P<0.05$). Error bars indicate s.e.m.

Development (2014) 141, 3399-3409 doi:10.1242/dev.106773

2001) and in muscles (Schnorrer et al., 2010) has been described previously.

To investigate the physiological importance of Gαo in the NMJ, we perturbed Gαo activity in the synapse. Gαo was modulated by the presynaptic expression of two previously tested *UAS* constructs: *RNAi-Gαo*, which downregulates Gαo (Purvanov et al., 2010) (see supplementary material Fig. S1I-K for the efficiency of downregulation); and *Gαo[Q205L]*, which is a constitutively active mutant form that is unable to hydrolyze GTP (Katanaev et al., 2005; Kopein and Katanaev, 2009). These two constructs were driven by the motoneuron driver *OK371-Gal4* (Mahr and Aberle, 2006). Excitatory junctional potentials (EJPs) were induced by light-activated channelrhodopsin-2 (Schroll et al., 2006) (see Materials and Methods). Analysis of EJPs in the NMJ of the control, *RNAi-Gαo* and *Gαo[Q205L]* larvae revealed a marked reduction in EJP amplitude and width with each perturbation of Gαo function (Fig. 1G-I).

We also analyzed spontaneous NMJ activity. Although the amplitude of miniature excitatory junctional potentials (mEJPs) was almost identical in the three conditions, their duration and frequency were strongly reduced upon overactivation and downregulation of Gαo (Fig. 1J-M). Decreased mEJP frequency with largely unperturbed mEJP amplitude suggests that motoneuron-specific modulation of Gαo function mainly induces presynaptic defects. The ratio of EJP to mEJP amplitudes provides the junctional quantal content. This measure of synaptic efficacy is significantly reduced in both mutant conditions (Fig. 1N), suggesting that the number of synaptic vesicles released upon stimulation is decreased in the *RNAi-Gαo* and *Gαo[Q205L]* conditions. These data might indicate that the number of mature boutons or their functionality is decreased by unbalancing Gαo activity in the presynapse. Additionally, we found that in *Gαo[Q205L]* larvae the overall crawling capacity was also perturbed (Fig. 1O).

Aberrant Gαo activity leads to morphological defects in the NMJ similar to those associated with abnormal Wg-Fz2 signaling

To examine why aberrant NMJ physiology accompanies reduced or increased Gαo activity, we performed immunostaining and a morphological investigation of the mutant synapses. We found reduced numbers of boutons in *RNAi-Gαo*-expressing NMJs (Fig. 2A). This reduction was rescued by re-expression of Gαo (but not of an unrelated protein; supplementary material Fig. S2A). Pertussis toxin (Ptx) is a specific inhibitor of Gαo in *Drosophila*, uncoupling it from cognate GPCRs (Katanaev and Tomlinson, 2006b), and its expression in motoneurons led to a ~50% reduction in the number of boutons (Fig. 2A). In addition to *OK371-Gal4*, other drivers such as the pan-neuronal *elav-Gal4* (Luo et al., 1994)

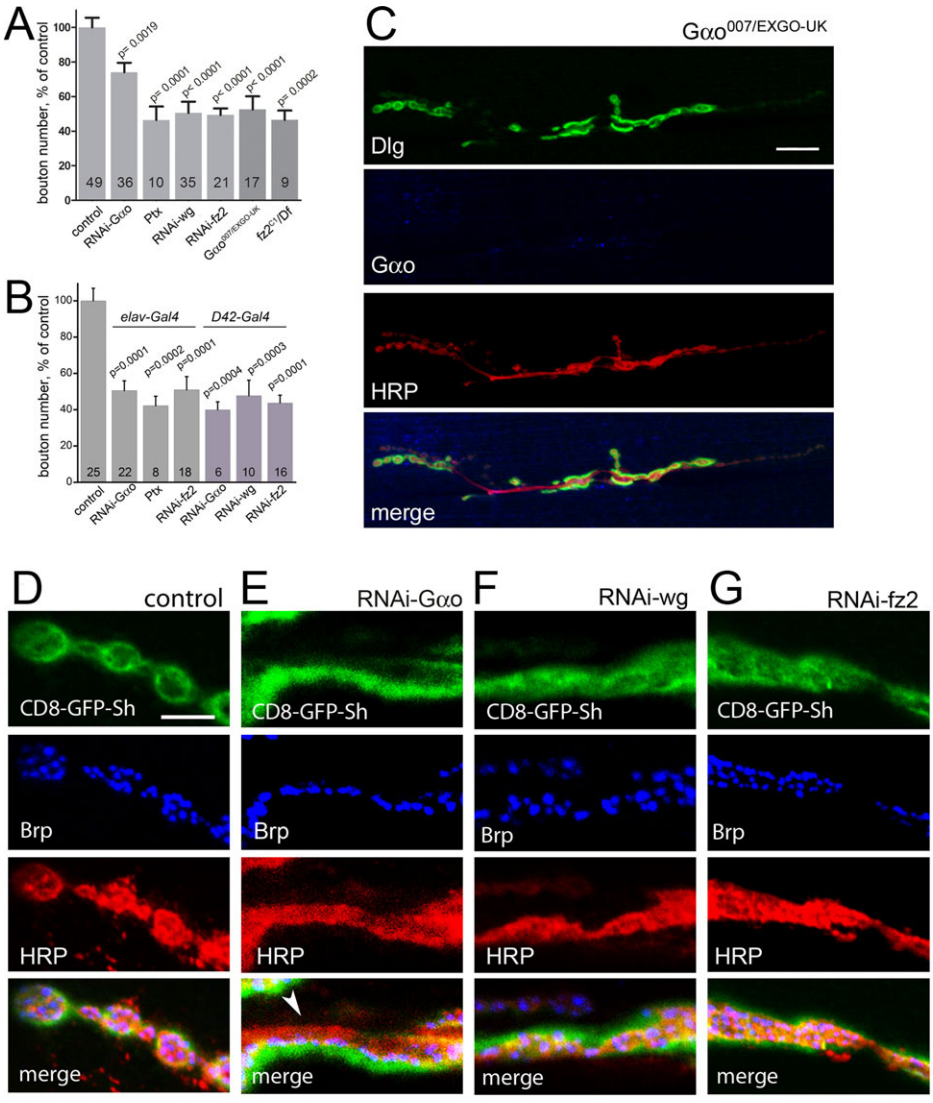

Fig. 2. Gαo is required for NMJ formation, similar to Wg and Fz2. (A) Quantitative analysis of bouton number on muscle 6/7. Presynaptic downregulation of Gαo, Wg and Fz2 with the driver *OK371-Gal4*, expression of Ptx, as well as genetic removal of *Gαo* or *Fz2* lead to a significant decrease in bouton number compared with the wild type (control). Data are represented as percentage of control; the number of NMJs analyzed for each genotype is shown in each bar; *P*-values compared with the control are indicated; error bars indicate s.e.m. (B) Downregulation of Gαo or Fz2 and expression of Ptx with the pan-neuronal driver *elav-Gal4* similarly decrease bouton numbers. The same effect is observed when RNAi against *Gαo*, *wg* or *fz2* is driven with motoneuron-specific *D42-Gal4*. (C) Genetic removal of *Gαo* leads to a strong reduction in bouton number and aberrant NMJ morphology (compare with Fig. 1A-F). Anti-Gαo staining (blue) confirms loss of the proteins; the remaining signal is non-specific. (D-G) Presynaptic downregulation of Gαo, Wg or Fz2 results in malformed boutons. Displayed is a detail of the NMJ on muscle 6/7 that is stained with anti-HRP to visualize the presynaptic cell membrane in red, with anti-Brp to stain the active zones in blue, and the postsynaptic marker CD8-GFP-Sh in green. All mutant genotypes lead to the development of elongated structures with defective overlap of pre- and postsynapse (E, arrowhead) instead of the circular postsynaptic boutons with postsynaptic staining encircling presynaptic staining as in the wild type (D). Scale bars: 20 µm in C; 5 µm in D-G.

Development (2014) 141, 3399-3409 doi:10.1242/dev.106773

(see supplementary material Fig. S1K,L) and the motoneuron-specific *D42-Gal4* (Parkes et al., 1998), when used to target Gαo through expression of RNAi or Ptx, also led to a substantial decrease in bouton numbers (Fig. 2B). The Wg-secreting type Ib boutons (Packard et al., 2002) appeared more severely affected by Gαo perturbations than type Is boutons (supplementary material Fig. S2B). Finally, genetic removal of *Gαo* replicated the Gαo downregulation data (Fig. 2A), resulting in a strong reduction in bouton numbers and aberrant NMJ morphology (Fig. 2C, compare with Fig. 1A-F); presynaptic re-expression of Gαo was able to rescue the $Gαo^{-/-}$ defects (supplementary material Fig. S2A). Thus, Gαo is presynaptically required for proper NMJ development. The decrease in bouton number induced by *RNAi-Gαo* parallels the reduced electric activity of the mutant NMJ (Fig. 1).

Gαo is a transducer of Fz2 (Katanaev et al., 2005; Katanaev and Tomlinson, 2006a; Purvanov et al., 2010), and the Wg-Fz2 pathway has been implicated in NMJ formation. In accordance with previous observations (Packard et al., 2002; Mathew et al., 2005), presynaptic downregulation of Wg (supplementary material Fig. S1M,N) or genetic loss of *fz2* led to a strong decrease in bouton numbers (Fig. 2A,B). Fz2 is present both pre- and postsynaptically (Packard et al., 2002), and the importance of the postsynaptic Fz2 for NMJ development has been demonstrated (Mathew et al., 2005; Mosca and Schwarz, 2010). Here we show that presynaptic Fz2 is also crucial for the NMJ, as specific presynaptic downregulation of Fz2 by various drivers (supplementary material Fig. S1O,P) reduces bouton numbers to the levels found in *fz2* null mutants (Fig. 2A,B). We also tested the ability of presynaptic re-expression of *fz2* to rescue bouton numbers in the *fz2* null background, and observed a complete rescue of bouton number (supplementary material Fig. S1Q,R), analogous to the rescue by postsynaptic *fz2* expression in *fz2* mutants (supplementary material Fig. S1Q) (Mathew et al., 2005), providing evidence for the important neuronal role of the Wg-Fz2 pathway in the NMJ.

This quantitative analysis was corroborated with morphological studies. Genetic removal of *Gαo* (Fig. 2C), expression of Ptx (supplementary material Fig. S1S) or silencing of *Gαo* resulted in clear morphological changes in the NMJ (Fig. 2D,E), similar to those previously described for *wg* loss-of-function mutations (Packard et al., 2002) and identical to those induced by downregulation of Wg and Fz2 (Fig. 2F,G), in which tube-like structures could be observed in the mutant NMJs instead of the normal separate circular boutons, often with diffuse presynaptic Brp and anti-HRP staining.

We next examined the effect of overexpression of different forms of Gαo in the presynapse. In addition to the constitutively GTP-loaded Gαo[Q205L] form used above, we also overexpressed wild-type Gαo and the Gαo[G203T] mutant (Katanaev et al., 2005), which has a reduced affinity for GTP (supplementary material Fig. S2C) but does not behave as a dominant-negative construct (see Discussion). Expression of all three *Gαo* forms with *OK371-Gal4* induced the formation of smaller and more compact boutons as compared with the normal NMJ (Fig. 3A-C). This morphological change was also observed when *wg* (Packard et al., 2002; Miech et al., 2008) or *fz2* was overexpressed presynaptically (Fig. 3D). Overexpression of *fz1* (also known as *fz* – FlyBase), by contrast, did not affect NMJ morphology (not shown). To further verify the influence of Wg signaling on NMJ formation we expressed *RNAi-sgg* in the presynapse, where Sgg localizes (Franco et al., 2004; Miech et al., 2008). Downregulation of this destruction complex protein resulted in a phenotype similar to that of overexpression of *Gαo* or *fz2* (Fig. 3E).

Quantitative analysis showed that overexpression of *Gαo* and its mutant forms, as well as overexpression of *wg* or *fz2* (but not *fz1*) and downregulation of *sgg*, significantly increased the total number of boutons and their density (the number of boutons per µm NMJ length; Fig. 3F; supplementary material Fig. S2D,E). Expression of different dominant-negative constructs of Sgg (SggDN) presynaptically was previously reported to increase bouton number, whereas postsynaptic expression of SggDN had no effect on NMJ formation (Franco et al., 2004; Miech et al., 2008). As the neurotransmitter release properties of Gαo[Q205L] NMJ are reduced (Fig. 1), the increased numbers of boutons observed upon overactivation of the Wnt pathway, as described here, might indicate

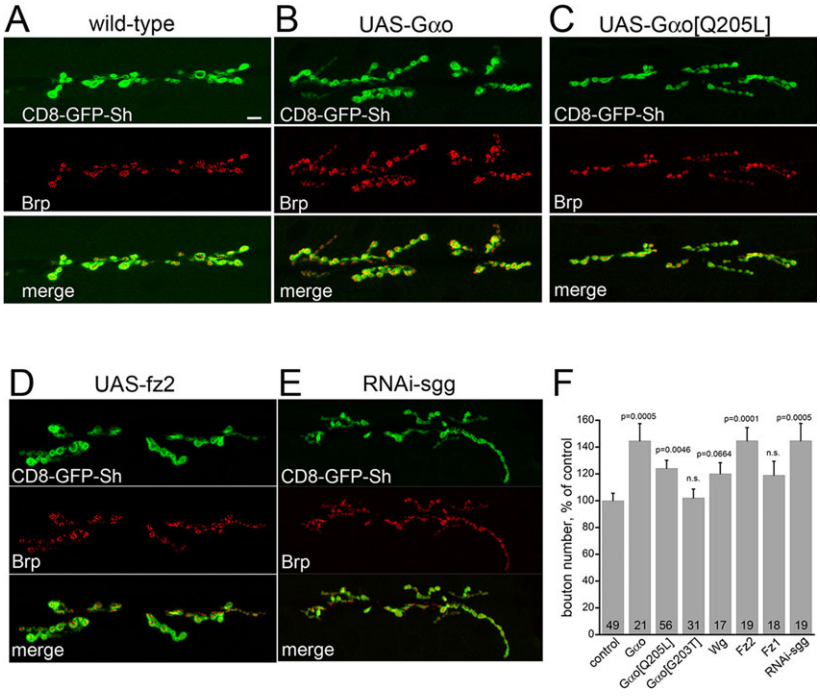

Fig. 3. Overexpression of Gαo or Fz2 in the presynaptic cell, as well as downregulation of Sgg, stimulates bouton formation in NMJ. (A) Wild-type NMJ stained for the presynaptic marker Brp (red); the postsynaptic cell is visualized by CD8-GFP-Sh (green). (B,C) Overexpression of Gαo and its mutant GTP-loaded form (Gαo[Q205L]) in the presynaptic cell leads to enhanced bouton formation. (D,E) Overexpression of *fz2* or expression of *RNAi-sgg* produces similar phenotypes. (F) Quantification of bouton numbers in the different genotypes (shown as in Fig. 2A). n.s., not significant (P>0.05). Scale bar: 10 µm.

Development (2014) 141, 3399-3409 doi:10.1242/dev.106773

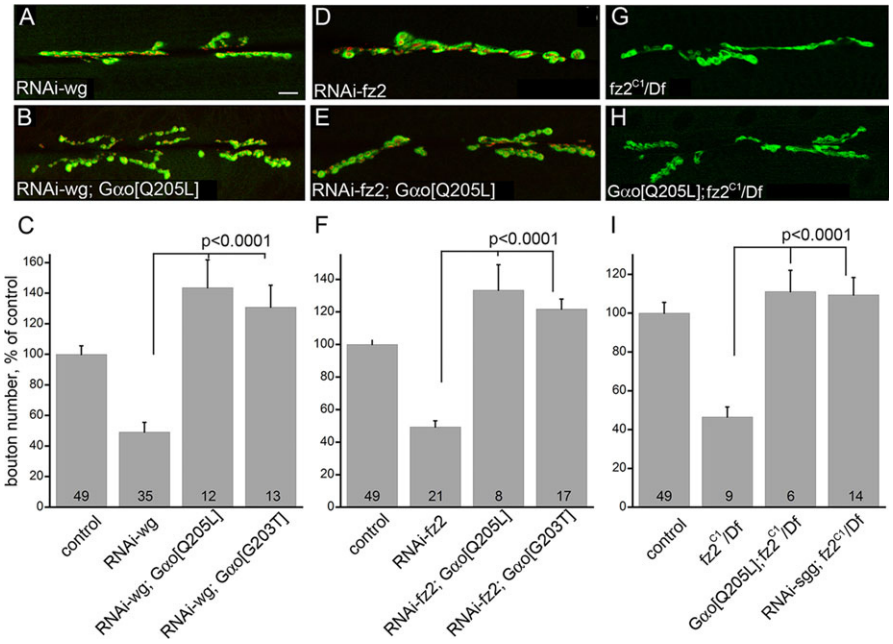

Fig. 4. Gαo acts downstream of Wg-Fz2 in the NMJ. Expression of the GDP-loaded and GTP-loaded mutant forms of Gαo (Gαo[G203T] and Gαo [Q205L], respectively) rescues the *RNAi-wg* (A-C), *RNAi-fz2* (D-F) and the *fz2* mutant (G-I) phenotypes. Brp (red) and CD8-GFP-Sh (green, A,B,D,E) or Dlg (G,H) visualize pre- and postsynaptic compartments, respectively. Quantification of bouton numbers (C,F,I) is as in Fig. 2A; *RNAi-sgg* also rescues the *fz2* null phenotype (I). Scale bar: 10 µm.

that these boutons are non-functional or that Gαo overactivation interferes with proper synaptic transmission.

Cumulatively, these findings suggest that Gαo acts as a transducer of the Wg-Fz2 pathway in the NMJ. Formally, Gαo might alternatively regulate Fz2 abundance in the NMJ. However, no discernible changes in Fz2 levels in the NMJ could be observed in the different *Gαo* backgrounds (supplementary material Fig. S2G).

Gαo is a transducer of Wg and Fz2 in the NMJ

To unequivocally demonstrate that Gαo is a downstream transducer of the Wg-Fz2 signal in the NMJ, we performed epistasis experiments among these proteins. Remarkably, regardless of its nucleotide state, overexpression of *Gαo* in the motoneurons was effective in rescuing the phenotypes obtained by neuronal downregulation of *wg* or *fz2* using RNAi constructs (Fig. 4A-F). In all cases, the morphology of the NMJ resembled that observed in *Gαo*-overexpressing larvae (Fig. 3B,C). The morphological rescue was confirmed by quantitative analysis of bouton numbers (Fig. 4C,F). We further confirmed the epistasis between Gαo and Fz2 using genetic null alleles of *fz2*. Complete loss of Fz2 substantially alters the morphology of the NMJ and decreases bouton numbers (Fig. 4G,I). These phenotypes could be completely rescued by neuronal expression of *Gαo[Q205L]* (Fig. 4H,I). The same rescue of the *fz2* null could be achieved by *RNAi-sgg* (Fig. 4I).

Thus, Gαo acts as a (presumably immediate) transducer of Wg-Fz2 signaling in the NMJ. The similar efficiencies of the GTP- and GDP-loaded forms of Gαo in executing the Wg-Fz2 signal suggest that the molecular target(s) of Gαo in this signaling pathway does not discriminate between the two nucleotide states of the G protein.

Ank2 physically binds to and acts downstream of Gαo in the *Drosophila* NMJ

To identify potential Gαo target proteins, we performed a yeast two-hybrid screen with a *Drosophila* head cDNA library as prey and Gαo as bait (Kopein and Katanaev, 2009). We identified three clones of Ank2 interacting with Gαo with high confidence. The interaction site could be narrowed to amino acids 47-123 of Ank2 (Fig. 5A; see Materials and Methods). In order to confirm the Gαo-Ank2 interaction and to investigate its dependence on guanine nucleotides, we bacterially expressed and purified a truncated maltose-binding protein (MBP)-tagged Ank2 construct (Ank2_12) that consisted of the first 12 ankyrin repeats containing the Gαo binding site (see supplementary material Fig. S3A for characterization of the resulting recombinant protein). We additionally purified highly active recombinant Gαo (Kopein and Katanaev, 2009). In the pull-down experiments, we found that Gαo and Ank2_12 efficiently interacted with each other, supporting the yeast two-hybrid data (Fig. 5B). The GDP- and GTPγS-loaded forms of Gαo were equally efficient in Ank2 binding, expanding the list of Gαo target proteins that do not discriminate between the two nucleotide forms of this G protein (Katanaev, 2010). Importantly, preincubation of Gαo with Gβγ dramatically reduced the amounts of Gαo pulled down by Ank2_12 (Fig. 5C, top). Furthermore, the small amounts of Gαo still interacting with Ank2_12 in this experiment remained Gβγ free, as no Gβγ was detected in Ank2 pull-downs (Fig. 5C, bottom). Thus, Ank2 behaves as a true effector of Gαo, interacting with the monomeric Gβγ-free form of this G protein.

The described (Koch et al., 2008; Pielage et al., 2008; see also Fig. 5D) phenotypes of *Ank2* mutants resemble those that we see upon RNAi-mediated presynaptic downregulation of *Gαo*, *fz2* and *wg*. To test whether Ank2 is epistatic to Wg-Fz2-Gαo signaling, we overactivated this pathway at different levels in the *Ank2* null background. Overexpression of *Gαo* or *Gαo[Q205L]* or downregulation of *sgg* failed to rescue the bouton morphology of the *Ank2* nulls (Fig. 5D-G), and the bouton density remained severely decreased (Fig. 5H), suggesting that Ank2 is epistatic to both Gαo and Sgg in synapse formation. However, Gαo could still localize to the NMJ despite Ank2 absence (supplementary material Fig. S3C), demonstrating that Ank2 does not merely control Go localization in the NMJ.

We also expressed RNAi against *Ank2L* (Pielage et al., 2008) with *OK371-Gal4*, producing morphological defects similar to those resulting from downregulation of *wg*/*fz2*/*Gαo* (Fig. 5I). Overexpression of *wg* or *fz2* in the *RNAi-Ank2L* background failed to restore or improve the synaptic morphology and bouton numbers of *Ank2* downregulation (Fig. 5J,K). Fz2 faithfully localizes to the NMJ despite reduced Ank2 levels (Fig. 5K; supplementary material Fig. S2G), again arguing that Ank2 does not simply regulate the

Development (2014) 141, 3399-3409 doi:10.1242/dev.106773

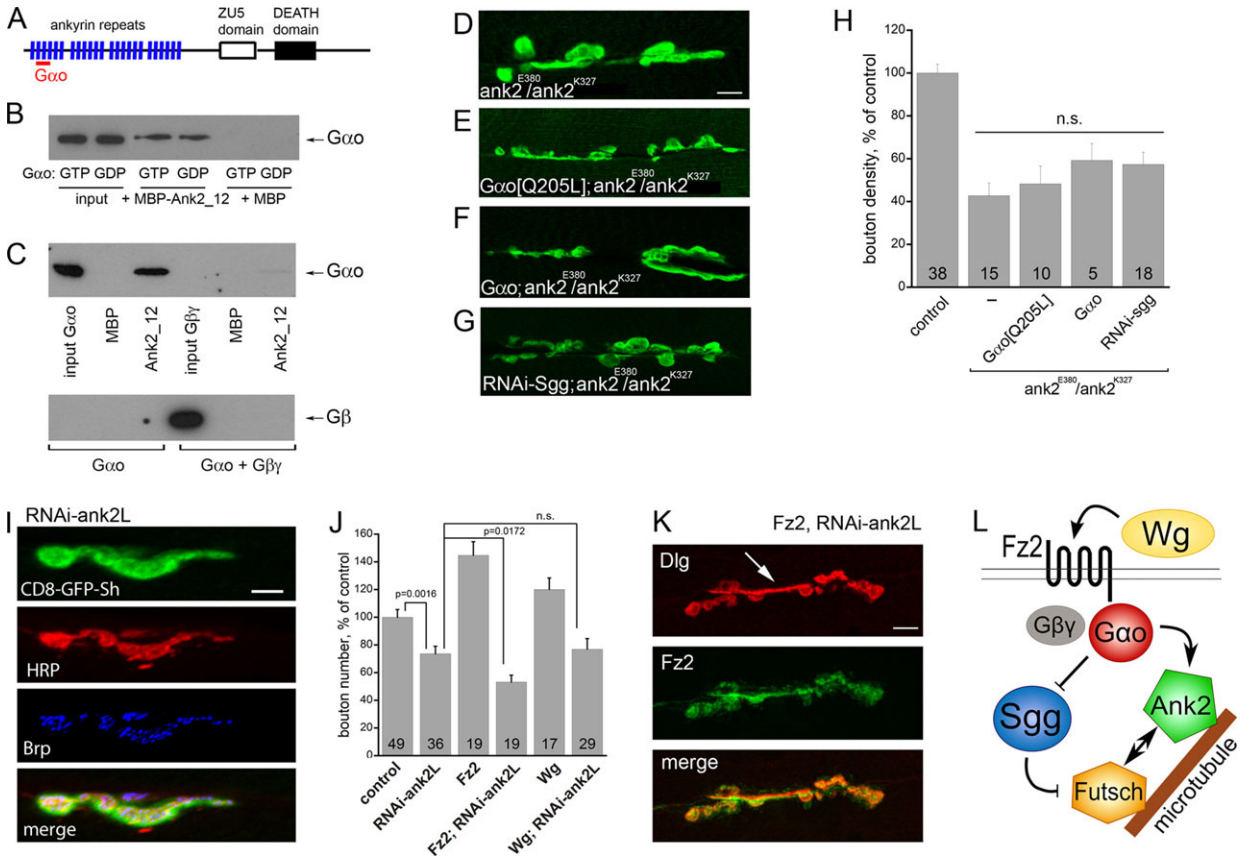

Fig. 5. Ank2 acts downstream from Gαo and physically interacts with it. (A) Structure of Ank2, displaying the four ankyrin-repeat domains (each composed of six ankyrin repeats), the ZU5 (spectrin binding) and the DEATH domains. The Gαo binding site detected in the yeast two-hybrid screen is located between amino acids 47 and 123 (red bar). (B) Pull-down experiments between Gαo and truncated Ank2 (Ank2_12, consisting of the first 12 ankyrin repeats) confirm the yeast two-hybrid interaction. Gαo efficiently interacts with Ank2 regardless of the guanine nucleotide with which it is preloaded (GDP or GTPγS). Maltose-binding protein (MBP) is the negative control showing no interaction with Gαo. (C) The binding between Gαo and Ank2 is outcompeted by Gβγ: preincubation of Gαo with equimolar Gβγ drastically diminishes the amounts of Gαo competent to interact with Ank2_12; Gβγ is not pulled down by Ank2. The bottom western blot panel is intentionally overexposed to show that no Gβγ is pulled down by Ank2. (D-G) *Ank2* null reveals severe NMJ phenotypes (D) that are not rescued by overexpression of *Gαo[Q205L]* (E), *Gαo* (F) or *RNAi-sgg* (G). (H) Bouton density in *Ank2* null phenotypes. Data are shown as bouton number per length of NMJ, as percentage of control; n.s., not significant (P>0.05). (I) High magnification of *RNAi-Ank2* shows morphological defects similar to downregulation of Wg, Fz2 or Gαo. (J,K) Overexpression of Wg or Fz2 fails to rescue the reduced bouton formation (J; data shown as in Fig. 2A) and morphological abnormalities (K) of *RNAi-Ank2*. (K) Immunostaining for Dlg provides a postsynaptic marker, whereas Fz2-GFP marks the presynapse. Elongated tube-like, bouton-less staining is visible (arrow). (L) Model of microtubule cytoskeleton regulation during NMJ formation. The Wg-Fz2 ligand-receptor complex activates the heterotrimeric Go protein, releasing Gαo, which in turn inhibits the Sgg-containing destruction complex. As a result, Sgg-mediated phosphorylation of Futsch is decreased. Futsch, in parallel, interacts with Ank2, the latter additionally being under direct control by Gαo. This combined action on microtubule-binding proteins coordinately regulates the microtubule cytoskeleton, as required for synaptic remodeling. Scale bars: 10 µm in D,K; 5 µm in I.

localization of Wg-Fz2-Gαo signaling components. Altogether, Ank2 appears to act downstream of the Wg-Fz2-Gαo pathway.

As Ank2 has been shown to regulate bouton stability (Hortsch et al., 2002; Koch et al., 2008; Pielage et al., 2008), we next analyzed the extent of synaptic retractions in *Ank2* mutants with or without activation of Gαo. Loss of the microtubule-binding protein Futsch is considered as the first step of synaptic retraction, followed by loss of cytoplasmic proteins such as Synapsin (Pielage et al., 2008). In accordance with previous studies (Koch et al., 2008; Pielage et al., 2008), we observed that ~40% of the $Ank2^{-/-}$ boutons lost Synapsin staining and ~60% lost Futsch (supplementary material Fig. S3D,F,H). As expected, expression of *Gαo[Q205L]* in the $Ank2^{-/-}$ NMJs failed to restore synaptic stability when evaluated at the level of Synapsin or Futsch (supplementary material Fig. S3E,G,H). Thus, Gαo cannot rescue synapse stability in the absence of Ank2, confirming that Ank2 is epistatic to the Wg-Fz2-Gαo pathway.

We next analyzed presynaptic abnormalities in NMJs with reduced Gαo and found that ~8% of *Gαo* mutant boutons and 5.4% of the *RNAi-Gαo* boutons are completely devoid of Ank2 immunostaining [supplementary material Fig. S3I; 7.91±2.71% (n=18) and 5.41±1.73% (n=23), respectively, as compared with 0.73±0.30% (n=31) in wild-type NMJs (mean±s.e.m.); P=0.0012 and P=0.0033, respectively]. Reciprocally, in the absence of Ank2, overactivation of Gαo induces a significant number of ghost boutons and neuronal processes [bouton-like structures and interconnecting processes containing presynaptic HRP staining but lacking postsynaptic CD8-GFP-Sh (Ataman et al., 2006)] (supplementary material Fig. S3J,K); such structures are rarely visible in other genotypes (Ataman et al., 2006). Thus, it can be suggested that the Wg-Fz2-Gαo pathway recruits Ank2 to build a synapse, and in the absence of the latter the synapse does not form properly.

Gαo-ankyrin interaction is conserved in the mammalian neurite outgrowth pathway

As an independent means of proving the mechanistic relationship between Gαo and ankyrins, and to show that this interaction is of

Development (2014) 141, 3399-3409 doi:10.1242/dev.106773

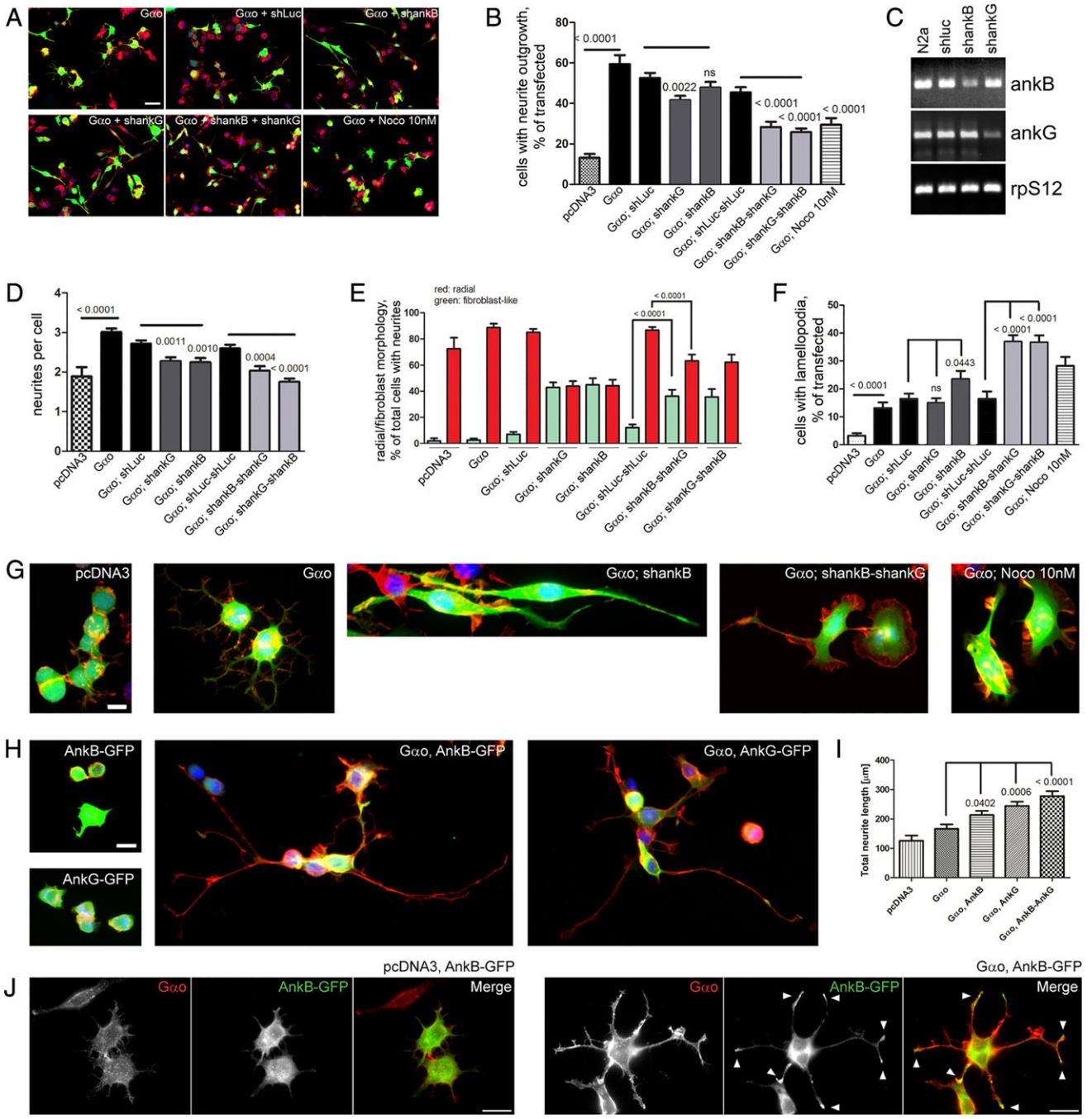

Fig. 6. Gαo-mediated neurite outgrowth and neuronal morphology in N2a cells require AnkB and AnkG. (A) Overexpression of Gαo stimulates the formation of neurites in parental mouse N2a cells and in cells stably transfected with control shRNA (shluc). Permanent shRNA-induced downregulation of *AnkB* (shankB) or *AnkG* (shankG) results in the formation of elongated fibroblast-like cells, increases lamellopodia formation and slightly reduces the percentage of cells growing neurites and the number of neurites per cell. Transient ankyrin double knockdowns achieved by transfection of the shankB and shankG stable cell lines with the shankG and shankB plasmids, respectively, strongly increase the effects observed in single knockdowns. Treatment of Gαo-overexpressing N2a cells with Nocodazole (Noco) mimics the ankyrin double-knockdown phenotypes. Co-expression of EGFP (green) marks transfected cells and staining with phalloidin-Rhodamine (red) and DAPI (blue) is used to visualize F-actin and nuclei, respectively. (B) Quantification of the effects of Gαo overexpression on neurite outgrowth as compared with control transfected (pcDNA3) N2a cells, in shRNA stably transfected cell lines and in the presence of 10 nM Nocodazole. Data represent mean±s.e.m.; horizontal black lines indicate groups of statistical analysis and *P*-values are given above each bar (ns, not significant). (C) RT-PCR analysis shows the reduction in *AnkB* and *AnkG* expression in shRNA stably transfected N2a cells. Expression of the ribosomal protein S12 gene (*Rps12*) served as control. (D-F) Quantification of effects on the number of neurites per cell (D), cell morphology (E) and lamellopodia formation (F) of overexpression of Gαo in parental and shRNA-treated N2a cells. Data representation and statistical analysis are as in B. (G) Representative images of control transfected (pcDNA3) N2a cells and Gαo overexpression in parental as well as in single and double AnkB and AnkG knockdowns. Nocodazole treatment mimics the effects of Gαo overexpression in ankyrin double knockdowns. (H) Representative images of N2a cells overexpressing EGFP-tagged AnkB or AnkG show a substantial increase in the length of neurites upon co-expression with *Gαo*, but not alone. Fluorescence as in A. (I) Quantification of total neurite length in H. Data representation and statistical analysis are as in B. (J) Overexpression of *Gαo* induced the local accumulation of AnkB-GFP at neurite tips (arrowheads), which is not observed in control cells transfected with AnkB-GFP alone. Red fluorescence indicates Gαo immunostaining. Scale bars: 20 µm in A; 10 µm in G,H,J.

Development (2014) 141, 3399-3409 doi:10.1242/dev.106773

importance beyond the *Drosophila* NMJ, we turned to the well-characterized neurite outgrowth pathway in mouse neuroblastoma N2a cells.

As previously reported (Jordan et al., 2005), we find that overexpression of *Gαo* induces strong neurite outgrowth in N2a cells (Fig. 6A,B), with ∼60% of cells forming neurites. N2a cells express both neuronal mammalian ankyrins: *AnkB* and *AnkG* (*Ank2* and *Ank3* – Mouse Genome Informatics) (Fig. 6C) (Santuccione et al., 2013). We downregulated *AnkB*, *AnkG* or both using shRNA constructs (Fig. 6C), and investigated whether Gαo was still capable of inducing neurite outgrowth in these mutant backgrounds. The overall number of N2a cells with neurite outgrowth, as well as the number of neurites per cell induced by Gαo, were decreased in *AnkB* and *AnkG* single knockdowns, and further decreased in double knockdowns (Fig. 6A,B,D).

However, the most dramatic effect of *AnkB*/*G* knockdown on Gαo-induced neurite outgrowth was seen at the level of overall cell morphology (Fig. 6E-G). Whereas *Gαo*-overexpressing cells (as well as N2a cells spontaneously producing neurites) possessed a radial morphology, with several neurites undergoing outgrowth in multiple directions (Fig. 6E,G), *Gαo* overexpression in *AnkB* and *AnkG* single knockdowns induced a very characteristic bilateral, fibroblast-like morphology (Fig. 6E,G), which often additionally included the formation of lamellopodia (Fig. 6G). Remarkably, the double knockdowns further increased the number of cells that were massively producing lamellopodia instead of neurites (Fig. 6F,G). It appears that the lamellopodial phenotype of *Gαo*-overexpressing, *AnkB*/*G* double-knockdown cells is a more severe manifestation of the fibroblast-like morphology seen in *Gαo*-overexpressing, *AnkB* or *AnkG* single-knockdown cells (Fig. 6E,F). By contrast, *AnkB*/*G* knockdowns in control cells do not change in cellular appearance (supplementary material Fig. S4A). As an independent means to induce neurite outgrowth, we overexpressed MARK2 (also known as PAR1b) (Biernat et al., 2002) and found that the resulting phenotype was unaffected by the double knockdown of *AnkB* and *AnkG* (supplementary material Fig. S4B,C), indicating that akyrins are specifically required for the Gαo-mediated neurite outgrowth pathway.

Thus, reduction in ankyrin levels dramatically alters the ability of Gαo to induce neurite outgrowth in neuronal cells and further changes the cytoskeletal response to Gαo – from neurite production to lamellopodial protrusion. We hypothesized that, in the absence of AnkB/G, the Gαo-responsive cellular program switches from the regulation of microtubules to the actin cytoskeleton. To test this, we treated the *Gαo*-overexpressing cells with different concentrations of nocodazole, which is a microtubule-depolymerizing agent known to impair neurite outgrowth (Heidemann et al., 1985). Remarkably, low nocodazole concentrations could mimic the effect of *AnkB*/*G* double knockdown in *Gαo*-overexpressing cells: the ability of Gαo to induce neurite outgrowth was reduced, with a concomitant increase in the number of lamellopodial cells (Fig. 6F,G; supplementary material Fig. S4D,E).

Next, we examined the effects of co-overexpression of *Gαo* with EGFP-tagged *AnkB* and/or *AnkG*. Notably, co-overexpression of *Gαo* and *AnkB*, *AnkG* or both induced a substantial increase in the total neurite length compared with *Gαo* overexpression alone (Fig. 6H,I), whereas the number of cells displaying neurites and the number of neurites per cell were unaffected (supplementary material Fig. S4F,G). As overexpression of *AnkB* and/or *AnkG* did not induce neurite outgrowth (Fig. 6H), these data further support the functional relationship between Gαo and ankyrins. Interestingly, AnkB (but not AnkG) significantly accumulates at the tips of neurites in *Gαo*-overexpressing cells, but not at spontaneously formed neurites in control N2a cells or at neurites induced by MARK2 co-expression (Fig. 6J; supplementary material Fig. S4H-J). These results indicate that Gαo activity is required to recruit AnkB to the growing neurite tips.

We conclude that the Gαo-Ank interaction is conserved from *Drosophila* to mammalian cells, and that this interaction is crucial for the ability of Gαo to regulate the neuronal microtubule cytoskeleton.

DISCUSSION

Synaptic plasticity underlies learning and memory. Both in invertebrates and vertebrates, activation of Wnt signaling is involved in several aspects of synapse formation and remodeling (Budnik and Salinas, 2011), and defects in this pathway may be causative of synaptic loss and neurodegeneration (Inestrosa and Arenas, 2010). Thus, understanding the molecular mechanisms of synaptic Wnt signaling is of fundamental as well as medical importance. The *Drosophila* NMJ is a powerful model system with which to study glutamatergic synapses (Collins and DiAntonio, 2007), and the Wnt pathway has been widely identified as one of the key regulators of NMJ formation (Packard et al., 2002; Mathew et al., 2005; Miech et al., 2008; Korkut et al., 2009; Mosca and Schwarz, 2010).

Here, we provide important mechanistic insights into Wnt signal transduction in the NMJ, identifying the heterotrimeric Go protein as a crucial downstream transducer of the Wg-Fz2 pathway in the presynapse. We further demonstrate that Ank2, a known player in the NMJ (Koch et al., 2008; Pielage et al., 2008), is a target of Gαo in this signaling.

We find that the α subunit of Go is strongly expressed in the presynaptic cell, and that under- or overactivation of this G protein leads to neurotransmission and behavioral defects. At the level of NMJ morphology, we find that presynaptic downregulation or Ptx-mediated inactivation of *Gαo* recapitulates the phenotypes obtained by similar silencing of *wg* and *fz2*. These data confirm that presynaptic Wg signaling, in addition to the Wg pathway active in the muscle (Mathew et al., 2005; Mosca and Schwarz, 2010), is crucial for proper NMJ formation (Miech et al., 2008), and that Go is required for this process. Furthermore, neuronal Gαo overexpression can rescue the *wg* and *fz2* loss-of-function phenotypes, demonstrating that, as in other contexts of Wnt/Fz signaling (Katanaev et al., 2005; Katanaev and Tomlinson, 2006a; Purvanov et al., 2010), Go acts as a transducer of Wg/Fz2 in NMJ formation. In contrast to its evident function and clear localization in the presynapse, Gαo localization on the muscle side of the synapse is much less pronounced or absent. Unlike Gαo, the main *Drosophila* Gβ subunit is strongly expressed in both the pre- and postsynapse. Thus, a heterotrimeric G protein other than Go might be involved in the postsynaptic Fz2 transduction, as has been implicated in Fz signaling in some other contexts (Egger-Adam and Katanaev, 2008; Koval and Katanaev, 2011; von Maltzahn et al., 2012; Nichols et al., 2013).

A recent study proposed a role for Gαo downstream of the octopamine receptor Octβ1R (Koon and Budnik, 2012). This signaling was proposed to regulate the acute behavioral response to starvation both on type II NMJs (octapaminergic) and on the type I NMJs (glutamatergic) studied here. In contrast to our observations, downregulation of Gαo in these NMJs was proposed to increase, rather than decrease, type I bouton numbers (Koon and Budnik, 2012). We suspect that the main reason for the discrepancy lies in the Gal4 lines used. The *BG439-Gal4* and *C380-Gal4* lines of Koon and Budnik are poorly characterized and, unlike the well-analyzed

Development (2014) 141, 3399-3409 doi:10.1242/dev.106773

pan-neuronal *elav-Gal4* (Luo et al., 1994) and motoneuron-specific *OK371-Gal4* (Mahr and Aberle, 2006) and *D42-Gal4* (Parkes et al., 1998) driver lines used in our study, might mediate a more acute expression. In this case, our study reflects the positive role of Gαo in the developmental formation of glutamatergic boutons, as opposed to a role in acute fine-tuning in response to environmental factors as studied by Koon and Budnik (2012).

Postsynaptic expression of *fz2* was found to fully rescue *fz2* null NMJs (Mathew et al., 2005) (supplementary material Fig. S1Q). Here, we find that presynaptic knockdown of Fz2 (and other components of Wg-Fz2-Gαo signaling) recapitulates *fz2* null phenotypes, whereas presynaptic overactivation of this pathway increases bouton numbers; furthermore, presynaptic overexpression of *fz2* or *Gαo* rescues the *fz2* nulls, just as postsynaptic overexpression of *fz2* does. Our data thus support a crucial role for presynaptic Wg-Fz2-Gαo signaling in NMJ formation. Interestingly, both pre- and postsynaptic re-introduction of Arrow, an Fz2 co-receptor that is normally present both pre- and postsynaptically, as is Fz2 itself, can rescue *arrow* mutant NMJs (Miech et al., 2008). Thus, it appears that the pre- and postsynaptic branches of Fz2 signaling are both involved in NMJ development. A certain degree of redundancy between these branches must exist. Indeed, wild-type levels of Fz2 in the muscle are not sufficient to rescue the bouton defects induced by presynaptic expression of *RNAi-fz2* (Fig. 2A,B,G), yet overexpression of *fz2* in the muscle can restore the bouton integrity of *fz2* nulls (supplementary material Fig. S1Q) (Mathew et al., 2005). One might hypothesize that postsynaptic Fz2 overexpression activates a compensatory pathway – such as that mediated by reduction in laminin A signaling (Tsai et al., 2012) – that leads to restoration in bouton numbers in *fz2* mutants. Our data showing that the targeted downregulation of Fz2 in the presynapse is sufficient to recapitulate the *fz2* null phenotype underpin the crucial function of presynaptic Fz2 signaling in NMJ formation.

We find that downregulation of *Ank2* produces NMJ defects similar to those of *wg*, *fz2* or *Gαo* silencing. However, *Ank2* mutant phenotypes appear more pronounced, indicating that Wg-Fz2-Gαo signaling might control a subset of Ank2-mediated activities in the NMJ. Ank2 was proposed to play a structural role in NMJ formation, binding to microtubules through its C-terminal region (Pielage et al., 2008). However, since the C-terminal region was insufficient to rescue *Ank2L* mutant phenotypes (Pielage et al., 2008), additional domains are likely to mediate Ank2 function through binding to other proteins. We demonstrate here in the yeast two-hybrid system and in pull-down experiments that the ankyrin repeat region of Ank2 physically binds Gαo, suggesting that the function of Ank2 in NMJ formation might be regulated by Wg-Fz2-Gαo signaling. Indeed, epistasis experiments place Ank2 downstream of Gαo in NMJ formation.

Upon dissociation of the heterotrimeric Go protein by activated GPCRs such as Fz2, the liberated Gαo subunit can signal to its downstream targets both in the GTP- and GDP-bound state (the latter after hydrolysis of GTP and before re-association with Gβγ) (Katanaev, 2010). The free signaling Gαo-GDP form is predicted to be relatively long lived (Katanaev and Chornomorets, 2007), and a number of Gαo target proteins have been identified that interact equally well with both of the nucleotide forms of this G protein (Kopein and Katanaev, 2009; Egger-Adam and Katanaev, 2010; Purvanov et al., 2010; Lin and Katanaev, 2013; Lin et al., 2014). In the context of NMJ formation, we find that Gαo-GTP and -GDP are efficient in the activation of downstream signaling, and identify Ank2 as a binding partner of Gαo that interacts with both nucleotide forms. The importance of signaling by Gα-GDP released from a heterotrimeric complex by the action of GPCRs has also been demonstrated in recent studies of mammalian chemotaxis, planar cell polarity and cancer (Ezan et al., 2013; Kamakura et al., 2013; Lin et al., 2014).

Gαo[G203T], which largely resides in the GDP-binding state owing to its reduced affinity for GTP, might be expected to act as a dominant-negative. However, in canonical Wnt signaling, regulation of asymmetric cell division as well as in planar cell polarity (PCP) signaling in the wing, Gαo[G203T] displays no dominant-negative activity but is simply silent (Katanaev et al., 2005; Katanaev and Tomlinson, 2006a), whereas in eye PCP signaling this form acts positively but is weaker than other Gαo forms (V.L.K. and A. Tomlinson, unpublished observations). Biochemical characterization of the mammalian Gαi2[G203T] mutant revealed that it can still bind Gβγ and GTP, but upon nucleotide exchange Gαi2[G203T] fails to adopt the activated confirmation and can further lose GTP (Inoue et al., 1995). Our biochemical characterization confirms that Gαo[G203T] still binds GTP (supplementary material Fig. S2C). Interestingly, Gαi2 [G203T] inhibited only a fraction of Gαi2-mediated signaling (Winitz et al., 1994), suggesting that the dominant-negative effects of the mutant are effector specific. Thus, we infer that a portion of Gαo[G203T] can form a competent Fz2-transducing complex, and a portion of overexpressed Gαo[G203T] resides in a free GDP-loaded form that is also competent to activate downstream targets – Ank2 in the context of NMJ formation.

Our experiments place Ank2 downstream of Gαo and also of Sgg (GSK3β). It remains to be investigated whether Ank2 can directly interact with and/or be phosphorylated by Sgg. Meanwhile, we propose that the microtubule-binding protein Futsch might be a linker between Sgg and Ank2. Futsch is involved in NMJ formation and is placed downstream of Wg-Sgg signaling, being the target of phosphorylation and negative regulation by Sgg as the alternative target to β-catenin, which is dispensable in Wg NMJ signaling (Hummel et al., 2000; Roos et al., 2000; Franco et al., 2004; Gogel et al., 2006; Miech et al., 2008). Abnormal Futsch localization has been observed in *Ank2* mutants (Pielage et al., 2008). In *Drosophila* wing and mammalian cells in culture, Gαo acts upstream of Sgg/GSK3β (Katanaev et al., 2005; Liu et al., 2005). Cumulatively, these data might suggest that the Wg-Fz2-Gαo cascade sends a signal to Futsch through Sgg, parallel to that mediated by Ank2 (Fig. 5L).

The importance of the Gαo-Ank2 interaction for *Drosophila* NMJ development is corroborated by our findings in mammalian neuronal cells, where we demonstrate that the ability of Gαo to induce neurite outgrowth is critically dependent on AnkB and AnkG. Knockdown of either or both ankyrin reduces neurite production. Remarkably, upon AnkB/G downregulation, Gαo switches its activity from the induction of microtubule-dependent processes (neurites) to actin-dependent protrusions (lamellopodia). Furthermore, Gαo recruits AnkB to the growing neurite tips. These data demonstrate that the Gαo-ankyrin mechanistic interactions are conserved from insects to mammals and are important for control over the neuronal tubulin cytoskeleton in the context of neurite growth and synapse formation. The novel signaling mechanism that we have uncovered (Fig. 5L) might thus be of general applicability in animal nervous system development and function.

MATERIALS AND METHODS

Fly stocks

Fly lines are described in supplementary material Methods. Fly crosses were performed at 25°C.

Development (2014) 141, 3399-3409 doi:10.1242/dev.106773

Immunostaining and microscopy analysis of NMJs

Wandering third instar larvae were dissected in PBS as described (Brent et al., 2009) before fixation and immunostaining using the antibodies described in supplementary material Methods. NMJs of muscle 6/7 in segment 2-4 were analyzed in all experiments. Maximally, two segments per animal were analyzed. NMJs were imaged with a Zeiss LSM 510 or LSM710 confocal microscope. For further details see supplementary material Methods.

Electrophysiology and muscle contraction

ChR2-mediated stimulation of synaptic potentials was performed as described (Schroll et al., 2006; Hornstein et al., 2009) and intracellular potentials were recorded in body wall muscles 6/7 (for details see supplementary material Methods).

Yeast two-hybrid screen, pull-down assay and GTP-binding assay

The yeast two-hybrid screen, biological significance score and analysis of the Gαo-interacting region in Ank2 were performed as described (Formstecher et al., 2005; Kopein and Katanaev, 2009). The first 12 ankyrin repeats of Ank2 (Ank2_12) were cloned into pMAL-c2x (New England BioLabs). The MBP-tagged Ank2_12 and MBP alone were bacterially expressed and purified. Recombinant *Drosophila* His_6-Gαo and His_6-Gαo[G203T] were purified in parallel and pull-downs and GTP-binding assays were performed as previously described (Kopein and Katanaev, 2009; Koval et al., 2010). Further details are provided in supplementary material Methods.

Mouse cell culture and neurite outgrowth assay

Mouse neuroblastoma N2a cells were cultured in MEM supplemented with 10% FCS, L-glutamine and penicillin/streptomycin (all from Gibco, Life Technologies). Vector transfections were carried out with X-tremeGENE 9 (Roche) according to the manufacturer's instructions. Permanent AnkB or AnkG depletion in N2a cells was achieved using the pRetroSuper vector (Oligoengine). For the analysis of neurite outgrowth, cells were transfected for 24 h, trypsinized and seeded on poly-L-lysine-coated coverslips for an additional 24 h to allow neurite formation. For Nocodazole (Sigma-Aldrich) treatment, transfected N2a cells were allowed to adhere on coverslips for 6 h before incubation for an additional 18 h with Nocodazole. Cells were finally fixed with 4% paraformaldehyde, stained with phalloidin-Rhodamine (Molecular Probes, Life Technologies) and DAPI (Sigma-Aldrich) or anti-Gαo antibody and mounted for microscopy analysis. For further details see supplementary material Methods.

Statistical analysis

Statistical analysis was performed with SAS JMP 7 and GraphPad Prism 5. Data are presented as mean±s.e.m. *P*-values were obtained by Student's *t*-test.

Acknowledgements

We thank Hermann Aberle, Vivian Budnik, Susan Cumberledge, Corey Goodman, Jean-Paul Vincent, Juergen Knoblich, Andrew Tomlinson, Vann Bennett, Clare Waterman, Bloomington Stock Center, Vienna *Drosophila* RNAi Stock Center, Developmental Studies Hybridoma Bank, and *Drosophila* Genomics Resource Center for generously providing fly stocks, antibodies and plasmids. We thank C. Giovanni Galizia, Claudia Stuermer and Andrew Tomlinson for critically reading the manuscript.

Competing interests

The authors declare no competing financial interests.

Author contributions

A.-M.L. performed the majority of the experiments and wrote the manuscript. G.P.S. designed and performed experiments of Fig. 6 and supplementary material Fig. S4. D.E.-A. participated in the early parts of the project. A.K. performed experiments for supplementary material Fig. S2C. C.L. produced antibodies to Gαo. M.G.B. and S.K. provided the experimental setup and consultation for electrophysiological measurements. V.L.K. designed and supervised the study, analyzed the data and wrote the manuscript.

Funding

This work was supported by grants from the Deutsche Forschungsgemeinschaft, Swiss National Science Foundation, and Synapsis Foundation to V.L.K. Deposited in PMC for immediate release.

Supplementary material

Supplementary material available online at
http://dev.biologists.org/lookup/suppl/doi:10.1242/dev.106773/-/DC1

References

Ataman, B., Ashley, J., Gorczyca, D., Gorczyca, M., Mathew, D., Wichmann, C., Sigrist, S. J. and Budnik, V. (2006). Nuclear trafficking of Drosophila Frizzled-2 during synapse development requires the PDZ protein dGRIP. *Proc. Natl. Acad. Sci. USA* **103**, 7841-7846.

Bennett, V. and Baines, A. J. (2001). Spectrin and ankyrin-based pathways: metazoan inventions for integrating cells into tissues. *Physiol. Rev.* **81**, 1353-1392.

Biernat, J., Wu, Y.-Z., Timm, T., Zheng-Fischhöfer, Q., Mandelkow, E., Meijer, L. and Mandelkow, E.-M. (2002). Protein kinase MARK/PAR-1 is required for neurite outgrowth and establishment of neuronal polarity. *Mol. Biol. Cell* **13**, 4013-4028.

Bouley, M., Tian, M. Z., Paisley, K., Shen, Y. C., Malhotra, J. D. and Hortsch, M. (2000). The L1-type cell adhesion molecule neuroglian influences the stability of neural ankyrin in the Drosophila embryo but not its axonal localization. *J. Neurosci.* **20**, 4515-4523.

Brent, J. R., Werner, K. M. and McCabe, B. D. (2009). Drosophila larval NMJ dissection. *J. Vis. Exp.* pii: 1107, doi: 10.3791/1107.

Budnik, V. and Salinas, P. C. (2011). Wnt signaling during synaptic development and plasticity. *Curr. Opin. Neurobiol.* **21**, 151-159.

Collins, C. A. and DiAntonio, A. (2007). Synaptic development: insights from Drosophila. *Curr. Opin. Neurobiol.* **17**, 35-42.

Dubreuil, R. R. and Yu, J. (1994). Ankyrin and beta-spectrin accumulate independently of alpha-spectrin in Drosophila. *Proc. Natl. Acad. Sci. USA* **91**, 10285-10289.

Egger-Adam, D. and Katanaev, V. L. (2008). Trimeric G protein-dependent signaling by Frizzled receptors in animal development. *Front. Biosci.* **13**, 4740-4755.

Egger-Adam, D. and Katanaev, V. L. (2010). The trimeric G protein Go inflicts a double impact on axin in the Wnt/frizzled signaling pathway. *Dev. Dyn.* **239**, 168-183.

Ezan, J., Lasvaux, L., Gezer, A., Novakovic, A., May-Simera, H., Belotti, E., Lhoumeau, A.-C., Birnbaumer, L., Beer-Hammer, S., Borg, J.-P. et al. (2013). Primary cilium migration depends on G-protein signalling control of subapical cytoskeleton. *Nat. Cell Biol.* **15**, 1107-1115.

Formstecher, E., Aresta, S., Collura, V., Hamburger, A., Meil, A., Trehin, A., Reverdy, C., Betin, V., Maire, S., Brun, C. et al. (2005). Protein interaction mapping: a Drosophila case study. *Genome Res.* **15**, 376-384.

Franco, B., Bogdanik, L., Bobinnec, Y., Debec, A., Bockaert, J., Parmentier, M.-L. and Grau, Y. (2004). Shaggy, the homolog of glycogen synthase kinase 3, controls neuromuscular junction growth in Drosophila. *J. Neurosci.* **24**, 6573-6577.

Gilman, A. G. (1987). G proteins: transducers of receptor-generated signals. *Annu. Rev. Biochem.* **56**, 615-649.

Gögel, S., Wakefield, S., Tear, G., Klämbt, C. and Gordon-Weeks, P. R. (2006). The Drosophila microtubule associated protein Futsch is phosphorylated by Shaggy/Zeste-white 3 at an homologous GSK3beta phosphorylation site in MAP1B. *Mol. Cell. Neurosci.* **33**, 188-199.

Guan, B., Hartmann, B., Kho, Y.-H., Gorczyca, M. and Budnik, V. (1996). The Drosophila tumor suppressor gene, dlg, is involved in structural plasticity at a glutamatergic synapse. *Curr. Biol.* **6**, 695-706.

Heidemann, S. R., Joshi, H. C., Schechter, A., Fletcher, J. R. and Bothwell, M. (1985). Synergistic effects of cyclic AMP and nerve growth factor on neurite outgrowth and microtubule stability of PC12 cells. *J. Cell Biol.* **100**, 916-927.

Hornstein, N. J., Pulver, S. R. and Griffith, L. C. (2009). Channelrhodopsin2 mediated stimulation of synaptic potentials at Drosophila neuromuscular junctions. *J. Vis. Exp.* e1133.

Hortsch, M., Paisley, K. L., Tian, M.-Z., Qian, M., Bouley, M. and Chandler, R. (2002). The axonal localization of large Drosophila ankyrin2 protein isoforms is essential for neuronal functionality. *Mol. Cell. Neurosci.* **20**, 43-55.

Hummel, T., Krukkert, K., Roos, J., Davis, G. and Klämbt, C. (2000). Drosophila Futsch/22C10 is a MAP1B-like protein required for dendritic and axonal development. *Neuron* **26**, 357-370.

Inestrosa, N. C. and Arenas, E. (2010). Emerging roles of Wnts in the adult nervous system. *Nat. Rev. Neurosci.* **11**, 77-86.

Inoue, S., Hoshino, S., Kukimoto, I., Ui, M. and Katada, T. (1995). Purification and characterization of the G203T mutant alpha i-2 subunit of GTP-binding protein expressed in baculovirus-infected Sf9 cells. *J. Biochem.* **118**, 650-657.

Jan, L. Y. and Jan, Y. N. (1982). Antibodies to horseradish peroxidase as specific neuronal markers in Drosophila and in grasshopper embryos. *Proc. Natl. Acad. Sci. USA* **79**, 2700-2704.
Jordan, J. D., He, J. C., Eungdamrong, N. J., Gomes, I., Ali, W., Nguyen, T., Bivona, T. G., Philips, M. R., Devi, L. A. and Iyengar, R. (2005). Cannabinoid receptor-induced neurite outgrowth is mediated by Rap1 activation through G (alpha)o/i-triggered proteasomal degradation of Rap1GAPII. *J. Biol. Chem.* **280**, 11413-11421.
Kamakura, S., Nomura, M., Hayase, J., Iwakiri, Y., Nishikimi, A., Takayanagi, R., Fukui, Y. and Sumimoto, H. (2013). The cell polarity protein mInsc regulates neutrophil chemotaxis via a noncanonical G protein signaling pathway. *Dev. Cell* **26**, 292-302.
Katanaev, V. L. (2010). The Wnt/Frizzled GPCR signaling pathway. *Biochemistry* **75**, 1428-1434.
Katanaev, V. L. and Chornomorets, M. (2007). Kinetic diversity in G-protein-coupled receptor signalling. *Biochem. J.* **401**, 485-495.
Katanaev, V. L. and Tomlinson, A. (2006a). Dual roles for the trimeric G protein Go in asymmetric cell division in Drosophila. *Proc. Natl. Acad. Sci. USA* **103**, 6524-6529.
Katanaev, V. L. and Tomlinson, A. (2006b). Multiple roles of a trimeric G protein in Drosophila cell polarization. *Cell Cycle* **5**, 2464-2472.
Katanaev, V. L., Ponzielli, R., Sémériva, M. and Tomlinson, A. (2005). Trimeric G protein-dependent frizzled signaling in Drosophila. *Cell* **120**, 111-122.
Katanayeva, N., Kopein, D., Portmann, R., Hess, D. and Katanaev, V. L. (2010). Competing activities of heterotrimeric G proteins in Drosophila wing maturation. *PLoS ONE* **5**, e12331.
Koch, I., Schwarz, H., Beuchle, D., Goellner, B., Langegger, M. and Aberle, H. (2008). Drosophila ankyrin 2 is required for synaptic stability. *Neuron* **58**, 210-222.
Koon, A. C. and Budnik, V. (2012). Inhibitory control of synaptic and behavioral plasticity by octopaminergic signaling. *J. Neurosci.* **32**, 6312-6322.
Kopein, D. and Katanaev, V. L. (2009). Drosophila GoLoco-protein pins is a target of Galpha(o)-mediated G protein-coupled receptor signaling. *Mol. Biol. Cell* **20**, 3865-3877.
Korkut, C., Ataman, B., Ramachandran, P., Ashley, J., Barria, R., Gherbesi, N. and Budnik, V. (2009). Trans-synaptic transmission of vesicular Wnt signals through Evi/Wntless. *Cell* **139**, 393-404.
Koval, A. and Katanaev, V. L. (2011). Wnt3a stimulation elicits G-protein-coupled receptor properties of mammalian Frizzled proteins. *Biochem. J.* **433**, 435-440.
Koval, A., Kopein, D., Purvanov, V. and Katanaev, V. L. (2010). Europium-labeled GTP as a general nonradioactive substitute for [(35)S]GTPgammaS in high-throughput G protein studies. *Anal. Biochem.* **397**, 202-207.
Lin, C. and Katanaev, V. L. (2013). Kermit interacts with galphao, vang, and motor proteins in Drosophila planar cell polarity. *PLoS ONE* **8**, e76885.
Lin, C., Koval, A., Tishchenko, S., Gabdulkhakov, A., Tin, U., Solis, G. P. and Katanaev, V. L. (2014). Double suppression of the Galpha protein activity by RGS proteins. *Mol. Cell* **53**, 663-671.
Liu, X., Rubin, J. S. and Kimmel, A. R. (2005). Rapid, Wnt-induced changes in GSK3beta associations that regulate beta-catenin stabilization are mediated by Galpha proteins. *Curr. Biol.* **15**, 1989-1997.
Logan, C. Y. and Nusse, R. (2004). The Wnt signaling pathway in development and disease. *Annu. Rev. Cell Dev. Biol.* **20**, 781-810.
Luo, L., Liao, Y. J., Jan, L. Y. and Jan, Y. N. (1994). Distinct morphogenetic functions of similar small GTPases: Drosophila Drac1 is involved in axonal outgrowth and myoblast fusion. *Genes Dev.* **8**, 1787-1802.
Mahr, A. and Aberle, H. (2006). The expression pattern of the Drosophila vesicular glutamate transporter: a marker protein for motoneurons and glutamatergic centers in the brain. *Gene Expr. Patterns* **6**, 299-309.
Mathew, D., Ataman, B., Chen, J., Zhang, Y., Cumberledge, S. and Budnik, V. (2005). Wingless signaling at synapses is through cleavage and nuclear import of receptor DFrizzled2. *Science* **310**, 1344-1347.
Miech, C., Pauer, H.-U., He, X. and Schwarz, T. L. (2008). Presynaptic local signaling by a canonical wingless pathway regulates development of the Drosophila neuromuscular junction. *J. Neurosci.* **28**, 10875-10884.
Mosca, T. J. and Schwarz, T. L. (2010). The nuclear import of Frizzled2-C by Importins-beta11 and alpha2 promotes postsynaptic development. *Nat. Neurosci.* **13**, 935-943.
Nichols, A. S., Floyd, D. H., Bruinsma, S. P., Narzinski, K. and Baranski, T. J. (2013). Frizzled receptors signal through G proteins. *Cell. Signal.* **25**, 1468-1475.
Packard, M., Koo, E. S., Gorczyca, M., Sharpe, J., Cumberledge, S. and Budnik, V. (2002). The Drosophila Wnt, wingless, provides an essential signal for pre- and postsynaptic differentiation. *Cell* **111**, 319-330.
Parkes, T. L., Elia, A. J., Dickinson, D., Hilliker, A. J., Phillips, J. P. and Boulianne, G. L. (1998). Extension of Drosophila lifespan by overexpression of human SOD1 in motorneurons. *Nat. Genet.* **19**, 171-174.
Pielage, J., Cheng, L., Fetter, R. D., Carlton, P. M., Sedat, J. W. and Davis, G. W. (2008). A presynaptic giant ankyrin stabilizes the NMJ through regulation of presynaptic microtubules and transsynaptic cell adhesion. *Neuron* **58**, 195-209.
Purvanov, V., Koval, A. and Katanaev, V. L. (2010). A direct and functional interaction between Go and Rab5 during G protein-coupled receptor signaling. *Sci. Signal.* **3**, ra65.
Roos, J., Hummel, T., Ng, N., Klämbt, C. and Davis, G. W. (2000). Drosophila Futsch regulates synaptic microtubule organization and is necessary for synaptic growth. *Neuron* **26**, 371-382.
Santuccione, A. C., Merlini, M., Shetty, A., Tackenberg, C., Bali, J., Ferretti, M. T., McAfoose, J., Kulic, L., Bernreuther, C., Welt, T. et al. (2013). Active vaccination with ankyrin G reduces beta-amyloid pathology in APP transgenic mice. *Mol. Psychiatry* **18**, 358-368.
Schaefer, M., Petronczki, M., Dorner, D., Forte, M. and Knoblich, J. A. (2001). Heterotrimeric G proteins direct two modes of asymmetric cell division in the Drosophila nervous system. *Cell* **107**, 183-194.
Schnorrer, F., Schönbauer, C., Langer, C. C. H., Dietzl, G., Novatchkova, M., Schernhuber, K., Fellner, M., Azaryan, A., Radolf, M., Stark, A. et al. (2010). Systematic genetic analysis of muscle morphogenesis and function in Drosophila. *Nature* **464**, 287-291.
Schroll, C., Riemensperger, T., Bucher, D., Ehmer, J., Völler, T., Erbguth, K., Gerber, B., Hendel, T., Nagel, G., Buchner, E. et al. (2006). Light-induced activation of distinct modulatory neurons triggers appetitive or aversive learning in Drosophila larvae. *Curr. Biol.* **16**, 1741-1747.
Sternweis, P. C. and Robishaw, J. D. (1984). Isolation of two proteins with high affinity for guanine nucleotides from membranes of bovine brain. *J. Biol. Chem.* **259**, 13806-13813.
Tsai, P.-I., Wang, M., Kao, H.-H., Cheng, Y.-J., Lin, Y.-J., Chen, R.-H. and Chien, C.-T. (2012). Activity-dependent retrograde laminin A signaling regulates synapse growth at Drosophila neuromuscular junctions. *Proc. Natl. Acad. Sci. USA* **109**, 17699-17704.
von Maltzahn, J., Bentzinger, C. F. and Rudnicki, M. A. (2012). Wnt7a-Fzd7 signalling directly activates the Akt/mTOR anabolic growth pathway in skeletal muscle. *Nat. Cell Biol.* **14**, 186-191.
Wagh, D. A., Rasse, T. M., Asan, E., Hofbauer, A., Schwenkert, I., Dürrbeck, H., Buchner, S., Dabauvalle, M.-C., Schmidt, M., Qin, G. et al. (2006). Bruchpilot, a protein with homology to ELKS/CAST, is required for structural integrity and function of synaptic active zones in Drosophila. *Neuron* **49**, 833-844.
Winitz, S., Gupta, S. K., Qian, N. X., Heasley, L. E., Nemenoff, R. A. and Johnson, G. L. (1994). Expression of a mutant Gi2 alpha subunit inhibits ATP and thrombin stimulation of cytoplasmic phospholipase A2-mediated arachidonic acid release independent of Ca2+ and mitogen-activated protein kinase regulation. *J. Biol. Chem.* **269**, 1889-1895.
Wolfgang, W. J., Quan, F., Goldsmith, P., Unson, C., Spiegel, A. and Forte, M. (1990). Immunolocalization of G protein alpha-subunits in the Drosophila CNS. *J. Neurosci.* **10**, 1014-1024.
Zito, K., Parnas, D., Fetter, R. D., Isacoff, E. Y. and Goodman, C. S. (1999). Watching a synapse grow: noninvasive confocal imaging of synaptic growth in Drosophila. *Neuron* **22**, 719-729.

SUPPLEMENTARY METHODS

Fly stocks

The following lines used were: *OK371-Gal4* (Mahr and Aberle, 2006); *CD8-GFP-Sh* (Zito et al., 1999); *UAS-RNAi-ank2L* (Pielage et al., 2008); *UAS-GFP-Wg* (Pfeiffer et al., 2002); *UAS-Ptx*, *UAS-Gαo*, *UAS-Gαo[Q205L]*, *UAS-Gαo[G203T]* (Katanaev et al., 2005); *UAS-Fz2* (Chen et al., 2004); *UAS-Fz* (Strapps and Tomlinson, 2001); *UAS-wg-GFP* (Pfeiffer et al., 2002); *omb-Gal4* (Lecuit et al., 1996). The following lines were from the Vienna *Drosophila* RNAi Center (Dietzl et al., 2007): *UAS-RNAi-fz2* (VDRC#44391), *UAS-RNAi-Gαo* (#19124 and #110552 were used with identical results), *UAS-RNAi-wg* (#13351), *UAS-RNAi-ank2* (#26121), *UAS-RNAi-sgg* (#7005). *Df(3L)ED4782* deficiency (Hummel et al., 2000), *UAS-ChR2* (Schroll et al., 2006), *elav-Gal4*, D42-Gal4, *BG487-Gal4*, *GMR-Gal4* and *UAS-myr-mRFP* were from the Bloomington Stock Center. The *fz2* mutant condition was $fz2^{C1}$/ *Df(3L)ED4782* following Mathew et al. (2005). The $ank2^{E380}$ and $ank2^{K327}$ alleles (Koch et al., 2008) were used in the transheterozygote combination to analyze the *Ank2* mutant phenotypes. Although *Gαo* mutant alleles are embryonic lethal (Fremion et al., 1999; Katanaev et al., 2005), we could obtain third instar larvae of the transheterozygous genotype $Gαo^{007}$/$Gαo^{EXGO-UK}$. The first allele is a hypomorph (Fremion et al., 1999), whereas the second is a small deletion in the region (gift from A. Tomlinson). The transheterozygous larvae emerged from the genetic cross at a frequency of 23% (expected frequency 33%) but developed 1-2 days later than their heterozygous siblings; they died during early pupal stages. For the *Gαo* rescue experiments, $Gαo^{EXGO-UK}$ was recombined with *OK371-Gal4*; the presence of the driver in the recombinant was confirmed by crossing to *UAS-myr-mRFP*; the presence of the mutation was confirmed by lethality over the parental and other *Gαo* alleles. The muscle size of the heterozygous larvae was somewhat reduced compared with control larvae (Fig. S2F). All crosses were performed at 25°C.

Antibodies and immunohistochemistry

Wandering third instar larvae were dissected in PBS as described (Brent et al., 2009), fixed in 3.7% formaldehyde/PBS or, in the case of anti-Wg staining, in Bouins fixative (Reactives RAL) for 15 min and washed three times in PBS for 10 min. The dissected larvae were incubated in PBS containing 0.05% Triton X-100 (PBT) + 5% normal goat serum (NGS) for at least 30 min at room temperature. Primary antibodies were diluted in PBT plus 5% NGS and incubated at room temperature for 2 h or at 4°C overnight. The following primary antibodies were used: Cy3-coupled goat anti-HRP (123-165-021, Jackson ImmunoResearch) at 1:200; rabbit anti-Wg (Reichsman et al., 1996) at 1:300; rabbit anti-Fz2 (Packard et al., 2002) at 1:10,000; rabbit anti-Gβ13F (Schaefer et al., 2001) at 1:250; and anti-Ank2XL (Koch et al., 2008) at 1:500; mouse anti-Brp (nc82), anti-Dlg (4F3), anti-Futsch (22C10) and anti-Synapsin (3C11) (all at 1:100; Developmental Studies Hybridoma Bank); rabbit anti-Gαo at 1:100 (Merck, #371726, raised against the C-terminal decapeptide of human Gαo and Gαi3). The specificity of these anti-Gαo antibodies to recognize *Drosophila* Gαo but not Gαi was confirmed in wing imaginal discs of *omb-Gal4; UAS-Gαo* and *omb-Gal4; UAS-Gαi* larvae (Fig. S1E,F). The efficiency of these overexpression lines had been tested previously (Katanaev and Tomlinson, 2006); wing discs were immunostained as described (Katanaev et al., 2005). Additionally, the specificity of these antibodies (1:1000) to *Drosophila* Gαo but not Gαi was proven by western blots of head extracts (Kopein and Katanaev, 2009) from wild-type, *UAS-Gαo; GMR-Gal4* and *UAS-Gαi; GMR-Gal4* flies (Fig. S1G). Gαi, migrating lower than Gαo on SDS-PAGE, was undetected in *Drosophila* heads without overexpression, but was efficiently overexpressed with the *UAS-Gαi* construct as detected by polyclonal anti-Gαi antibodies (Merck, #371723, raised against the C-terminal decapeptide of human Gαi1 and Gαi2; used at 1:1000); these antibodies also recognized *Drosophila* Gαo (Fig. S1G). Additional rabbit polyclonal antibodies against *Drosophila* Gαo

were raised using the recombinant protein purified from bacteria (Kopein and Katanaev, 2009); the antiserum was used at 1:100 for immunostaining. Specificity of this antiserum was confirmed by western blots on *Drosophila* head extracts, as well as by immunostaining of wing imaginal discs. Secondary antibodies were HRP labeled for western blots (1:4000) or Cy3- and Cy5-labeled in immunostaining (1:400 in PBT, 2h incubation at room temperature). The preparations were mounted in Vectashield (Vector Labs), dorsal side up.

Microscopy and analysis of NMJs

The well-characterized NMJs of muscle 6/7 in segment 2-4 were analyzed in all experiments. Maximally, two segments per animal (e.g. segment A3 and A4, both in the same hemisphere, or both segments A3 in the two hemispheres) were analyzed. NMJs were imaged with a confocal microscope (Zeiss LSM 510 or Zeiss LSM710). For statistical analysis, one optical slice with a thickness of 2.3 µm was taken with a 20x or a 25x objective in the optical plane of each NMJ and the boutons were measured manually with the help of the program AxioVision 4.7 (Zeiss). A bouton was identified by the CD8-GFP-Sh, anti-Dlg and/or anti-HRP staining as a circular or slightly oval structure with clear borders, connected by neurites to the neighboring bouton; all these methods resulted in identical bouton quantifications. Type 1b boutons were distinguished from type Is by more intense anti-Dlg staining and their larger size (Packard et al., 2002). Bouton number values are depicted as percentage of the respective control. The length of the NMJ was measured from the first to the last bouton along the synaptic cleft and all side branches on the muscle surface with more than three boutons were measured and added to the total length of the NMJ. The lengths of the NMJ slightly varied depending on the phenotype, in agreement with (Mathew et al., 2005) (Fig. S2E).

To confirm that the *OK371-Gal4/UAS-RNAi* system was efficient to downregulate Gαo, Wg and Fz2, respective immunostainings of wild-type and *RNAi*-expressing NMJs were

performed in parallel. NMJs were imaged with a LSM710 (Zeiss) confocal microscope using identical settings for all images. Quantification of the fluorescence was performed with ImageJ (NIH). The presynaptic cell was outlined with the freehand selection tool following the borders of the staining and the mean value of the fluorescence of this area was measured with the measure tool. A noticeable downregulation in the levels of the respective proteins was achieved (Fig. S1I,M,O), and quantification revealed a ~50% decrease in anti-Gαo/Wg/Fz2 staining in the NMJ (Fig. S1J,N,P). However, this is likely to be a gross underestimation of the efficiency of the RNAi-mediated downregulation: using a pan-neuronal driver (*elav-Gal4*), we find a comparable decrease in anti-Gαo immunostaining (Fig. S1K), but in western blots on whole-head extracts of the control versus the *RNAi-Gαo* constructs, a dramatic decrease in Gαo levels could be seen (Fig. S1L). Mouse anti-tubulin (Sigma, 1:2500) staining served as loading control.

Electrophysiology and muscle contraction

ChR2-mediated stimulation of synaptic potentials was performed as described (Schroll et al., 2006; Hornstein et al., 2009). Larvae expressing ChR2 in motoneurons using the driver *OK371-Gal4* were grown on standard corn food supplemented with 1 mM *all-trans*-retinal (Sigma) at 25°C in the dark. Wandering third instar larvae were dissected in cold Ca^{2+}-free HL-3 saline (Zhang and Stewart, 2010) and washed three times in cold HL-3 supplemented with 1.5 mM $CaCl_2$ before performing the measurements in same buffer. Intracellular potentials were recorded in body wall muscles 6/7 using a pipette with a resistance of 15-30 MΩ when filled with 1 M KCl. To evoke single action potentials, animals were stimulated by a 20 ms light pulse of 470 nm using a high-power LED placed 10 cm from the larvae (light pulse triggered at 1.2V, Thorlabs) controlled by Chart Master software (HEKA). Electrophysiological signals were pre-amplified (without filtering) using the LPF-8 signal conditioner (Warner Instruments) and the 50 Hz noise was reduced using the HumBug (Quest scientific) noise reducer. Finally, analog signals were

measured using a KS-700 amplifier (World Precision Instruments) then digitized using LIH8+8 (HEKA). Data were acquired using the Chart Master software at a sampling frequency of 20 kHz. The data were low-pass filtered at 2 kHz before analysis of EJPs and mEJPs with the Mini analysis program (Synaptosoft). The threshold for detection of peaks was set to 0.3 mV. For analysis only muscles with a resting potential more negative than –46 mV were used. Note that the optogenetic measurements used here and the traditional electrophysiological recordings produce identical EJP amplitudes when measured side-by-side (Pulver et al., 2011) (note also that, in this particular work, utilizing the same *OK371-Gal4* driver as used by us, the EJP amplitude in the wild-type is measured as ~12.5 mV, very similar to our measurement of 11 mV; see Fig. 1H). Furthermore, when performing our own optogenetic measurements, we sometimes (rarely) observed non-stimulated, spontaneous action potentials which were of the same amplitude as the light-induced ones (such an example is shown on Fig. S1T).

For the locomotion test, third instar larvae were placed on a 1% agarose plate and allowed to adjust for 1 min. The number of whole body contractions per minute was counted.

Yeast two-hybrid screen

Isoform II of *Drosophila* Gαo was used as the bait, and the cDNA library from *Drosophila* head was used as the prey in the screening custom-performed by Hybrigenics (Paris, France). Fifty four million clones were screened and analyzed as described (Kopein and Katanaev, 2009). The three clones of Ank2 representing partial open reading frames each had the high confidence interaction score]biological significance score (Formstecher et al., 2005)] (B, *E*-value < 1e–5). The Gαo-interacting region in Ank2 was determined as described (Formstecher et al., 2005; Kopein and Katanaev, 2009).

Biochemistry

We amplified the first 12 ankyrin repeats of Ank2 from cDNA clone RE55168 (*Drosophila* Genomics Resource Center, EST collection) using primers 5'-GGGCATGCATGGCCCAGTTTGTGACC-3' and 5'-CCGGTACCGGCACTAATGCTGGCACC-3' and inserted the fragment into pMAL-c2x (New England Biolabs). The MBP-tagged protein was expressed in TOP10F' cells (Invitrogen). Transformed cells were grown at 37°C until OD_{600} = 0.7, cooled to 17°C before induction with 0.1 mM IPTG and subsequent growth overnight at 17°C, and then harvested by 15 min centrifugation at 4000 ***g***. The pellet was resuspended in column buffer [20 mM Tris-HCl, 200 mM NaCl, 1 mM EDTA, 1 mM DTT, 1 mg/ml lysozyme, 1x Complete protease inhibitor cocktail (Roche)] and incubated on ice for 30-60 min before sonification lysis, followed by centrifugation for 30 min at 16,000 ***g*** to remove cell debris. The protein was bound to amylose resin (New England BioLabs) by incubation at 4°C for at least 1 h. The amylose beads were washed three times for 10-15 min with column buffer and the protein was eluted with 10 mM maltose in column buffer. Control MBP was prepared using the pMAL-c2x plasmid in parallel.

The Gαo[G203T] mutation was introduced by site mutagenesis using pQE32-Gαo (Kopein and Katanaev, 2009) as the template. The following primers were used: sense, AATTGTTTGACGTGACCGGTCAGCGCTC; antisense, GAGCGCTGACCGGTCACGTCAAACAATT. Recombinant *Drosophila* His_6-Gαo was prepared and preloaded with 1 mM GDP or GTPγS as described (Kopein and Katanaev, 2009); His_6-Gαo[G203T] was purified in parallel.

Pull-down assays

Thirty micrograms of His_6-Gαo were incubated with a twofold molar excess of MBP or MBP-Ank2_12 in HKB* buffer (100 mM KCl, 50 mM HEPES-KOH, 10 mM NaCl, 5 mM $MgCl_2$, 2 mM EGTA, 1 mM DTT, 5% glycerol, 0.5% NP40, 0.1% Tween) at 17°C for 1.5 h, prior to

addition to 100 µl 50% amylose resin slurry (New England BioLabs) pre-equilibrated with HKB* for an additional 1.5 h incubation at 17°C. The resin was washed four times with 1.5 ml HKB* for 15 min. The retained proteins were eluted by a 15 min incubation with 50 µl 10 mM maltose in HKB*. The proteins were resolved on 10% SDS-PAGE, electrotransferred to nitrocellulose membranes (Whatman) and detected by immunoblotting using rabbit anti-Gαo/i at 1:1000 (Merck). Equal loading was ensured by immunoblotting using rabbit anti-MBP antibodies at 1:4000 (New England Biolabs). For experiments with Gβγ, His6-Gαo was pre-incubated with the βγ dimer purified from porcine brains (Koval et al., 2010) for 45 min at room temperature before addition of equimolar amounts of MBP-Ank2_12 or MBP and incubation for an additional 1.5 h at 4°C. The pre-equilibrated resin was added to the proteins, incubated for 1.5 h and washed as described above. Proteins were eluted by addition of 5x sample buffer and boiling.

GTP-binding assay

Poorly hydrolysable fluorescent GTP analog Eu-GTP (PerkinElmer) was used in the GTP-binding assay with purified His_6-tagged *Drosophila* Gαo and Gαo[G203T] as described (Koval et al., 2010). The indicated (Fig. S2C) concentrations of the proteins were incubated for 2 hours in the presence of 5 nM GTP-Eu in 1xHKB buffer (10 mM HEPES-NaOH, 135 mM KCl, 10 mM NaCl, 2 mM EGTA, pH 7.5) supplemented with 5 mM $MgCl_2$. The reaction mixtures were subsequently transferred to AcroWell BioTrace NT 96-well plates (Pall), filtered using a vacuum manifold, and the membranes were washed twice with ice-cold washing buffer (20 mM Tris-HCl, 0.1 mM $MgCl_2$, pH 8.0). Fluorescence of the label retained on the membranes was measured immediately in a Victor^3 multilabel counter (PerkinElmer) in TRF mode. All experimental points were measured in duplicate. Curve fitting was performed in Prism 5 software (GraphPad).

Cell culture

Mouse neuroblastoma N2a cells were cultured in MEM supplemented with 10% FCS, L-glutamine and penicillin/streptomycin (all from Gibco, Life Technologies). Vector transfections were carried out with X-tremeGENE 9 (Roche) according to the manufacturer's instructions. Permanent AnkB or AnkG depletion in N2a cells was obtained by shRNA interference using annealed primers inserted into the *Bam*HI and *Hin*dIII sites of the pRetroSuper vector. Specific target sequences for murine *AnkB* and *AnkG* were previously described (Ayalon et al., 2008). Primers used for *AnkB*: 5′ sense strand, 5′-gatccccGAGTGGCCAACATCATATAttcaagagaTATATGATGTTGGCCACTCttttta-3′; and 3′ antisense strand, 5′-agcttaaaaaGAGTGGCCAACATCATATAtctcttgaaTATATGATGTTGGCCACTCggg-3′. For *AnkG*: 5′ sense strand, 5′-gatccccGGCAGACAGACGCCAGAGCttcaagagaGCTCTGGCGTCTGTCTGCCttttta-3′; and 3′ antisense strand, 5′-agcttaaaaaGGCAGACAGACGCCAGAGCtctcttgaaGCTCTGGCGTCTGTCTGCCggg-3′. A shluc vector expressing an shRNA against firefly luciferase was used as control. To generate stable lines, shRNA vectors were transfected into N2a cells and selection was performed in normal medium supplemented with 10 μg/ml puromycin. Downregulation of *AnkB* and *AnkG* expression was confirmed by standard RT-PCR methods using primers that recognize all ankyrin isoforms: ankB-For 5′-ACAGGTGATGGGGGAGAATAC-3′; ankB-Rev 5′-GAGTCCATTGTGTCTGCATCC-3′; ankG-For 5′-GCCTGCTCATAGGAAGAGGAA-3′; ankG-Rev 5′-GTCATGACCTTGTTGCAGAGC-3′. Primers to detect expression of the ribosomal protein S12 gene were used as control: S12-For 5′-GGGGCTAGCGCCACCATGGCCGAGGAAGGCATTGC-3′; S12-Rev 5′-GGGAGATCTTCATTTCTTGCATTTGAAATAC-3′.

Neurite outgrowth assay

N2a cells were co-transfected for 24 h with pEGFP-C1 (Clontech) and pcDNA3.1+ (Invitrogen) or a plasmid encoding human Gαo (Missouri S&T cDNA Resource Center). Cells were trypsinized and seeded on poly-L-lysine-coated coverslips for an additional 24 h to allow neurite formation. Alternatively, cells were transfected with EGFP-tagged ankyrin-B or ankyrin-G vectors (Ayalon et al., 2008) or co-transfected with the Gαo plasmid and prepared as above. Transient ankyrin double knockdowns were obtained by co-transfection of the shRNA-stably transfected N2a cell lines with the shRNA vectors shluc, shankB or shankG in addition to the plasmids described above. Ankyrin-independent neurite outgrowth was analyzed using an EGFP-tagged MARK2 (PAR1b) plasmid (Nishimura et al., 2012) under the transient double ankyrin knockdown conditions described above. Additionally, an mRFP-tagged MARK2 plasmid was generated by subcloning the *Bgl*II-*Kpn*I fragment including the MARK2 sequence into the same sites of the pmRFP-C1 vector. Then, N2a cells were co-transfected with the mRFP-MARK2 and AnkB-GFP plasmids and prepared as above. AnkB-GFP mean fluorescence intensities at the rear end of neurites (10-20 μm^2) and at whole neurites were scored from 40-80 neurites per condition using ImageJ, and the ratio values were used to determine AnkB-GFP accumulation at neurite tips in cells co-transfected with control pcDNA3.1+, Gαo or mRFP-MARK2 plasmids. For Nocodazole treatment, transfected N2a cells were allowed to adhere on coverslips for 6 h before incubation for an additional 18 h with Nocodazole (Sigma-Aldrich) in normal medium at the concentrations indicated in the corresponding figures. Cells were finally fixed with paraformaldehyde, stained with phalloidin-Rhodamine (Molecular Probes, Life Technologies) and DAPI (Sigma-Aldrich) or anti-Gαo antibody and mounted for microscopy analysis. Samples were recorded with an α-Plan-Apochromat 63x/1.4 or a Plan-Neofluar 20x/0.50 objective on an

AxioImager M1 microscope equipped with an AxioCam HRc camera and analyzed using AxioVision software (all from Zeiss). The number of transfected cells displaying neurites and lamellopodia, neurites per cell, total neurite length, and cell morphology were scored from 15-20 randomly taken images (>200 cells per condition).

Supplementary references

Ayalon, G., Davis, J. Q., Scotland, P. B. and Bennett, V. (2008) 'An ankyrin-based mechanism for functional organization of dystrophin and dystroglycan', *Cell* 135(7): 1189-200.

Brent, J. R., Werner, K. M. and McCabe, B. D. (2009) 'Drosophila larval NMJ dissection', *J Vis Exp*(24).

Chen, C. M., Strapps, W., Tomlinson, A. and Struhl, G. (2004) 'Evidence that the cysteine-rich domain of Drosophila Frizzled family receptors is dispensable for transducing Wingless', *Proceedings of the National Academy of Sciences of the United States of America* 101(45): 15961-6.

Dietzl, G., Chen, D., Schnorrer, F., Su, K. C., Barinova, Y., Fellner, M., Gasser, B., Kinsey, K., Oppel, S., Scheiblauer, S. et al. (2007) 'A genome-wide transgenic RNAi library for conditional gene inactivation in Drosophila', *Nature* 448(7150): 151-6.

Formstecher, E., Aresta, S., Collura, V., Hamburger, A., Meil, A., Trehin, A., Reverdy, C., Betin, V., Maire, S., Brun, C. et al. (2005) 'Protein interaction mapping: a Drosophila case study', *Genome Research* 15(3): 376-84.

Fremion, F., Astier, M., Zaffran, S., Guillen, A., Homburger, V. and Semeriva, M. (1999) 'The heterotrimeric protein Go is required for the formation of heart epithelium in Drosophila', *Journal of Cell Biology* 145(5): 1063-76.

Hornstein, N. J., Pulver, S. R. and Griffith, L. C. (2009) 'Channelrhodopsin2 mediated stimulation of synaptic potentials at Drosophila neuromuscular junctions', *J Vis Exp*(25).

Hummel, T., Krukkert, K., Roos, J., Davis, G. and Klambt, C. (2000) 'Drosophila Futsch/22C10 is a MAP1B-like protein required for dendritic and axonal development', *Neuron* 26(2): 357-70.

Katanaev, V. L., Ponzielli, R., Semeriva, M. and Tomlinson, A. (2005) 'Trimeric G protein-dependent frizzled signaling in Drosophila', *Cell* 120(1): 111-22.

Katanaev, V. L. and Tomlinson, A. (2006) 'Dual roles for the trimeric G protein Go in asymmetric cell division in Drosophila', *Proceedings of the National Academy of Sciences of the United States of America* 103(17): 6524-9.

Koch, I., Schwarz, H., Beuchle, D., Goellner, B., Langegger, M. and Aberle, H. (2008) 'Drosophila ankyrin 2 is required for synaptic stability', *Neuron* 58(2): 210-22.

Kopein, D. and Katanaev, V. L. (2009) 'Drosophila GoLoco-protein pins is a target of Galpha(o)-mediated G protein-coupled receptor signaling', *Molecular Biology of the Cell* 20(17): 3865-77.

Koval, A., Kopein, D., Purvanov, V. and Katanaev, V. L. (2010) 'Europium-labeled GTP as a general nonradioactive substitute for [(35)S]GTPgammaS in high-throughput G protein studies', *Analytical Biochemistry* 397(2): 202-207.

Lecuit, T., Brook, W. J., Ng, M., Calleja, M., Sun, H. and Cohen, S. M. (1996) 'Two distinct mechanisms for long-range patterning by Decapentaplegic in the Drosophila wing', *Nature* 381(6581): 387-93.

Mahr, A. and Aberle, H. (2006) 'The expression pattern of the Drosophila vesicular glutamate transporter: a marker protein for motoneurons and glutamatergic centers in the brain', *Gene Expr Patterns* 6(3): 299-309.
Mathew, D., Ataman, B., Chen, J., Zhang, Y., Cumberledge, S. and Budnik, V. (2005) 'Wingless signaling at synapses is through cleavage and nuclear import of receptor DFrizzled2', *Science* 310(5752): 1344-7.
Nishimura, Y., Applegate, K., Davidson, M. W., Danuser, G. and Waterman, C. M. (2012) 'Automated screening of microtubule growth dynamics identifies MARK2 as a regulator of leading edge microtubules downstream of Rac1 in migrating cells', *PLoS One* 7(7): e41413.
Packard, M., Koo, E. S., Gorczyca, M., Sharpe, J., Cumberledge, S. and Budnik, V. (2002) 'The Drosophila Wnt, wingless, provides an essential signal for pre- and postsynaptic differentiation', *Cell* 111(3): 319-30.
Pfeiffer, S., Ricardo, S., Manneville, J. B., Alexandre, C. and Vincent, J. P. (2002) 'Producing cells retain and recycle Wingless in Drosophila embryos', *Current Biology* 12(11): 957-62.
Pielage, J., Cheng, L., Fetter, R. D., Carlton, P. M., Sedat, J. W. and Davis, G. W. (2008) 'A presynaptic giant ankyrin stabilizes the NMJ through regulation of presynaptic microtubules and transsynaptic cell adhesion', *Neuron* 58(2): 195-209.
Pulver, S. R., Hornstein, N. J., Land, B. L. and Johnson, B. R. (2011) 'Optogenetics in the teaching laboratory: using channelrhodopsin-2 to study the neural basis of behavior and synaptic physiology in Drosophila', *Advances in physiology education* 35(1): 82-91.
Reichsman, F., Smith, L. and Cumberledge, S. (1996) 'Glycosaminoglycans can modulate extracellular localization of the wingless protein and promote signal transduction', *Journal of Cell Biology* 135(3): 819-27.
Schaefer, M., Petronczki, M., Dorner, D., Forte, M. and Knoblich, J. A. (2001) 'Heterotrimeric G proteins direct two modes of asymmetric cell division in the Drosophila nervous system', *Cell* 107(2): 183-94.
Schroll, C., Riemensperger, T., Bucher, D., Ehmer, J., Voller, T., Erbguth, K., Gerber, B., Hendel, T., Nagel, G., Buchner, E. et al. (2006) 'Light-induced activation of distinct modulatory neurons triggers appetitive or aversive learning in Drosophila larvae', *Current Biology* 16(17): 1741-7.
Strapps, W. R. and Tomlinson, A. (2001) 'Transducing properties of Drosophila Frizzled proteins', *Development* 128(23): 4829-35.
Zhang, B. and Stewart, B. (2010) 'Electrophysiological recording from Drosophila larval body-wall muscles', *Cold Spring Harb Protoc* 2010(9): pdb prot5487.
Zito, K., Parnas, D., Fetter, R. D., Isacoff, E. Y. and Goodman, C. S. (1999) 'Watching a synapse grow: noninvasive confocal imaging of synaptic growth in Drosophila', *Neuron* 22(4): 719-29.

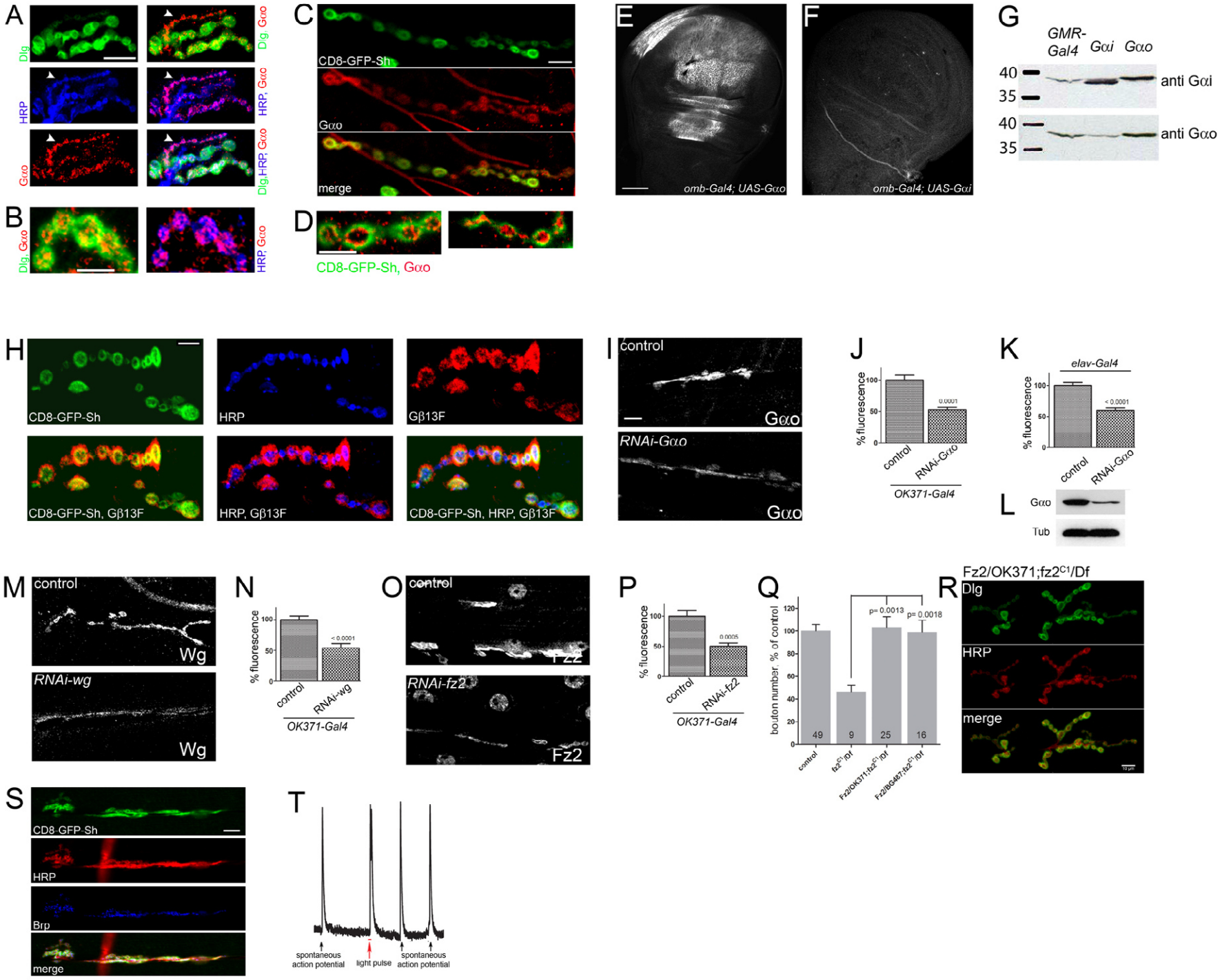
A
Dlg
Dlg, Gαo
HRP
HRP, Gαo
Gαo
Dlg,HRP, Gαo
B
Dlg, Gαo
HRP, Gαo
C
CD8-GFP-Sh
Gαo
merge
D
CD8-GFP-Sh, Gαo
E
omb-Gal4; UAS-Gαo
F
omb-Gal4; UAS-Gαi
G
GMR-Gal4
Gαi
Gαo
40
35
anti Gαi
anti Gαo
H
CD8-GFP-Sh
HRP
Gβ13F
CD8-GFP-Sh, Gβ13F
HRP, Gβ13F
CD8-GFP-Sh, HRP, Gβ13F
I
control
Gαo
RNAi-Gαo
J
% fluorescence
control
RNAi-Gαo
OK371-Gal4
K
elav-Gal4
L
Gαo
Tub
M
control
Wg
RNAi-wg
N
RNAi-wg
O
Fz2
RNAi-fz2
P
Q
bouton number, % of control
p= 0.0013
p= 0.0018
49
9
25
16
R
Fz2/OK371;fz2C1/Df
Dlg
HRP
merge
S
CD8-GFP-Sh
HRP
Brp
merge
T
spontaneous action potential
light pulse
spontaneous action potential

Figure S1. Characterization of the anti-Gαo antibodies and the RNAi lines.

(A) Gαo (red) is expressed in the presynaptic side of NMJ and is barely detected postsynaptically, as judged by colocalization with anti-HRP (blue) but only partial overlap with Dlg (green). Arrowhead points to the types Is boutons depicting low anti-Dlg staining. Scale bar 10μm. (B) High-magnification anti-Dlg (green), -Gαo (red), and -HRP (blue) staining. Scale bar 5μm. (C) Rabbit polyclonal antiserum raised against recombinant *Drosophila* Gαo produces the same staining pattern as shown in Figure 1. Scale bar 10μm. (D) High-magnification CD8-GFP-Sh (green) and anti-Gαo (red) staining. Scale bar 5μm. (E, F) The *omb-Gal4* driver was used to overexpress *Drosophila* Gαo (E) or Gαi (F) in wing imaginal discs. The anti-Gαo antibodies (Merck, raised against the C-terminal peptide corresponding to human Gαo, used in Figure 1) recognized overexpressed Gαo in the characteristic *omb* domain. In contrast, Gαi was not detected even with enhanced microscope settings. Scale bar 50μm. (G) Western blot of fly head extracts (wild type or overexpressing Gαo or Gαi) probed with antibodies against Gαo or Gαi. The anti-Gαo antibodies (Merck) recognize only the higher-migrating Gαo, both endogenous and overexpressed. The anti-Gαi antibodies (Merck) recognize both *Drosophila* Gαo and Gαi; Gαi migrates lower than Gαo and is not detectable in the non-Gαi-overexpressing samples. (H) Gβ13F (red) is found both in the presynapse colocalizing with anti-HRP (blue) and in the postsynapse colocalizing with, and even expanding the domain of, CD8-GFP-Sh (green). Scale bar 5μm. (I) Immunostainings of the wild-type (control) and *RNAi-Gαo*-expressing NMJ driven with *OK371-Gal4* at muscle 6/7 performed in parallel and recorded with identical microscope settings show a clear although incomplete downregulation in the levels of the proteins. (J) Quantification of the mean fluorescence in the NMJ indicates a two-fold decrease of fluorescence levels. Scale bar 10μm. (K) Expression of *RNAi-Gαo* with the driver *elav-Gal4* leads to a comparable decrease of Gαo in the NMJ determined by quantification of mean fluorescence. Western blot of fly head extracts expressing *RNAi-Gαo* with *elav-Gal4* however clearly demonstrates a drastic decrease in protein levels (L). (M-P) *RNAi-wg* and *RNAi-fz2* driven by *OK371-Gal4* also result in a clear downregulation of the Wg (M, N) and Fz2 (O, P) proteins as judged by immunostainings and quantification of the fluorescence in the NMJ. Immunostaining and image acquisition was performed like in (I, J). Anti-Fz2 antibodies have immunoreactivity in the muscle nuclei; note similar nuclear postsynaptic signal in control and *RNAi-fz2* samples (O). (Q) Quantification of total number of boutons show a rescue of the *fz2* mutant phenotype both by presynaptic and postsynaptic overexpression. (R) Representative image of presynaptic Fz2 rescue. Scale bar 10 μm. (S) Expression of Ptx in motoneurons results in reduced bouton numbers and aberrant NMJ morphology, similar to the phenotype of loss of Gαo (see Figure 2C). Scale bar 10μm. (T) Examples of spontaneous action potentials (black arrows) generated in the same recording session as a light-induced action potential (red arrow). The EJP amplitude and duration of the light-induced and spontaneous action potentials are similar. Scale as on Figure1G.

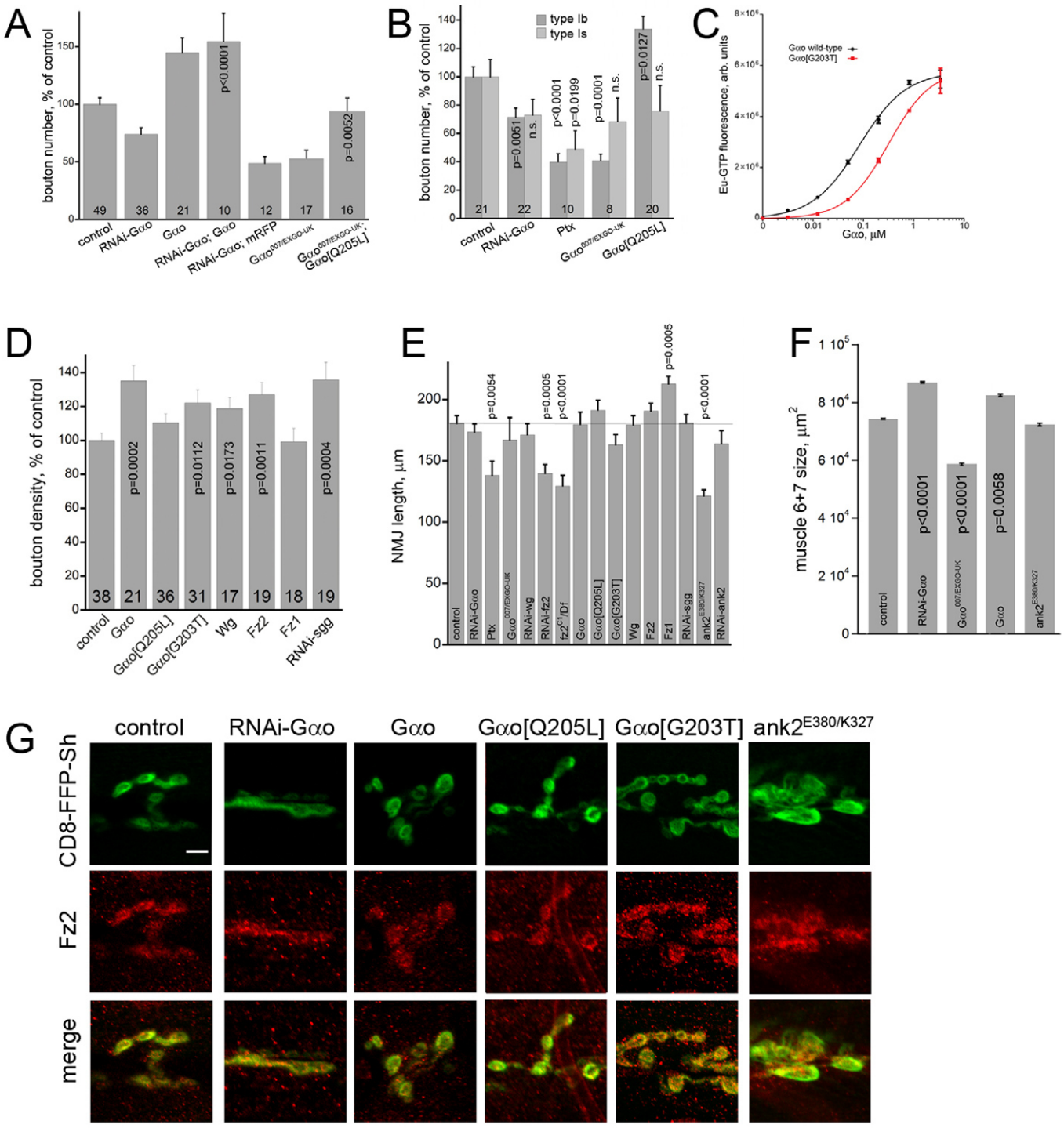

Figure S2. NMJ characterization and Fz2 localization in different genotypes; characterization of Gαo[G203T].

(A) The decrease of bouton number induced by downregulation of Gαo by RNAi is rescued by presynaptic co-overexpression of *Gαo* (p-value refers to the difference from *RNAi-Gαo*) to the level of *Gαo* overexpression. mRFP fails to restore bouton number of *RNAi-Gαo*. Pre-synaptic expression of activated Gαo rescues the *Gαo* genetic mutants (p-value refers to the difference from *Gαo*$^{-/-}$). (B) Change in type Ib and type Is bouton numbers upon alteration of Gαo levels or functionality. (C) Saturation binding curves of recombinant Gαo (black circles) and Gαo[G203T] (red squares) demonstrate that both proteins can be charged with Eu-GTP. Their affinities to the nucleotide analog differ, with that of the wild-type protein being about 4 times higher as judged by the calculated EC_{50} values of these proteins (83±8 nM for Gαo *vs* 316±37 nM for Gαo[G203T]). (D) Bouton density upon overactivation of the Wg pathway; p-values compared to the control are indicated. (E) Length of the NMJ of the indicated genotypes. (F) Muscle area of the indicated genotypes. p-values show significant differences to the control. (G) Localization of Fz2 in boutons of the denoted genotypes. Synaptic Fz2 localization is unaffected upon perturbations in Gαo or Ank2 levels. Scale bar 5μm.

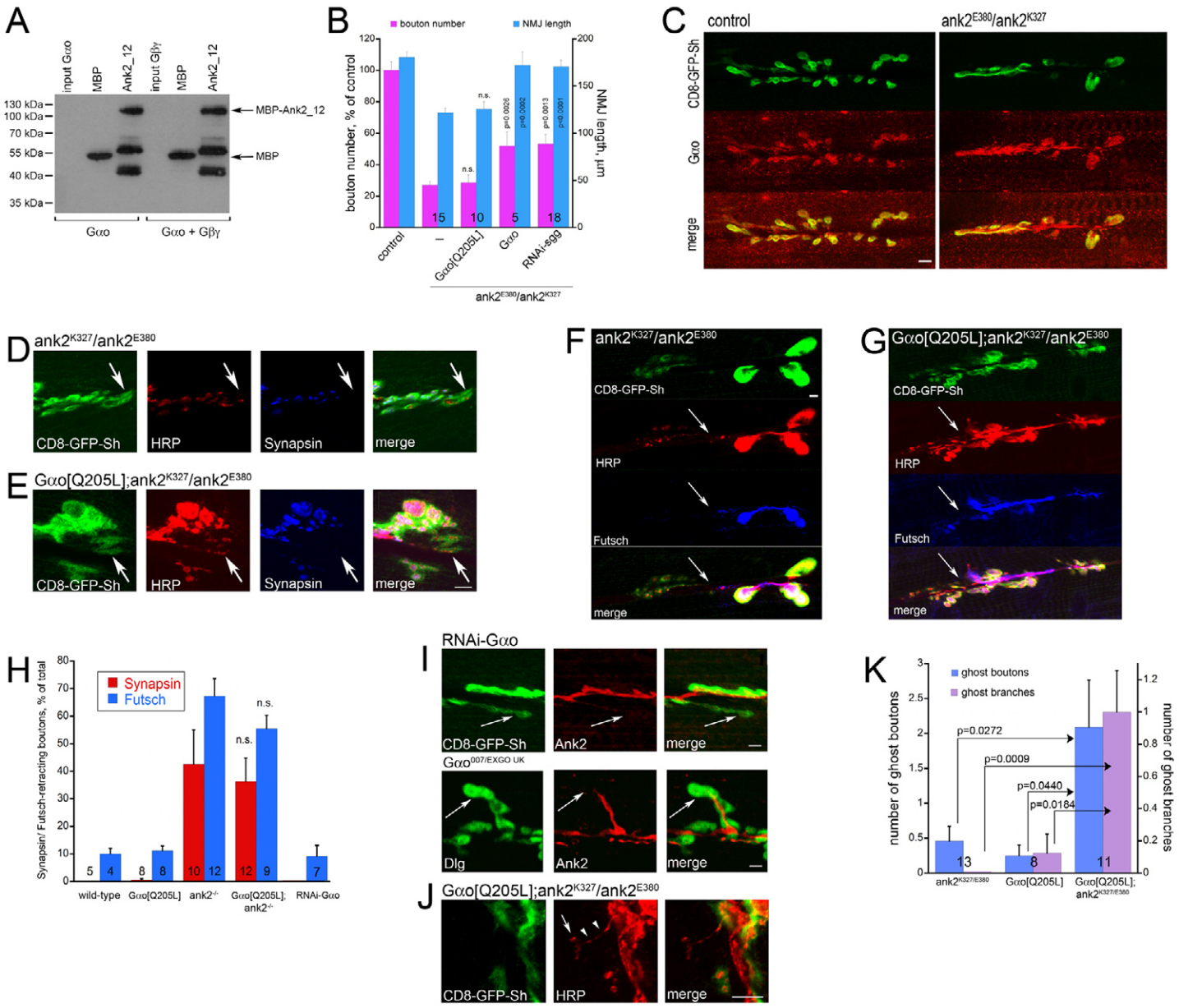

Figure S3. Additional controls to Western blotting, bouton quantification and analysis of presynaptic defects.

(A) Probing the western blot of Figure 5C with anti-MBP antibody demonstrates equal loading of the MBP control and MBP-Ank2_12. MBP-Ank2_12 is purified as a mixture of the full-length protein (ca. 120kDa) and two major degradation products. (B) Bouton number and NMJ length are increased in the *Gαo; ank2$^{E380/K327}$* and *RNAi-sgg; ank2$^{E380/K327}$* genotypes compared to *ank2$^{E380/K327}$*. Numbers of NMJ analyzed and p-values are indicated, n.s. means 'not significant'. (C) Synaptic Gαo localization is unaffected upon loss of Ank2. Scale bar 10 µm. (D-G) Synaptic retractions in *ank2$^{-/-}$* (D, F) or *ank2$^{-/-}$; Gαo[Q205L]* (E, G) seen at the level of synaptic loss of Synapsin (D, E) or Futsch (F, G). Arrows in (D, E) point to some boutons having HRP but no Synapsin staining. Arrows in (F, G) point to the "border" where Futsch staining starts to be lost. Scale bar 5 µm. (H) Quantitation of synaptic retractions in different genotypes. (I) Ghost boutons (arrow) in boutons that still present in RNAi-Gαo and Gαo mutant NMJs. Scale bar 5 µm. (J) Neuronal processes (arrowheads) containing presynaptic HRP but lacking the postsynaptic structures can be seen upon overactivation of Gαo in the absence of Ank2. Scale bar 5 µm. (K) represents quantification of the phenotypes.

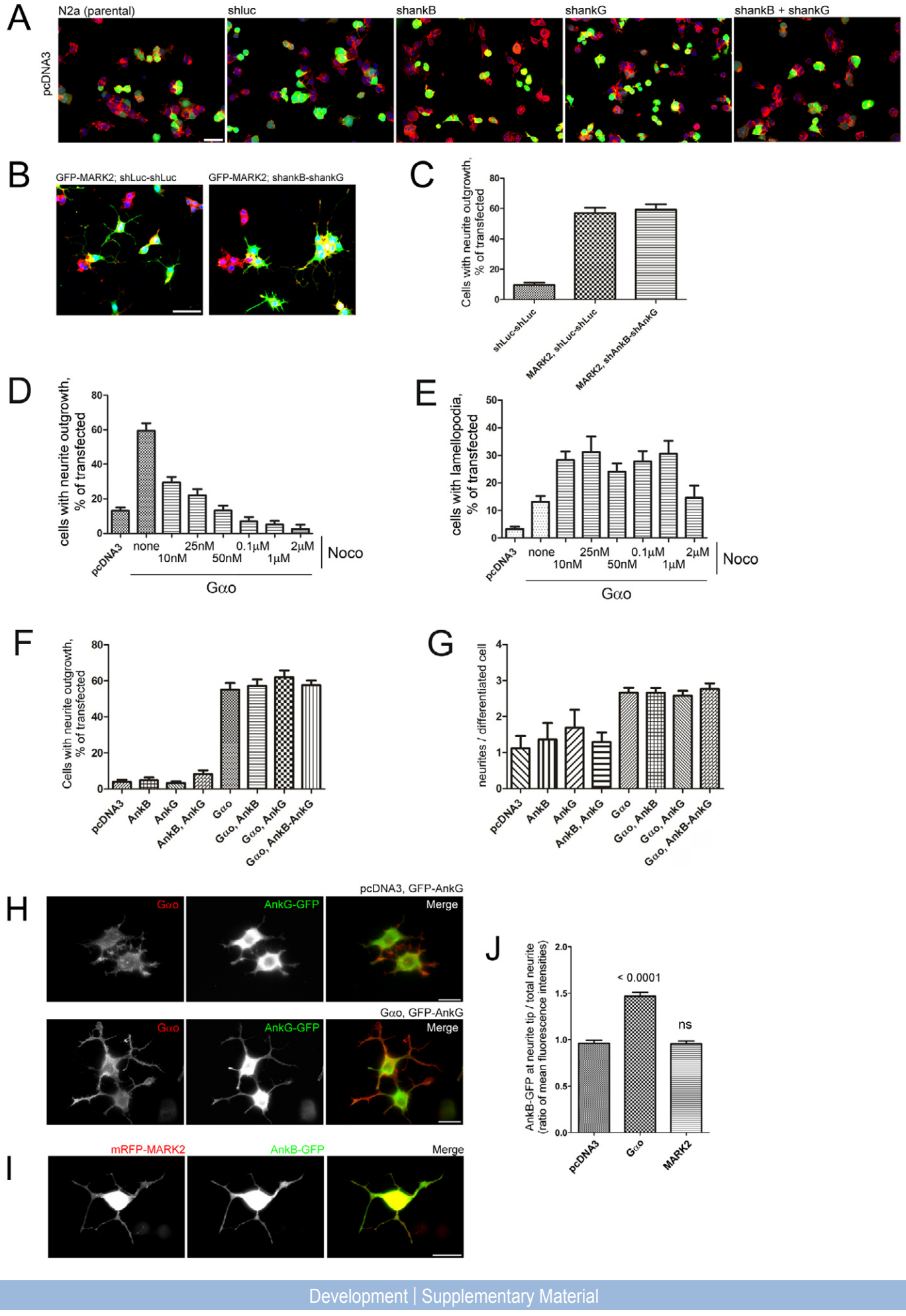
A
N2a (parental)
shluc
shankB
shankG
shankB + shankG
pcDNA3
B
GFP-MARK2; shLuc-shLuc
GFP-MARK2; shankB-shankG
C
Cells with neurite outgrowth, % of transfected
shLuc-shLuc
MARK2, shLuc-shLuc
MARK2, shAnkB-shAnkG
D
cells with neurite outgrowth, % of transfected
pcDNA3
none
10nM
25nM
50nM
0.1μM
1μM
2μM
Noco
Gαo
E
cells with lamellopodia, % of transfected
F
Cells with neurite outgrowth, % of transfected
pcDNA3
AnkB
AnkG
AnkB, AnkG
Gαo
Gαo, AnkB
Gαo, AnkG
Gαo, AnkB-AnkG
G
neurites / differentiated cell
H
pcDNA3, GFP-AnkG
Gαo
AnkG-GFP
Merge
Gαo, GFP-AnkG
I
mRFP-MARK2
AnkB-GFP
J
AnkB-GFP at neurite tip / total neurite (ratio of mean fluorescence intensities)
< 0.0001
ns
MARK2

Figure S4. N2a cell treatments.

(A) Transfection of parental N2a cells with pcDNA3 empty vector poorly induces formation of neurites and lamellopodia. shRNA-stably transfected control (shluc) as well as *ankB* (shankB) and *ankG* (shankG) single and double knockdowns do not show any apparent phenotype after pcDNA3 transfection. Co-expression of EGFP (green) shows transfected cells and Rhodamine phalloidin (red) and DAPI (blue) are used to visualize F-actin and nuclei, respectively. Scale bar: 20 mm. (B) Overexpression of EGFP-tagged MARK2 (GFP-MARK2) induced neurite outgrowth in control shRNA-transfected (shluc-shluc) cells which is not affected in *ankB/G* double know-down (shankB-shankG) cells. Scale bar: 50 mm. (C) Quantification of the experiment described in (B). (D-E) Quantification of the Nocodazole (Noco) effects on neurite outgrowth (B) and lamellopodia formation (C) in Gαo overexpressing N2a cells. Nocodazole treatment blocks neurite outgrowth in a concentration dependent manner (B), while formation of lamellopodia is increased at any Nocodazole concentration (C). (F-G) Quantification of the effects on neurite outgrowth and neurite per cells by the overexpression of EGFP-tagged *ankB* (AnkB-GFP) or *ankG* (AnkG-GFP) in combination with Gαo or empty pcDNA3 vector. (H) Representative images of N2a cells overexpressing AnkG-GFP alone (pcDNA3, AnkG-GFP) or together with Gαo (Gαo, AnkG-GFP). Red fluorescence indicates Gαo immunostaining. (I) No accumulation of AnkB-GFP in neurite tips (and a more homogeneous distribution along the whole of the neurite instead) was observed upon overexpression of an mRFP-tagged MARK2 (mRFP-MARK2) construct (cf. Figure 7J). Scale bar: 10µm. (J) Ratio values of mean fluorescence intensities of AnkB-GFP at neurite tips vs. whole neurites indicate that AnkB significantly accumulates at the rear end of neurites formed by Gαo overexpression, but not at spontaneously formed neurites (pcDNA3) or at neurites induced by mRFP-MARK2 co-expression. P-value (Students t-test) is shown for Gαo co-overexpression. ‘ns’: non-significant (P>0.05).

Molecular Brain

SHORT REPORT Open Access

Lack of evidence of the interaction of the Aβ peptide with the Wnt signaling cascade in *Drosophila* models of Alzheimer's disease

Anne-Marie Lüchtenborg and Vladimir L Katanaev*

Abstract

Background: Alzheimer's disease (AD) is the leading form of dementia worldwide. The Aβ-peptide is believed to be the major pathogenic compound of the disease. Since several years it is hypothesized that Aβ impacts the Wnt signaling cascade and therefore activation of this signaling pathway is proposed to rescue the neurotoxic effect of Aβ.

Findings: Expression of the human Aβ42 in the *Drosophila* nervous system leads to a drastically shortened life span. We found that the action of Aβ42 specifically in the glutamatergic motoneurons is responsible for the reduced survival. However, we find that the morphology of the glutamatergic larval neuromuscular junctions, which are widely used as the model for mammalian central nervous system synapses, is not affected by Aβ42 expression. We furthermore demonstrate that genetic activation of the Wnt signal transduction pathway in the nervous system is not able to rescue the shortened life span or a rough eye phenotype in *Drosophila*.

Conclusions: Our data confirm that the life span is a useful readout of Aβ42 induced neurotoxicity in *Drosophila*; the neuromuscular junction seems however not to be an appropriate model to study AD in flies. Additionally, our results challenge the hypothesis that Wnt signaling might be implicated in Aβ42 toxicity and might serve as a drug target against AD.

Keywords: Alzheimer's disease, Aβ peptide, *Drosophila*, Wnt signaling

Findings

Alzheimer's disease (AD) is a major neurodegenerative malady, affecting today more than 35 million people worldwide with the tendency to double in the prevalence every twenty years [1]. The two major hallmarks of AD are the intracellular neurofibrillary tangles consisting of the hyperphosphorylated tau protein and the extracellular plaques mainly containing the aggregated Aβ peptide. According to the amyloid hypothesis, Aβ peptides in their various aggregation states are the major pathogenic compounds in AD.

Already more than a decade ago, first experiments suggested the interaction of Aβ with the Wnt (Wingless [Wg] in *Drosophila*) signaling cascade and its contribution to Aβ toxicity [2,3]. Wnt signaling is involved in numerous developmental processes and regulates synaptic formation and stability in the adult organism [4]. In the canonical pathway, the ligand Wnt activates the receptor Frizzled (Fz) and its co-receptor LRP5/6 to induce reorganization of the β-catenin-destruction complex, a protein complex consisting of Axin, APC, glycogen synthase kinase 3β (GSK3β, Shaggy [Sgg] in *Drosophila*) and casein kinase, through the scaffolding protein Dishevelled and the trimeric Go protein [4,5]. Thus Wnt signaling leads to stabilization of β-catenin and its translocation to the nucleus where it induces transcription of Wnt target genes. GSK3β also phosphorylates tau and might be the integration point of Aβ and tau induced toxicity [6].

Lithium is a well-established drug against psychiatric disorders that inhibits, amongst other targets, GSK3β [7]. Due to its neuroprotective effect, it has been used in small-scale trials in patients with AD, although with contradictory results [8]. In transgenic mouse models of AD, lithium treatment reduced behavioral impairments and the Aβ load in mouse brains [9]. Likewise, the destabilization of cytosolic β-catenin and the neurotoxicity

* Correspondence: vladimir.katanaev@unil.ch
Department of Pharmacology and Toxicology, Faculty of Biology and Medicine, University of Lausanne, Rue du Bugnon 27, Lausanne 1005, Switzerland

BioMed Central

© 2014 Lüchtenborg and Katanaev; licensee BioMed Central Ltd. This is an Open Access article distributed under the terms of the Creative Commons Attribution License (http://creativecommons.org/licenses/by/4.0), which permits unrestricted use, distribution, and reproduction in any medium, provided the original work is properly credited. The Creative Commons Public Domain Dedication waiver (http://creativecommons.org/publicdomain/zero/1.0/) applies to the data made available in this article, unless otherwise stated.

induced by Aβ in cell culture could be attenuated by LiCl, potentially implying Wnt signaling in Aβ toxicity [10]. Additionally, incubation with Wnt3a reduces the neurotoxic effect of Aβ in cell culture assays – an effect mediated by Fz1 [11,12]. Furthermore, it has been demonstrated that the Aβ peptide can bind to the receptor Fz5 [13]. Therefore, the Wnt cascade was suggested to serve as a potential drug target against AD [3].

Most investigations on Wnt signaling and Aβ have mainly been carried out in mice and cell culture where the inhibition or activation of the signal pathway can be achieved pharmacologically. The genetic model organism *Drosophila melanogaster* has also been used to study the mechanisms of AD [14]. In this model, several possibilities to mimic AD are available; amongst others the neuronal expression of human Aβ42 peptide [15,16]. These flies recapitulate several aspects of AD observed in patients: they show learning deficits, reduced locomotion, shorter life span and neurodegeneration and amyloid deposition in the brain [15].

However, the link between the Wnt signaling and Aβ has not been so far investigated using the *Drosophila* models. We have recently provided an in-depth characterization of the Wg-Fz2-Go-Ankyrin2 signaling pathway active on the presynaptic side of *Drosophila* neuromuscular junctions (NMJs) [17]. NMJs are composed of synaptic boutons – circular structures containing active zones for neurotransmitter release. Being a glutamatergic synapse (unlike most other synapses in *Drosophila*), NMJ provides an especially useful model for mammalian synapses [18]. Expression of human Aβ42 in *Drosophila* NMJs has already been performed and reports to induce defective NMJ formation and functioning [19-21]. Thus we aimed at investigation of the details of the expected interaction of Aβ42 and the Wnt signaling pathway in this system.

Pan-neuronal expression of secreted Aβ42 (using the *elav-Gal4* driver) has previously been shown to reduce the life span of *Drosophila* [15,16]. We recapitulated these findings (Figure 1A) and further showed that a similar reduction in the life span can be achieved through Aβ42 expression by a motoneuron-specific driver *D42-Gal4* (Figure 1B). Indeed, Aβ42 caused a reduction of the median survival from 30 days (*elav-Gal4* control, n = 62) to 10 days (*elav-Gal4; UAS-Aβ42*, n = 74) ($p < 0.0001$, Log-rank test) and of the maximal life span from 42 to 16 days when the pan-neuronal driver was used (Figure 1A), and from 35 days (*D42-Gal4* control, n = 60) to 12 days (*D42-Gal4; UAS-Aβ42*, n = 59) ($p < 0.0001$, Log-rank test) and the maximal life span from 49 to 19 days when the motoneuron-specific driver was used (Figure 1B). This effect is dose-dependent: increasing the amount of Gal4 produced per cell by adding another motoneuron-specific driver *OK371-Gal4* to *D42-Gal4* to express the Aβ42 peptide further reduced the median life span to 10 days ($p = 0.0028$, Log-rank test) and the maximal survival to 14 days (Figure 1B). Cumulatively, these findings suggest that the major effect of Aβ42 on the life span observed previously [15,16] by the pan-neuronal Aβ42 expression takes place in glutamatergic neurons.

We further investigated this effect of Aβ42 by analyzing the morphology of the NMJs in *Drosophila* larvae. We expressed Aβ42 through *elav-Gal4*, *D42-Gal4*, and the combination of *D42-Gal4* and *OK371-Gal4* to increase the expression levels in the motoneurons. In contrast to previously published results where Aβ42 expression induced small morphological changes in NMJs and expression of human APP and BACE led to a reduction in bouton number [20,21], we could not detect an influence of Aβ42 on the larval synapse. Both in terms of the overall morphology (Figure 2A) and in bouton number (Figure 2B), NMJs appear to be unaffected by Aβ42.

We further aimed at investigating the potential interaction of Aβ42 and the Wnt signaling cascade. Given the absence of the expected phenotypes of Aβ42 expression

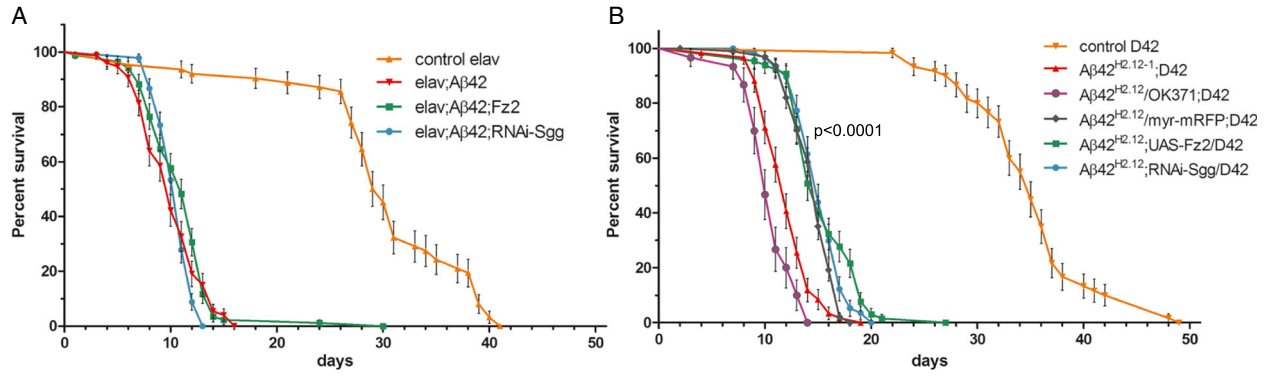

Figure 1 Expression of Aβ42 in the nervous system dramatically reduces the life span. (A-B) Survival curves of the indicated genotypes expressed either with the pan-neuronal driver *elav-Gal4* **(A)** or the driver *D42-Gal4* which expresses in the glutamatergic motoneurons **(B)**. $P < 0.0001$ comparing the controls *elav-Gal4* and *D42-Gal4* to Aβ42 expression, respectively. $p = 0.0028$ comparing *Aβ42; D42-Gal4* and *Aβ42/OK371-Gal4; D42-Gal4*. Co-expression of Fz2 or RNAi-Sgg did not rescue life span. P-values are calculated with the Log-rank test.

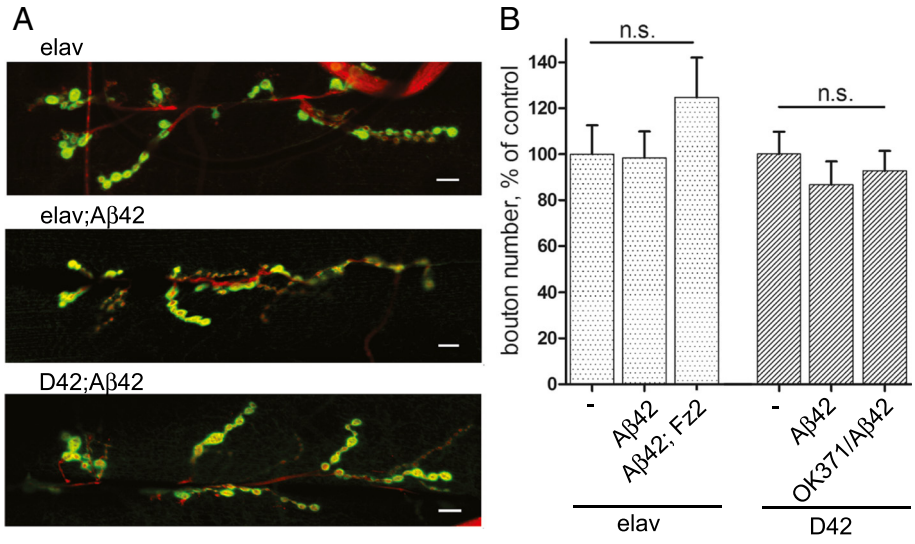

Figure 2 The morphology and bouton number of NMJ are unaffected by neuronal Aβ42 expression. (A) Representative images of NMJs on muscle 6/7 of *elav-Gal4*, *Aβ42; elav-Gal4*, and *Aβ42; D42-Gal4* stained with Dlg to visualize the postsynaptic side and HRP to visualize the neuron. Aβ42 expression does not change NMJ morphology. **(B)** quantification of the bouton number as mean ± sem in percent of control. n.s. means 'not significant' compared to control as calculated with student's t-test.

on NMJ morphology and bouton numbers (Figure 2), we could not use this readout to study the potential interaction between Aβ42 and the pathway. We thus decided to use the life span reduction as the readout. To this end, we co-expressed Aβ42 together with Fz2 – the main Wnt receptor in the *Drosophila* nervous system [17] – or together with the RNAi construct targeting Sgg to activate Wg signaling [17]. We used both the *elav-Gal4* and *D42-Gal4* drivers. We also tried co-expression of Aβ42 with the constitutively active form of Gαo (Gαo [Q205L]) – the Fz2 transducer in the NMJs [17], but this was lethal with either driver, probably due to involvement of the trimeric Go protein in other neuronal activities.

In the motoneurons, co-expression of Fz2 or RNAi-Sgg together with Aβ42 slightly increased the survival compared to Aβ42 expression alone (Figure 1B). However, this was due to a titration effect since an unrelated protein (myr-mRFP) was also able to similarly rescue the life span. In pan-neuronal expression, neither Fz2 nor RNAi-Sgg could significantly increase the median survival, although the maximum life span was increased upon co-expression of Fz2 (Figure 1A). Cumulatively, these results indicate that overactivation of the Wnt signaling transduction pathways in neurons using the genetic tools available in *Drosophila* does not rescue the toxicity (manifested by a shortened life span) induced by secreted Aβ42.

This conclusion is further corroborated using another *Drosophila* readout – insect's eye. Aβ42 expression in the eyes using the *GMR-Gal4* driver leads to a rough eye

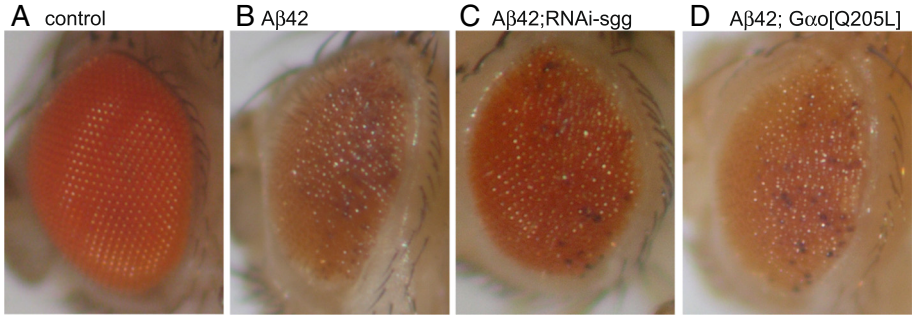

Figure 3 The rough eye phenotype induced by Aβ42 is not rescued by RNAi-Sgg or Gαo [Q205L]. (A) In the control eye (Aβ42 without driver) ommatidia are arranged in a regular array. The other parental line, *GMR-Gal4*, also shows similar wild-type arrangement. **(B)** Expression of Aβ42 in the eyes with the driver *GMR-Gal4* results in a rough eye phenotype. This is not rescued by co-expression of neither RNAi-Sgg **(C)** nor Gαo [Q205L] **(D)**.

phenotype (Figure 3, [16]). We co-expressed RNAi-Sgg and Gαo [Q205L] with Aβ42 and could not observe a rescue of the eye roughness (Figure 3). This confirms in a different setting that genetic activation of the Wnt signaling cascade does not rescue Aβ42 induced toxicity in *Drosophila*.

However, it has been previously reported that expression of the dominant-negative form of Sgg, SggS9E, rescues the shortened life span of *Drosophila* that express the arctic Aβ42 peptide [22]. The arctic peptide was shown to decrease Ser9 phosphorylation of Sgg and thereby upregulate its activity [22]. In contrast another study shows no change in phosphorylation of Sgg when wild-type Aβ42 is expressed [20]. The arctic variant accumulates intracellularly in mice [23,24]; therefore it is likely that the arctic variant of Aβ42 exerts a different pathogenic mechanism than the wild-type peptide. Our data suggest that secreted wild-type Aβ42 acts primarily on glutamatergic neurons in *Drosophila*, but induces the toxicity independently from Wnt signaling.

Taken together, our results demonstrate that Aβ42 expression in glutamatergic neurons is responsible for the dramatic shortened life span manifested in *Drosophila* models of AD. However, the glutamatergic NMJs seem not to be appropriate to study the Aβ42-induced changes on a single cell level. In addition, our genetic interaction analysis challenges the widely accepted idea that Aβ42 inhibits Wnt signaling and that Wnt pathway overactivation might reduce the Aβ42 toxicity. This concept is based on numerous studies, mainly relying on the usage of LiCl and its effects on the AD phenotypes. We suggest that caution is taken when interpreting these data, as LiCl is not a specific inhibitor of GSK3β/Sgg, and further since this kinase has many other functions outside the Wnt signaling pathway [7].

Methods

Life span, eye analysis and *Drosophila* stocks

For the life span test, flies were crossed at 25°C and 5 male and 5 female newly hatched flies were pooled and transferred to 28.5°C. Flies were transferred to fresh food every other day and time-to-death was recorded for individual flies. 59 to 90 flies were analyzed for each genotype. Analysis of survival was performed with GraphPad Prism 5, p-values were calculated with the Log-rank test.

Eye phenotypes were analyzed after crossing to *GMR-Gal4* at 25°C.

The following stock were used: *elav-Gal4*, *D42-Gal4*, *GMR-Gal4* (all from Bloomington stock center), *UAS-RNAi-Sgg* (VCRC #7005), *UAS-Aβ42* [16]. The lines *OK371-Gal4*, *UAS-Fz2*, and *UAS-Gαo [Q205L]* were used as described [17].

Immunohistochemistry

For the analysis of the neuromuscular junctions, crosses were set up at 28.5°C and wandering third instar larvae were dissected and stained as previously described [17]. Primary antibodies were: Cy3-coupled goat anti-HRP (123-165-021, Jackson ImmunoResearch) at 1:200 and mouse anti-Dlg (4 F3, Developmental Studies Hybridoma Bank) at 1:100. Boutons were identified based on presynaptic HRP and postsynaptic Dlg staining. Statistical analysis was performed with GraphPad Prism 5. Data are present as mean ± sem.

Competing interests

The authors declare that they have no competing interests.

Authors' contributions

AML designed, performed and interpreted the data and wrote the manuscript; VLK designed and interpreted the data and wrote the manuscript. Both authors read and approved the final manusrcipt.

Acknowledgements

We thank Gonzalo Solis for critically reading the manuscript. The work was funded by a grant of Synapsis Foundation to VLK.

Received: 27 August 2014 Accepted: 28 October 2014
Published online: 12 November 2014

References

1. Prince M, Bryce R, Albanese E, Wimo A, Ribeiro W, Ferri CP: **The global prevalence of dementia: a systematic review and metaanalysis.** *Alzheimers Dement* 2013, **9:**63–75.e62.
2. Inestrosa NC, Alvarez A, Godoy J, Reyes A, De Ferrari GV: **Acetylcholinesterase-amyloid-beta-peptide interaction and Wnt signaling involvement in Abeta neurotoxicity.** *Acta Neurol Scand Suppl* 2000, **176:**53–59.
3. Inestrosa NC, Varela-Nallar L: **Wnt signaling in the nervous system and in Alzheimer's disease.** *J Mol Cell Biol* 2014, **6:**64–74.
4. Blagodatski A, Poteryaev D, Katanaev V: **Targeting the Wnt pathways for therapies.** *Mol Cell Ther* 2014, **2:**28.
5. Egger-Adam D, Katanaev VL: **The trimeric G protein go inflicts a double impact on axin in the Wnt/frizzled signaling pathway.** *Dev Dyn* 2010, **239:**168–183.
6. Qu ZS, Li L, Sun XJ, Zhao YW, Zhang J, Geng Z, Fu JL, Ren QG: **Glycogen synthase kinase-3 regulates production of amyloid- beta peptides and Tau phosphorylation in diabetic Rat brain.** *Sci World J* 2014, **2014:**878123.
7. O'Brien WT, Klein PS: **Validating GSK3 as an in vivo target of lithium action.** *Biochem Soc Trans* 2009, **37:**1133–1138.
8. Forlenza OV, de Paula VJ, Machado-Vieira R, Diniz BS, Gattaz WF: **Does lithium prevent Alzheimer's disease?** *Drugs Aging* 2012, **29:**335–342.
9. Toledo EM, Inestrosa NC: **Activation of Wnt signaling by lithium and rosiglitazone reduced spatial memory impairment and neurodegeneration in brains of an APPswe/PSEN1DeltaE9 mouse model of Alzheimer's disease.** *Mol Psychiatry* 2010, **15:**272–285. 228.
10. De Ferrari GV, Chacon MA, Barria MI, Garrido JL, Godoy JA, Olivares G, Reyes AE, Alvarez A, Bronfman M, Inestrosa NC: **Activation of Wnt signaling rescues neurodegeneration and behavioral impairments induced by beta-amyloid fibrils.** *Mol Psychiatry* 2003, **8:**195–208.
11. Alvarez AR, Godoy JA, Mullendorff K, Olivares GH, Bronfman M, Inestrosa NC: **Wnt-3a overcomes beta-amyloid toxicity in rat hippocampal neurons.** *Exp Cell Res* 2004, **297:**186–196.
12. Chacon MA, Varela-Nallar L, Inestrosa NC: **Frizzled-1 is involved in the neuroprotective effect of Wnt3a against Abeta oligomers.** *J Cell Physiol* 2008, **217:**215–227.
13. Magdesian MH, Carvalho MM, Mendes FA, Saraiva LM, Juliano MA, Juliano L, Garcia-Abreu J, Ferreira ST: **Amyloid-beta binds to the extracellular cysteine-rich domain of Frizzled and inhibits Wnt/beta-catenin signaling.** *J Biol Chem* 2008, **283:**9359–9368.
14. Prussing K, Voigt A, Schulz JB: **Drosophila melanogaster as a model organism for Alzheimer's disease.** *Mol Neurodegener* 2013, **8:**35.
15. Iijima K, Liu HP, Chiang AS, Hearn SA, Konsolaki M, Zhong Y: **Dissecting the pathological effects of human Abeta40 and Abeta42 in drosophila: a**

potential model for Alzheimer's disease. *Proc Natl Acad Sci U S A* 2004, **101:**6623–6628.

16. Sanokawa-Akakura R, Cao W, Allan K, Patel K, Ganesh A, Heiman G, Burke R, Kemp FW, Bogden JD, Camakaris J, Raymond BB, Konsolaki M: **Control of Alzheimer's amyloid beta toxicity by the high molecular weight immunophilin FKBP52 and copper homeostasis in Drosophila.** *PLoS One* 2010, **5:**e8626.
17. Luchtenborg AM, Solis GP, Egger-Adam D, Koval A, Lin C, Blanchard MG, Kellenberger S, Katanaev VL: **Heterotrimeric Go protein links Wnt-Frizzled signaling with ankyrins to regulate the neuronal microtubule cytoskeleton.** *Development* 2014, **141:**3399–3409.
18. Collins CA, DiAntonio A: **Synaptic development: insights from drosophila.** *Curr Opin Neurobiol* 2007, **17:**35–42.
19. Chiang HC, Iijima K, Hakker I, Zhong Y: **Distinctive roles of different beta-amyloid 42 aggregates in modulation of synaptic functions.** *FASEB J* 2009, **23:**1969–1977.
20. Folwell J, Cowan CM, Ubhi KK, Shiabh H, Newman TA, Shepherd D, Mudher A: **Abeta exacerbates the neuronal dysfunction caused by human tau expression in a Drosophila model of Alzheimer's disease.** *Exp Neurol* 2010, **223:**401–409.
21. Mhatre SD, Satyasi V, Killen M, Paddock BE, Moir RD, Saunders AJ, Marenda DR: **Synaptic abnormalities in a Drosophila model of Alzheimer's disease.** *Dis Model Mech* 2014, **7:**373–385.
22. Sofola O, Kerr F, Rogers I, Killick R, Augustin H, Gandy C, Allen MJ, Hardy J, Lovestone S, Partridge L: **Inhibition of GSK-3 ameliorates Abeta pathology in an adult-onset Drosophila model of Alzheimer's disease.** *PLoS Genet* 2010, **6:**e1001087.
23. Lord A, Kalimo H, Eckman C, Zhang XQ, Lannfelt L, Nilsson LN: **The arctic Alzheimer mutation facilitates early intraneuronal Abeta aggregation and senile plaque formation in transgenic mice.** *Neurobiol Aging* 2006, **27:**67–77.
24. Sahlin C, Lord A, Magnusson K, Englund H, Almeida CG, Greengard P, Nyberg F, Gouras GK, Lannfelt L, Nilsson LN: **The arctic Alzheimer mutation favors intracellular amyloid-beta production by making amyloid precursor protein less available to alpha-secretase.** *J Neurochem* 2007, **101:**854–862.

doi:10.1186/s13041-014-0081-y
Cite this article as: Lüchtenborg and Katanaev: **Lack of evidence of the interaction of the Aβ peptide with the Wnt signaling cascade in *Drosophila* models of Alzheimer's disease.** *Molecular Brain* 2014 **7**:81.

Submit your next manuscript to BioMed Central and take full advantage of:

- **Convenient online submission**
- **Thorough peer review**
- **No space constraints or color figure charges**
- **Immediate publication on acceptance**
- **Inclusion in PubMed, CAS, Scopus and Google Scholar**
- **Research which is freely available for redistribution**

Submit your manuscript at
www.biomedcentral.com/submit

BioMed Central